Efficient Hybrid Iterative Detector for Signal Detection in Massive MIMO Uplink System over AWGN Channel

Zelalem Melak Gebeyehu

A Thesis Submitted to

The Department of Electronics and Communication Engineering

School of Electrical Engineering and Computing

Presented in Partial Fulfillment of the Requirement for the Degree of Master's in Electronics and Communication Engineering

Office of Post Graduate Studies

Adama Science and Technology University

June, 2022

Adama, Ethiopia

Efficient Hybrid Iterative Detector for Signal Detection in Massive MIMO Uplink System over AWGN Channel

Zelalem Melak Gebeyehu

Major Advisor: - Dr. Ram Sewak Singh (PhD)

Co-advisor: -Dr. Satyasis Mishra (PhD)

A Thesis Submitted to

The Department of Electronics and Communication Engineering

School of Electrical Engineering and Computing

Presented in Partial Fulfillment of the Requirement for the Degree of Master's in Electronics and Communication Engineering

Office of Post Graduate Studies

Adama Science and Technology University

June, 2022

Adama, Ethiopia

APPROVAL PAGE of M.SC. THESIS

We, the advisors of the thesis entitled **"Efficient Hybrid Iterative Detector for Signal Detection in Massive MIMO Uplink System over AWGN Channel"** and developed by **Zelalem Melak Gebeyehu,** hereby certify that the recommendation and suggestions made by the board of examiners are appropriately incorporated into the final version of the thesis.

Dr. Ram Sewak Singh	________________	___________
Major Advisor	Signature	Date
Dr. Satyasis Mishra	________________	___________
Co-Advisor	Signature	Date

We, the undersigned members of the board of Examiners of the thesis by **Zelalem Melak Gebeyehu** have read and evaluated the thesis entitled **"Efficient Hybrid Iterative Detector for Signal Detection in Massive MIMO Uplink System over AWGN Channel"** and examined the candidate during open defense. This is, therefore, to certify that the thesis is accepted for partial fulfillment of the requirement of the degree of Master of Science in Electronics and Communication engineering.

_______________	_____________	___________
Chairperson	Signature	Date
_______________	________________	___________
Internal Examiner	Signature	Date
_______________	________________	___________
External Examiner	Signature	Date

Finally, approval and acceptance of the thesis is contingent upon submission of its final copy to the Office of Postgraduate Studies (OPGS) through the Department Graduate Council (DGC) and School Graduate Committee (SGC).

_______________	________________	___________
Department Head	Signature	Date
_______________	________________	___________
School Dean	Signature	Date
______________	_______________	__________
Office of Postgraduate Studies, Dean	Signature	Date

DECLARATION

I hereby declare that this Master Thesis entitled "**Efficient Hybrid Iterative Detector for Signal Detection in Massive MIMO Uplink System over AWGN Channel**" is my own work and has not been submitted to any university for the award of any academic degree, diploma or certificate. The references used in this thesis are duly recognized by proper citations.

Zelalem Melak Gebeyehu	________________	___________
Name of student	Signature	Date

RECOMMENDATION

We, the advisors of this thesis, hereby certify that we have read the revised version of the thesis entitled **"Efficient Hybrid Iterative Detector for Signal Detection in Massive MIMO Uplink System over AWGN Channel''** prepared under our guidance by Zelalem Melak Gebeyehu submitted in partial fulfillment of the requirements for the degree of Mater's of Science in Electronics and Communication Engineering. Therefore, we recommend the submission of revised version of the thesis to the department following the applicable procedures.

Dr. Ram Sewak Singh	________________	___________
Major Advisor	Signature	Date
Dr. Satyasis Mishra	________________	___________
Co-Advisor	Signature	Date

ACKNOWLEDGEMENT

First and foremost, praise and thanks to the Almighty God for his mercies in allowing me to finish this thesis successfully.

I would like to express my thanks to my advisor, Dr. Ram Sewak Singh (PhD), for his encouragement and sacrifice of valuable time to encourage me to work in my own way and for giving me the freedom to explore this thesis deeply. Without his assistance, it would not have been possible to achieve the ultimate goal of this thesis. He was a great help whenever I had a problem with my thesis.

I would like to express my sincere gratitude to my co-advisor, Dr. Satyasis Mishra (PhD), for his continuous support of my M.Sc. research and for his patience, motivation, and enthusiasm. His guidance helped me in all the research and writing of this thesis.

In addition, I would like to thank Adama Science and Technology University (ASTU) and all members of the School of Electrical Engineering and Computing (SoEEC), particularly the program of electronics and communication engineering, for providing such an excellent educational and research environment. I am grateful to all of the students in the Communication Engineering division who have shared their knowledge with me.

Finally, I am grateful to my family for always allowing me to go my own way and making me feel as if I could do whatever I wanted without feeling pressed.

TABLE OF CONTENTS

Contents

LIST OF TABLES

LIST OF FIGURES

LIST OF ACRONYMS AND ABBREVIATIONS

3D	Three Dimensional
4G	Fourth Generations
4G/LTE	Fourth Generation Long Term Evolution
5G	Fifth Generations
ADMM	Alternating Direction Method of Multiplier
AWGN	Additive White Gaussian Noise
B5G	Beyond Fifth Generation
BER	Bit Error Rate
BGS	Block-Gauss Seidel
BLER	Block Error Rate
BS	Base Station
BUAR	Base Station-to-User Antenna Ratio
CG	Conjugate-Gradient
CGLS	Conjugate-Gradient Linear Square
CSI	Channel State Information
DJ	Damped Jacobi
DL	Downlink
FPGA	Field Programmable Gate Array
Gbps	Giga bits per second
GS	Gauss-Seidel
IEEE	Institute of Electrical and Electronics Engineers
LS	Linear Square
MATLAB	Matrix Laboratory
MF	Matched Filter
MIMO	Multiple-Input Multiple-Out
M-MIMO	Massive- Multiple-Input Multiple-Out
ML	Maximum Likelihood
MMSE	Minimum Mean Square Error
MRC	Maximum Ratio Combining
MS	Mobile Station

MSE	Mean Squared Error
MU-MIMO	Multi-User Multiple-Input Multiple-Out
M-QAM	M-ary Quadrature Amplitude Modulation
NR	New Radio
NSA	Neumann Series Approximation
OCD	Optimized Coordinate Descent
PAPR	Peak to Average Power Ratio
PLL	Phase-Locked Loop
SER	Symbol Error Rate
SNR	Signal-to-Noise ratio
SOR	Successive Over Relaxation
SU-MIMO	Single-User Multiple-Input Multiple-Out
UL	Uplink
VLSI	Very Large Scale Integration
ZF	Zero forcing

ABSTRACT

Massive Multiple Input Multiple Output (Massive MIMO) is a key technology in fifth-generation (5G) and beyond fifth-generation (B5G) networks. It improves energy efficiency, spectral efficiency and throughput. Because of the large number of users and antennas, sophisticated processing is required to detect the transmitted message signal. One of the challenges in massive MIMO systems is transmitted message signal detection. To respond to these challenges, several detection algorithms have been developed, including Minimum Mean Squared Error (MMSE), Zero Forcing (ZF), Matched Filter (MF), Conjugate-Gradient (CG), Gauss-Seidel (GS) and Optimized Coordinate Descent (OCD). Although the ZF and MMSE algorithms perform well, their computational complexity is high due to direct matrix inversion. When the number of users is much lower than the number of antennas, the MF algorithm performs well. However, as the number of users increases, the performance of the MF algorithm degrades. Although the OCD, CG, and GS algorithms have less computational complexity than the MMSE algorithm, they perform poorly in comparison. To address the shortcomings of existing methods, this thesis proposed an efficient iterative algorithm that is a hybrid of MMSE with the Alternating Direction Method of Multipliers (ADMM) technique and Gauss-Seidel method. The initial vector has a large influence on the performance, complexity, and convergence rate of such iterative algorithms. The proposed detector's initial solution is determined using the diagonal matrix and MMSE with the ADMM technique. The proposed algorithm's performance is compared to existing algorithms based on BER, MSE and SER. The complexity of proposed algorithm also compared based on number of multiplications. The simulation results show that the proposed algorithm achieved the best BER, SER and MSE performance with a small number of iterations and a significant reduction in computational complexity.

Keywords: *5G; Massive MIMO; Signal Detection; Hybrid Minimum Mean Squared Error with Alternating Direction Method of Multiplier and Gauss-Seidel; Cholesky Decomposition*

CHAPTER ONE

1. INTRODUCTION

1.1 Background of the Study

Nowadays, users' demands for high data rates, high spectral efficiency, high energy efficiency and throughput in wireless communication systems are increasing. Multiple input multiple output (MIMO) systems are an essential component of today's wireless systems, and they have been extensively used in recent years to obtain high spectral efficiency and high energy efficiency (Larsson et al., 2014). Prior to the introduction of MIMO, single-input, single-output systems were commonly used, which had very low throughput and could not support a large number of users with high reliability. To meet this massive user demand, various new MIMO technologies such as single-user MIMO (SU-MIMO), multi-user MIMO (MU-MIMO), and network MIMO were developed (Chataut & Akl, 2020). However, these new technologies are not sufficient to meet the ever-increasing demands. Wireless users have increased exponentially in recent years, and these users generate trillions of bytes of data that must be handled efficiently and with greater reliability.

The current MIMO technologies used in fourth generation long term evolution (4G/LTE) networks are incapable of handling this massive influx of data traffic with greater speed and reliability. To address consumer requests for high performance and data rates, 5G mobile networks are now being introduced. To achieve high data rate, high energy efficiency, better throughput, and high spectral efficiency, 5G used one of the enabling technologies known as massive multiple input multiple output (Massive MIMO). The most enticing technology for 5G and B5G wireless networks is the massive MIMO system (Borges et al., 2021). It is a development of current MIMO wireless network systems that combine a high number of antennas at the base station and serve several users at the same time as shown in figure 1.1 (Chataut & Akl, 2020). Because Massive MIMO employs many more antennas than the number of users in the cell, the beam is much narrower, allowing the base station to deliver radio frequency (RF) energy to the user with greater precision and efficiency. The large number of antennas in Massive MIMO help the energy to focus on a smaller region of space, improving spectral efficiency and throughput (Nguyen, 2018). Radiated beams in a Massive MIMO system become narrower and more spatially focused toward the users as the number of antennas increases. These spatially focused antenna beams improve throughput for the intended user while reducing interference for the neighboring user.

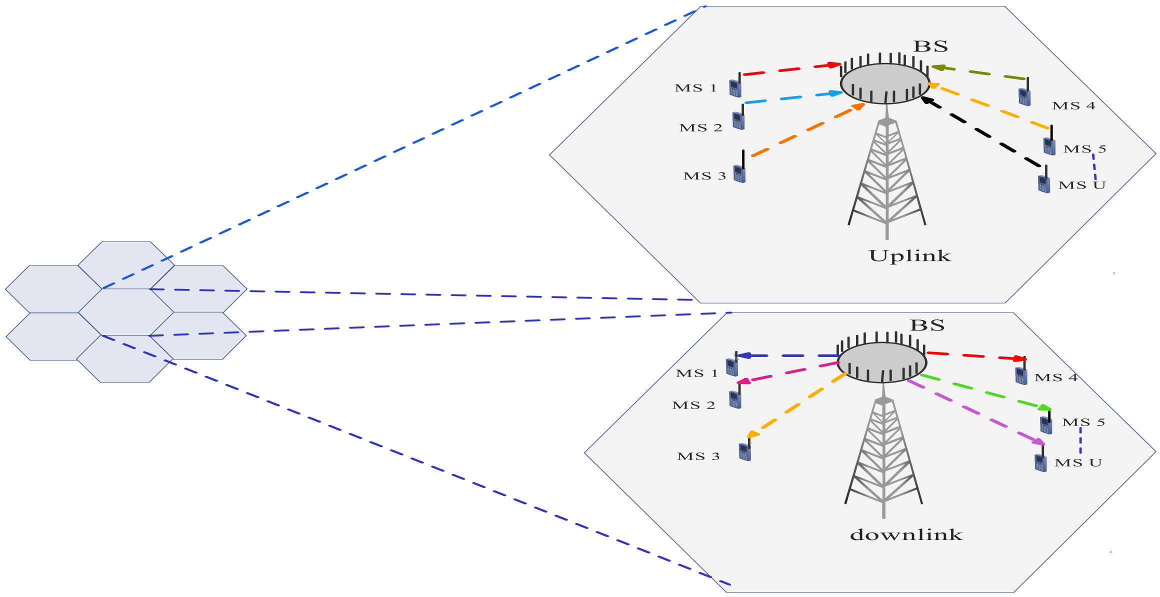

Figure 1. 1: Massive MIMO architecture with U number of mobile station (MS) users (Chataut & Akl, 2020)

Massive MIMO is an emerging technology that enables the use of large-scale antenna arrays by installing hundreds or even thousands of antennas at the base station (BS) to simultaneously serve multiple single-antenna users within the same bandwidth (Shafivulla et al., 2020). Massive MIMO's ability to enhance throughput and spectral efficiency has made it a critical technology for emerging wireless standards. In comparison to traditional MIMO systems, the number of antennas in massive MIMO systems has increased significantly, and the utilization efficiency of the spectrum and link reliability have both improved. Furthermore, Massive MIMO can reduce power consumption at the BS. In general, Massive MIMO technology in 5G provides higher spectral efficiency, higher data rates, low latency, robustness, high link reliability, reliable and accurate user tracking, higher energy efficiency, and enhanced security. Although this massive MIMO scenario benefits the communication system, it faces several difficulties during deployment. These difficulties are signal detection, pilot contamination, precoding, channel estimation, user scheduling, and hardware impairment. Several studies are being conducted to discover mitigation techniques for these difficulties. This research focuses on the signal detection challenge and its mitigation techniques.

1.2 Motivation

Because the Massive MIMO technology concept was introduced just a few years ago, it has reached new heights every year. Massive MIMO has emerged as one of the most recent research topics in wireless communication networks due to its enormous benefits in 5G standardization. The current MIMO systems are insufficient to cope with the massive increase in wireless network data traffic. Massive MIMO technology is being considered by the 5G network as a potential solution to the problem caused by massive data traffic and users. The study and investigation of Massive MIMO wireless access technology has been motivated by the global bandwidth scarcity in the wireless communication sector.

1.3 Statement of Problem

Due to the large number of antennas and users in massive MIMO systems, the uplink transmitted signal detection becomes complex. To solve this problem, there are conventional signal detection algorithms such as ZF and MMSE. But these algorithms have high computational complexity due to direct matrix inversion. To overcome this problem, iterative algorithms such as GS, CG, and OCD should be used, but the performance of these algorithms is less than that of ZF and MMSE algorithms. To solve this problem, a high-performance and low-complexity algorithm is required. In this study, a hybrid algorithm based on minimum mean square error with the ADMM technique and Gauss-Seidel algorithm is proposed to obtain a high performance and low computational complexity signal detection method.

1.4 Objectives

1.4.1 General objective

The main objective of this thesis is to develop high performance and low computational complexity hybrid iterative algorithm for transmitted signal detection in massive MIMO systems.

1.4.2 Specific Objectives

- To develop a hybrid algorithm based on MMSE with ADMM technique and GS algorithm for transmitted signal detection of Massive MIMO uplink systems.
- To apply hybrid algorithm on M-ary QAM for transmitted signal detection of Massive MIMO uplink systems using AWGN channel.

- To compare the performance of hybrid algorithm with existing algorithms.
- To compare the Computational complexity of hybrid algorithm with existing algorithms.

1.5 Scope of the Study

This thesis focuses on finding the signal detector for uplink massive systems that is efficient in performance and complexity. The complexity and performance of existing detectors such as ZF, MF, MMSE, CG, GS, and OCD are compared with the proposed algorithm and analysis is made about the performance and computational complexity.

1.6 Significance of the Study

As the number of users increases in a massive MIMO system, so does the complexity of the transmitted signal detection algorithm. The thesis provides an optimal, low-complexity, high-performance signal detection algorithm that is a hybrid of the minimum mean square error with the Alternating Direction Method of Multiplier Algorithm and the Gauss-Seidel algorithm.

1.7 Thesis Contribution

Massive MIMO is the key enabling technology for 5G networks. However, during deployment, it faces the challenges of uplink signal detection. The main contribution of this thesis is to develop a hybrid efficient detector to address this challenge. This thesis analyze the performance of the developed detector with existing detectors based on parameters such as bit error rate, mean squared error, and symbol error rate. The complexity is also analyzed based on the number of multiplications required in the algorithm.

1.8 Limitation of the Thesis

The investigation for the thesis is limited to simulations.

1.9 Outline of the Thesis

The remaining part of the thesis is outlined as follows:

Chapter Two presents basic introduction, working principle, characteristics, limitations, challenges and main advantage of massive MIMO systems. Review of different related works on massive MIMO uplink signal detection also included in this chapter.

Chapter Three describes the methods used in this thesis. System model, mathematical models of different methods and proposed method, and performance metrics are included in this chapter.

Chapter Four describes simulation results and detailed discussion of the obtained results.

The last part contains the conclusion and recommendation for the future work.

CHAPTER TWO

2. LITERATURE REVIEW

2.1 Introduction to Massive MIMO

5G mobile networks use a number of different technologies to deliver a far superior experience to customers than previous 4G LTE networks (Elsherbiny et al., 2020). MIMO is an antenna technology that is used in 4G LTE networks, however its improved version, Massive MIMO, is a key component in 5G New Radio (NR) networks (Rahmawati et al., 2021).

Massive MIMO is a type of wireless communications technology in which base stations are equipped with a large number of antenna elements to improve spectral and energy efficiency. Massive MIMO technology combines antennas, radios, and spectrum to increase capacity and speed for the upcoming 5G networks. Massive MIMO is a multi-user MIMO technology that allows wireless terminals in high-mobility environments to receive consistently good service. The key idea is to employ base stations with multiple antenna arrays that can simultaneously serve multiple user terminals at the same time-frequency resource. The term "massive" indicates the number of antennas, not the size of the antennas.

Massive MIMO effectively uses radio network resources to enhance network capacity, resulting in higher throughput and multi-user support. Massive MIMO is an advanced antenna technology being used in 5G NR network systems that improves spectral efficiency, network capacity, coverage, and achievable data rates. It supports multiple users at the same time by utilizing a massive number of antenna elements within the transmitter and receiver antenna panels.

2.2 Massive MIMO Working Principle in 5G Networks

Massive MIMO uses a large number of antenna elements within a single antenna panel of a 5G base station and employs spatial multiplexing, diversity, and beamforming to improve network capacity, throughput, and radio link quality. The extra capacity is used to serve multiple users at the same time. The foundation for enhancing signal reliability and data rate while minimizing interference is provided by transmitter and receiver diversity, spatial multiplexing, and beamforming.

2.2.1 Diversity in Transmitter and Receiver

Diversity is defined as the use of many antennas at the transmitter or receiver end to reduce the influence of signal fading (Chen et al., 2017). A radio signal transmission can take several paths between such a transmitter and a receiver. A few paths are clear of obstacles, such as high-rise buildings, but others may be obstructed. As a consequence, the different versions of the signal that travel through the different pathways may fade at varying rates. Diversity takes advantage of the signal's nature by using multiple antennas to catch various versions of the signal, which can then be merged to improve overall signal quality. Massive MIMO significantly increases the number of antennas in 5G networks. By enhancing the radio link's reliability, diversity improves the signal's robustness.

2.2.2 Spatial Multiplexing

One of the most crucial components of Massive MIMO systems for increasing frequency chan nel efficiency is spatial multiplexing (Iwakuni et al., 2015). This increase in spectral efficiency results in increased overall capacity and, as a result, higher data rates. Massive MIMO involves a huge number of antenna arrays that are differentiated in space and can transmit and receive multiple data streams at the same time as shown in figure 2.1. The total data stream designed for a particular customer can be divided into multiple specific data streams. At the receiver side, these data streams are collected by an array of receiving antenna elements, which combine the numerous specific data streams into a single data stream. This procedure increases data rates for a specific user.

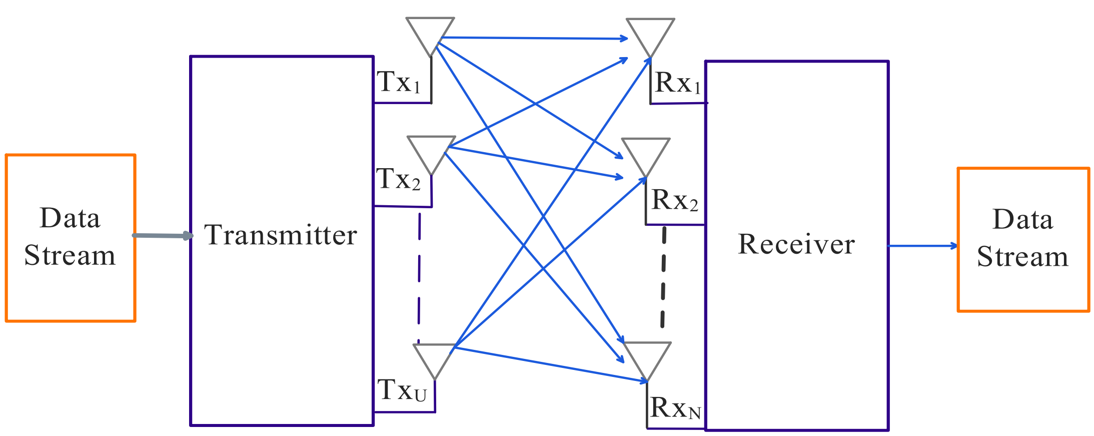

Figure 2. 1: Massive MIMO Spatial multiplexing (Iwakuni et al., 2015)

2.2.3 Beamforming

MIMO systems use beamforming, which is an advanced antenna technology. It refers to the base station's ability to change the radiation pattern of the antenna. Beamforming is the process of focusing a signal transmitted through several antenna elements in one direction rather than transmitting the signal in all directions (Yarrabothu & Telagathoti, 2019). Beamforming makes effective use of existing transmission power to direct the signal's various beams in the right direction. Beamforming assists the base station in determining the best route to take in order to offer data to the user while also reducing interference from neighboring customers along the path.

Massive MIMO beamforming is three-dimensional (3D beamforming), which means beams can be horizontal or vertical to enhance data rates for all customers. Beamforming improves spectrum efficiency in massive MIMO systems. In massive MIMO, the BS can transmit the data to the user via multiple paths, and beamforming coordinates packet motion and arrival time to allow more customers to transmit data at the same time. Beamforming increases the signal's range by helping to shape the transmission so that the intended beam receives the majority of the transmission power, causing it to become greater while suppressing the non-desired beams. Massive MIMO employs the beamforming technique to direct transmission power in specific directions, thereby increasing network coverage while reducing interference. Figure 2.2 indicates the beamforming in massive MIMO systems.

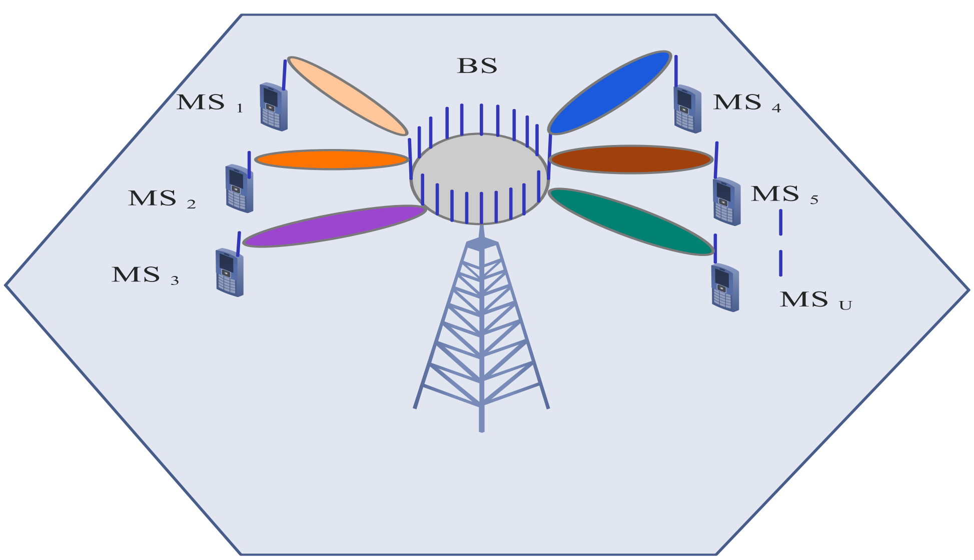

Figure 2. 2: Massive MIMO Beamforming (Yarrabothu & Telagathoti, 2019)

2.3 The Advantages of Massive MIMO Technology for 5G Networks

The following are the main advantages of massive MIMO technology (Chataut & Akl, 2020):

I. Spectral Efficiency: Massive MIMO improves spectral efficiency by allowing its antenna array to focus narrow beams towards a user. It is possible to achieve a spectral efficiency that is more than ten times greater than that of the current MIMO system used for 4G/LTE.

II. Energy Efficiency: Since the antenna array is focused on a small specific section, it requires less radiated power and thus reduces the energy requirement in massive MIMO systems.

III. High Data Rate: Massive MIMO increases the data rate and capacity of wireless systems by providing array gain and spatial multiplexing.

IV. User Tracking: Because massive MIMO uses narrow signal beams towards the user, user tracking becomes more reliable and accurate.

V. Low Power Consumption: Massive MIMO is built with ultra-low power linear amplifiers, which eliminates the need for bulky electronic equipment in the system. This power consumption can be significantly reduced.

VI. Less Fading: Having a large number of antennas at the receiver makes massive MIMO resilient to fading.

VII. Low Latency: Massive MIMO reduces the latency on the air interface.

VIII. Robustness: Massive MIMO systems are resistant to unintentional interference and internal jamming. Furthermore, due to the large number of antennas, these systems are resistant to one or a few antenna failures.

IX. Reliability: The use of a large number of antennas in massive MIMO provides more diversity gain, which improves link reliability.

X. Enhanced Security: Because of the orthogonal mobile station channels and narrow beams, massive MIMO provides greater physical security.

2.4 Characteristics of Massive MIMO System

- There are many more antennas at the base station than there are users, implying that the number of antennas at the base station is greater than the number of users' antennas.
- Multiplexing gain: Massive MIMO channels provide a linear increase in capacity without the need for additional power or bandwidth. This is known as multiplexing gain.

- Highly directive signals: Since the signal beam used in massive MIMO is narrow, the system becomes highly directive.
- Smaller antenna array size: Because the wavelength is shorter at higher frequencies, the antenna array size for high-frequency Massive MIMO is smaller.
- Low-power antennas: Because antenna arrays are focused on a small particular section and beams are narrow, less radiated power is required.
- Reduced interference: Massive MIMO systems reduce intra-and inter-cell interference by narrowing and focusing radiated energy in the direction of the intended user.

2.5 Limitation of Massive MIMO

I. Pilot contamination as a result of a limited number of orthogonal pilot subcarriers with a constrained coherent interval as well as bandwidth.

II. Due to the use of a large number of antennas and the multiplexing of users' equipment, signal processing complexity is high.

III. Beam alignment is critical because a highly narrow beam is being used, which is attentive to mobile station movement or moving of the antenna array.

2.6 Massive MIMO Uplink System

The uplink (UL) transmission channel is used to send message signals from the mobile station to the base station. The base station in the UL with N antennas receives transmitted data from all U user terminals using the same frequency-time resource (X. Yang et al., 2020). Consider a massive MIMO uplink system with N antennas at the base station communicating with U ($N >> U$) single-antenna users at the same time; the figure 2.3 illustrates massive MIMO uplink transmission. Signal detection at the base station is the major challenge in massive MIMO uplink transmission systems due to the huge number of antennas.

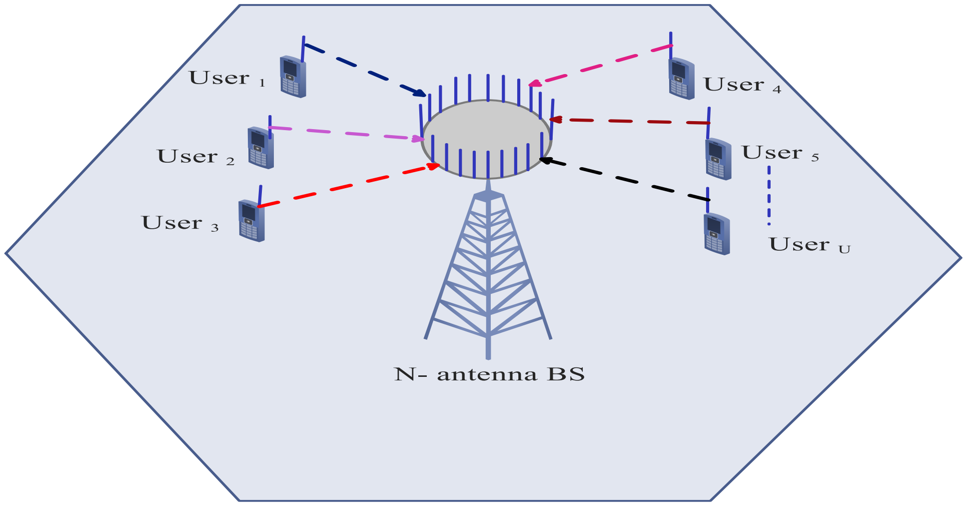

Figure 2. 3: Massive MIMO uplink transmission (X. Yang et al., 2020)

2.7 Massive MIMO Downlink System

The downlink transmission channel is used to send data from the base station to the mobile stations. The base station transmits signals to all U users in the downlink from the same time-frequency resource (Xia et al., 2017). Consider a downlink massive MIMO system in which the base station has N antennas and serves up to U mobile stations with a single antenna at the same time. The figure below shows massive MIMO downlink transmission.

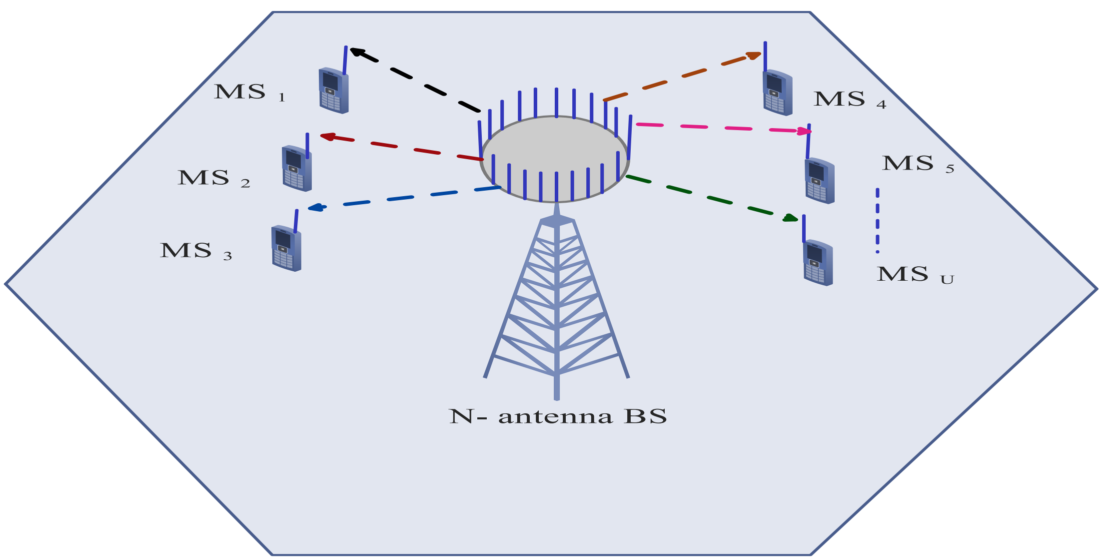

Figure 2. 4: Massive MIMO downlink transmission (Xia et al., 2017)

2.8 Massive MIMO Technology Challenges

Massive MIMO technology is more than just an extension of MIMO technology, and there are still many issues and challenges to be addressed in order to make it a reality (Chataut & Akl, 2020). Signal detection, pilot contamination, channel estimation, precoding, user scheduling, and hardware impairment are the main challenges in massive MIMO systems.

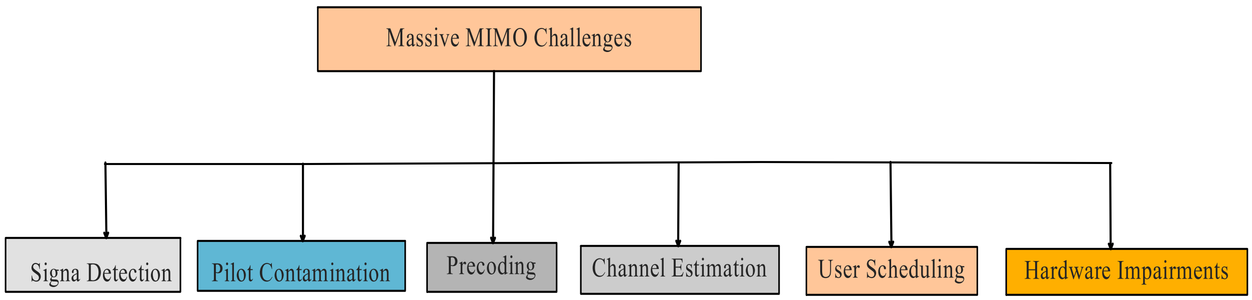

Figure 2. 5: Difficulties in Massive MIMO systems deployment

2.8.1 Signal Detection

Finding the transmitted symbol from the received signal at the base station is referred to as uplink signal detection. The signal detection for massive MIMO uplink systems becomes computationally complex due to the massive number of antennas. Figure 2.6 show signal detection for massive MIMO uplink system with U user terminals and N antennas at the base station. All of the signals sent from the U user terminal travel through different wireless paths, the noise is added at the channel on the signal and finally meet at the BS, making signal detection at the BS difficult.

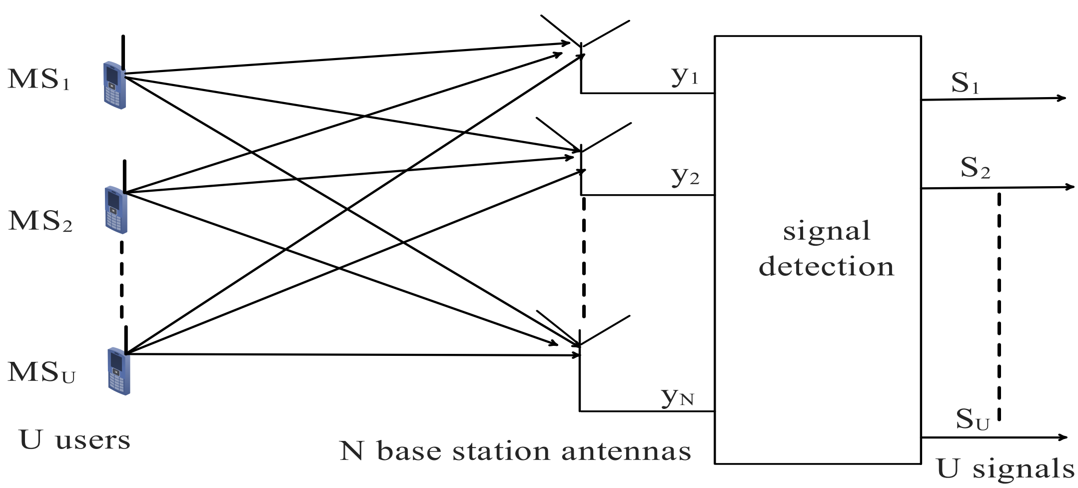

Figure 2. 6: signal detection for Massive MIMO uplink system (Dan et al., 2020)

Numerous studies have been conducted to find best signal detection algorithm for massive MIMO uplink systems, one that provides good performance while requiring less computational complexity.

In massive MIMO, a number of linear detectors, such as ZF, MF, and MMSE have been used for uplink signal detection. For massive MIMO uplink signal detection, ZF and MMSE can achieve near-optimal bit error rate (BER) performance (Dan et al., 2020). However, due to the direct and complicated matrix inversion, both the ZF and MMSE detection methods have high computational complexity. The matched filter method is simple in comparison to more complex detectors, but it performs poorly (Albreem et al., 2019). Iterative methods such as CG, GS, and OCD have been developed to avoid direct matrix inversion. The Gauss-Seidel algorithm has low computational complexity, but the performance is less as compared to ZF and MMSE detector. The use of optimized coordinate descent method yields an approximate solution with low computational complexity. The conjugate gradient method solves the system equation with low computational complexity through the nth iteration. However, the performance of both the OCD and the CG methods is inferior to that of the MMSE and ZF methods. The Neumann series expansion (NSE) method (Gustafsson et al., 2017) is used to approximate matrix inversion, which reduces the complexity of the linear detector. However, the complexity of NS increased as the number of iterations increased and it perform poorly as compared to ZF and MMSE. Table 2.1 shows the advantage and disadvantage summary of existing uplink signal detection algorithms for massive MIMO systems based on of performance and complexity.

Table 2. 1: Summary of signal detection algorithms based on advantage and disadvantage

Algorithms	Advantage	Disadvantage
MF	• Low complexity. • It works properly if the propagation matrix's columns are approximately orthogonal.	• Its performance is poor.
ZF	• It performs better.	• High computational complexity
MMSE	• It has the best performance.	• High computational complexity due to direct matrix inversion.
GS	• Low computational complexity. • If good initial solution is considered, it has good convergence.	• Less performance as compared to MMSE. • If the initial solution is not select properly it needs more number of iteration.
OCD	• It has Better performance for the large value of BUAR.	• The calculated solution contains an inverse component that increases complexity.
CG	• When the ratio of BS antennas to user antennas is large, it achieves near-optimal performance.	• It requires large number of iterations.

2.8.2 Pilot Contamination

All operating channels between the transmitter and receiver must be estimated by the massive MIMO system. The pilot signals are used to estimate the channels and must be orthogonal with a limited number of set numbers. As a result, in massive MIMO systems, one must reuse the pilots more frequently, which causes more interference between the pilots (Lu et al., 2014) as their reuse distance becomes shorter. Once two terminals are using the same pilot sequence, it results in pilot contamination. The same sequence of orthogonal pilots used in neighboring cells will interfere, and the base station will receive a linear combination of channel responses from the domestic cell and the neighboring cells. This is known as "pilot contamination," and it reduces achievable throughput, as illustrated in the figure 2.7.

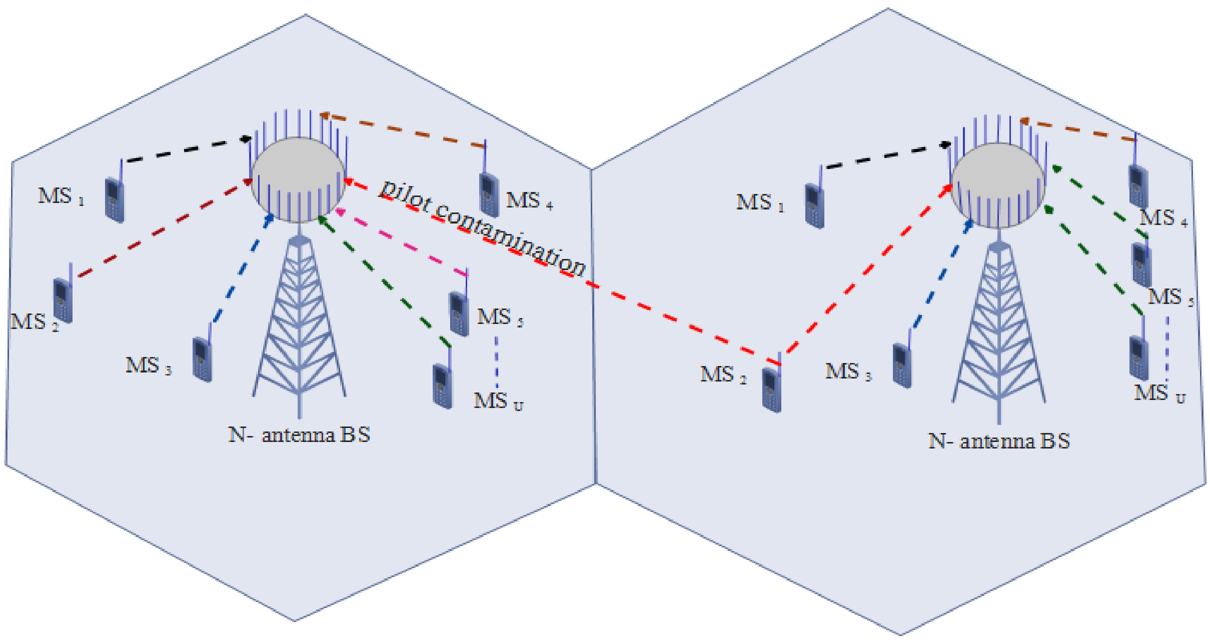

Figure 2. 7: Pilot contamination effect in Massive MIMO (Lu et al., 2014)

Several techniques, such as pilot-based estimation approaches (Appaiah et al., 2010), subspace-based estimation approaches (Van der Veen et al., 1997), pilot contamination precoding (Li et al., 2012), pilot decontamination (Mohammadghasemi et al., 2019), and blind pilot decontamination (Müller et al., 2014), have been developed to mitigate the effect of pilot contamination in massive MIMO systems.

2.8.3 Precoding

Precoding is a beamforming concept that enables multi-stream transmission in systems with multiple antennas. Precoding is a method that takes advantage of transmit diversity by weighting the data stream, i.e., the transmitter transmits the coded information to the receiver in order to gain channel knowledge. Precoding is important in massive MIMO systems because it reduces the effect of path loss and interference while increasing throughput. The base station estimates channel state information (CSI) in massive MIMO systems using uplink pilot signals or feedback from the user equipment. The performance of DL massive MIMO is dependent on the accuracy of CSI estimation and the precoding technique used. The figure 2.8 shows precoding in massive MIMO systems.

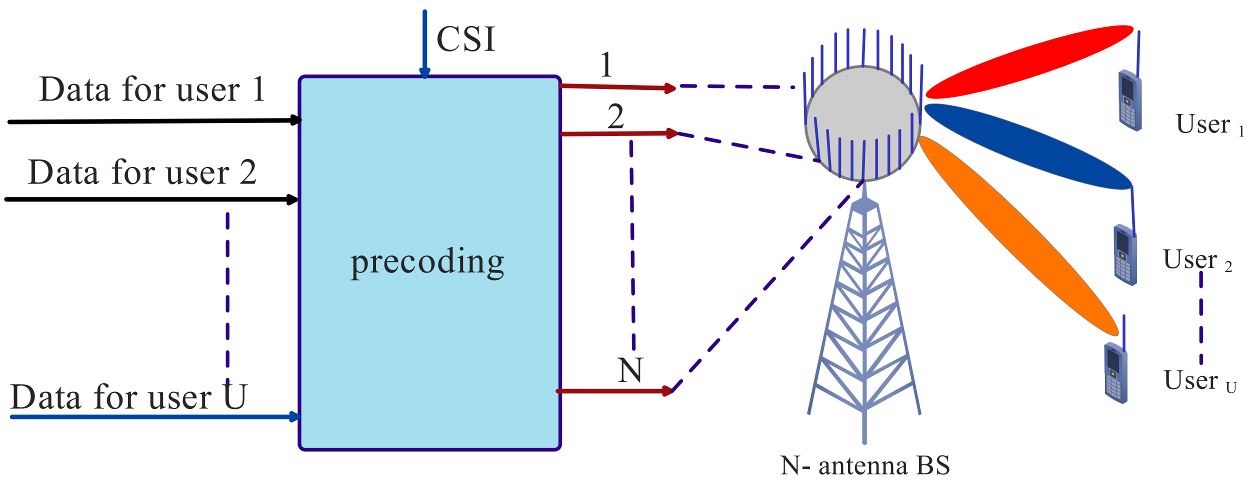

Figure 2. 8: Massive MIMO precoding with N base station antenna and U users (Mukubwa et al., 2017)

Even though the precoding method gives significant benefits to massive MIMO systems, it also increases the overall system's computational complexity by adding extra computations. The computational complexity rises in direct proportion to the number of antennas. To address this problem, several precoders have been used, including maximum ratio combination (MRC) (Xiang Gao et al., 2011), MMSE (Mukubwa et al., 2017), and ZF (Park et al., 2014)

2.8.4 Channel Estimation

In massive MIMO systems, the channel estimation technique is used to provide channel state information for precoding and decoding (MOQBEL et al., 2017). CSI is the status of the communication link between the transmitter and the receiver. This data shows how a signal travels from the transmitter to the receiver. Massive MIMO performance increases linearly with the number of transmitting or receiving antennas if the CSI is perfect. The user will send orthogonal pilot signals to the base station during uplink, and the base station will estimate the CSI to the user terminal based on these pilot signals (Lu et al., 2014). The base station will then beamform DL data towards the users' terminal based on the estimated CSI. The pilot contamination problem arises as a result of the limited number of orthogonal pilots that can be reused from one cell to the other during massive MIMO channel estimation. Several algorithms have recently been introduced for massive MIMO systems channel estimation, including Least Square (LS) (Xinyu Gao et al., 2014), MMSE (Adhikary et al., 2017), Blind Estimation (Jiang et al., 2014), Compressed Sensing (Ding et al., 2014), and Convolutional Blind Denoising (MOQBEL et al., 2017). The figure 2.9 shows the channel estimation in massive MIMO system with N base station antennas and U users antenna. y indicates the received signal at the BS and $\hat{H}$ represents the estimated channel.

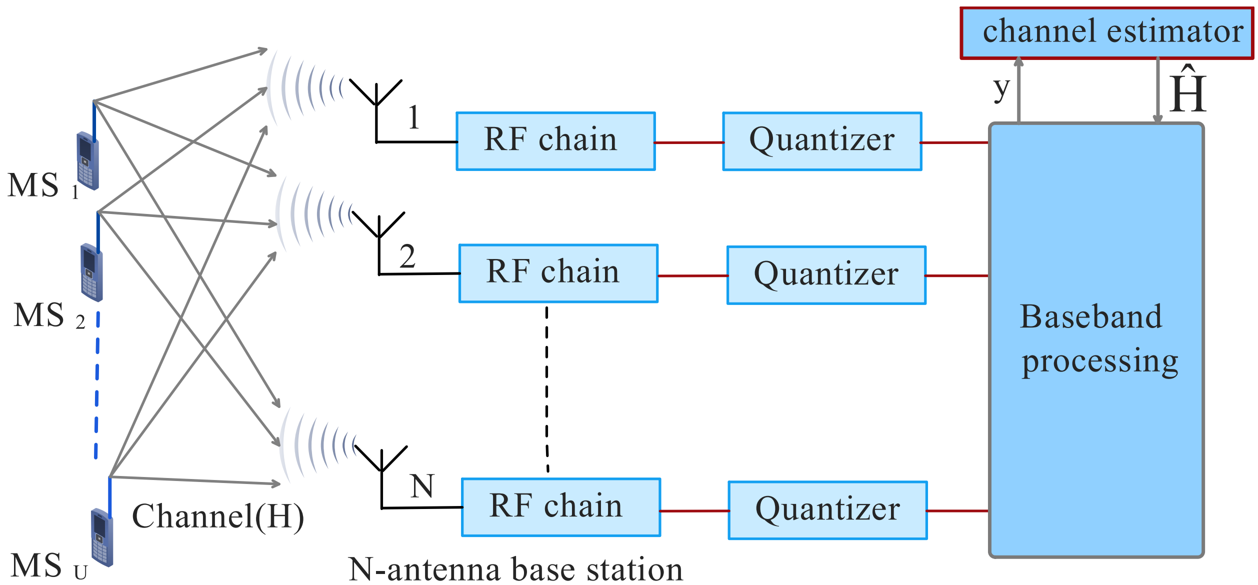

Figure 2. 9: Massive MIMO Channel estimation (MOQBEL et al., 2017)

2.8.5 User Scheduling

Massive MIMO base stations installed with a massive number of antennas can communicate with multiple users at the same time. Simultaneous communication with a large number of users leads to multi-user interference, which reduces throughput performance (Huang et al., 2021). As illustrated in Figure 2.10, precoding techniques are used during the downlink to minimize the influence of multi-user interference. If the number of users exceeds the number of antennas, a good user scheduling system has been implemented prior to precoding to obtain higher throughput and sum rate performance.

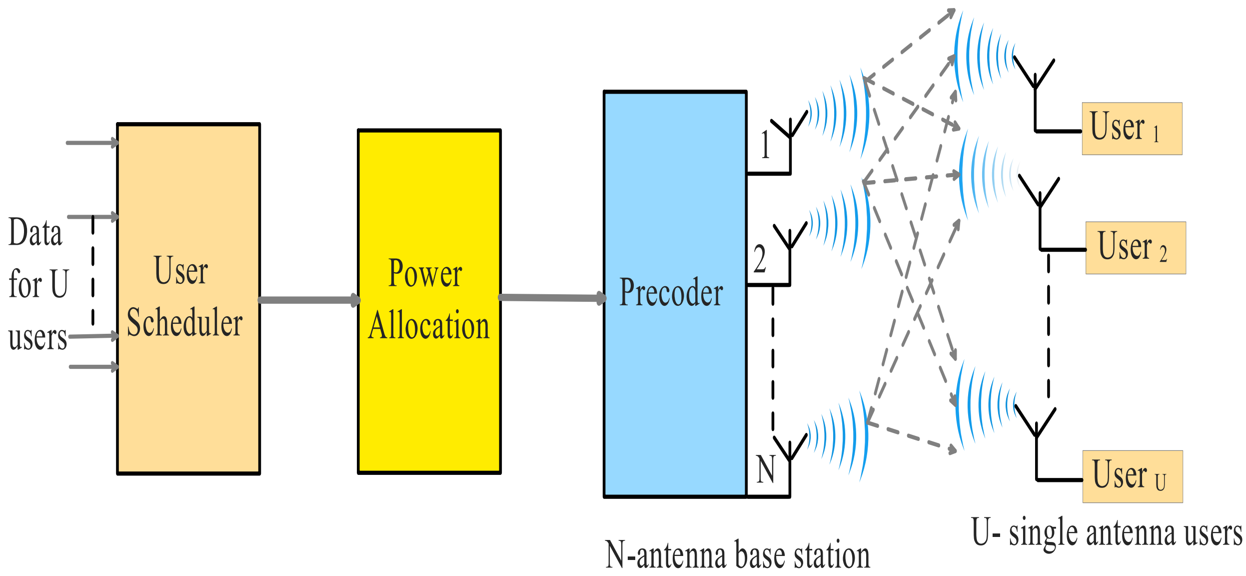

Figure 2. 10: User Scheduling in Massive MIMO (Huang et al., 2021)

Numerous studies have been conducted in order to find the best scheduling algorithm for massive MIMO. At various times, many methods have been proposed, including ZF (H. Yang, 2018), MMSE (Lyu, 2016), and Multi-user Grouping (Meng et al., 2018).

2.8.6 Hardware Impairments

To mitigate the effects of noise, fading, and interference, massive MIMO systems employ a large number of antennas (Bjornson et al., 2014). Massive MIMO's use of a huge number of antennas increases system complexity and hardware cost. To reduce computational complexity and hardware size, massive MIMO should be built with low-cost and small components. The use of a low-cost component will significantly increase hardware imperfections such as phase noise, magnetization noise, amplifier distortion, and IQ imbalance (Studer et al., 2010). These problems have a big influence on system performance. Because of the large number of antennas, there is a cooperative connection between the antenna elements, which alters the load impedance and causes distortions (Gustavsson et al., 2014). Even though massive MIMO intends to minimize radiated power by a factor of 100 compared to conventional MIMO systems, the power consumed by baseband hardware and data converters increases linearly with the number of antennas. The use of low-cost phase-locked loops (PLL) and oscillators increases the phase shift between the times when the pilot and data signals are received at each antenna, limiting the massive MIMO performance. Figure 2.11 illustrates the hardware impairment at a massive MIMO base station.

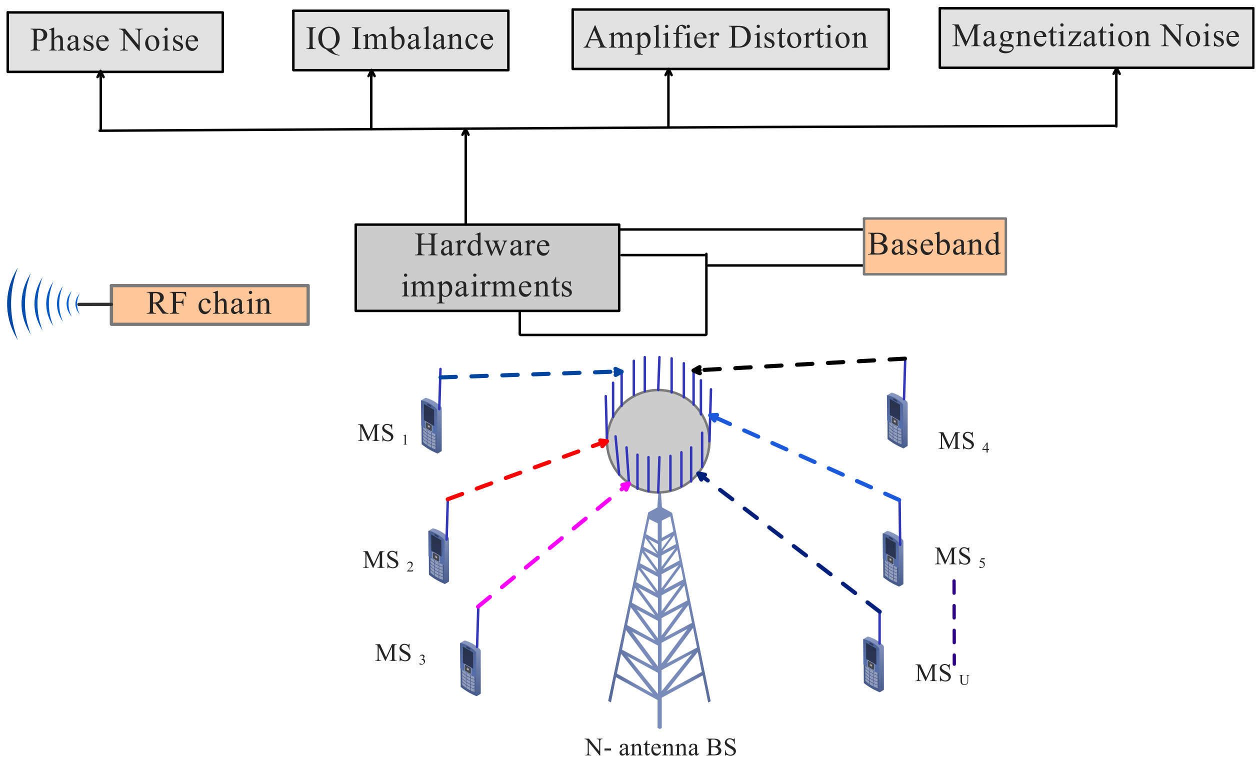

Figure 2. 11: Massive MIMO Hardware Impairments (Bjornson et al., 2014)

Even though the hardware impairment cannot be completely eliminated, its impact can be reduced by employing appropriate compensation techniques. To mitigate the effect of hardware impairments, methods such as Digital Pre-Distortion (Gustavsson et al., 2014) and Peak to Average Power Ratio (PAPR) (Björnson et al., 2014) have been used.

2.9 M-ary Quadrature Amplitude Modulation

M-ary quadrature amplitude modulation (M-QAM) is a modulation scheme that transmits data by modulating the amplitude of the data transmission using two carrier signals. These two signals, known as the in-phase (I) and quadrature (Q) components, are required for quadrature modulation to implement complex carrier amplitude and phase states (Besnoff & Ricketts, 2015). Each has the same frequency but varies in phase by 90 degrees, or one-quarter of a cycle, which is the foundation for the name quadrature. M-QAM is a technique that simultaneously combines amplitude and phase variations in a carrier. This technique enables higher data rates to be transmitted within the same bandwidth. M-QAM is commonly used for data transmission because it achieves higher levels of spectral efficiency than other types of modulation. The technique entails sending multiple bits for every time period of the carrier symbol. The term M in M-QAM refers to the number of QAM states, which is given by 2^K, where K is the number of bits per symbol. The main advantage of M-QAM modulation types is the effective use of bandwidth. This is because M-QAM represents a greater number of bits per symbol. It is utilized to attain high levels of spectrum utilization efficiency. This is performed by modulating both the amplitude and phase components. In the 5G new wireless networks, M-ary quadrature amplitude modulations have been used. 16-QAM, 64-QAM, and 256-QAM are some of the formats utilized in 5G mobile communications systems.

2.10 Additive White Gaussian Noise (AWGN) channel

AWGN is a basic noise model used in information theory to model the effect of many random processes that occur in nature. Specific characteristics are denoted by the modifiers:

- It is additive because it is added to any noise that may exist in the information system.
- White refers to the idea that the information system has uniform power across the frequency band. It is analogous to the color white, which emits uniformly across all frequencies in the visible spectrum.
- Gaussian because it has a time domain normal distribution with an average time domain value of zero.

The AWGN channel model is frequently used as a channel model in which the only impediment to communication is a linear addition of wideband or white noise with a constant spectral density and a Gaussian amplitude distribution. The AWGN channel is a well-known model for indicating line of sight (LOS) conditions. An AWGN channel adds white Gaussian noise to the signal that passes through it. The model does not take fading, frequency selectivity, interference, nonlinearity, or dispersion into account. However, it generates simple and tractable mathematical models that are useful for gaining insight into the underlying behavior of a system before considering these other phenomena (Varasteh et al., 2017).

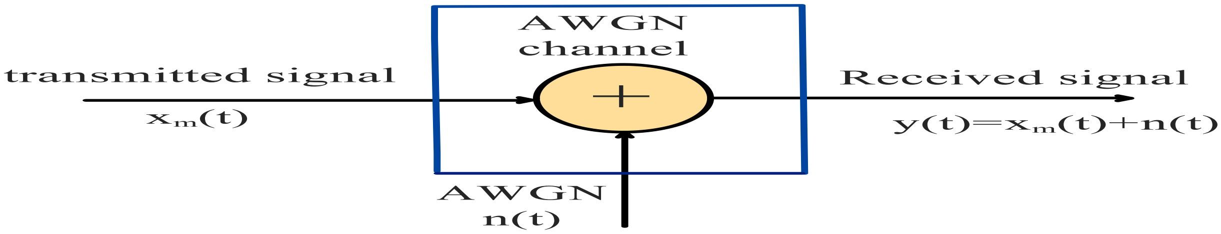

Figure 2. 12: Block diagram of AWGN channel (Varasteh et al., 2017)

2.11 Related Works

Several studies are being carried out in order to find low-complexity and high-performance signal detection algorithms for massive MIMO uplink systems. Some of them are the following:

In (Z. Wu et al., 2016), a GS based-soft detection algorithm is proposed. To accelerate the convergence rate of the conventional GS method while maintaining an acceptable overhead complexity, for initialization, the first two terms of the truncated Neumann series are used. The GS technique is used to solve the U-dimension linear problem. In this paper, the complexity of the proposed method is lowered from $O(U^3)$ to $O(U^2)$ where U represents the number of users antenna, and its performance is compared to the Cholesky decomposition approach and the NSE-based algorithm based on BER for antenna configurations of 8×128 and 16×128. The GS-based algorithm proposed here outperforms the NSE-based method.

A robust and joint low complexity detection algorithm based on the Jacobi (JA) and Gauss-Seidel methods. is suggested in (Albreem et al., 2020). The proposed technique takes advantage of the JA and GS methods' minimal complexity. The performance, complexity, and convergence rate of such iterative algorithms are greatly dependent on the initial vector. In this paper, an initial solution is presented by using the benefits of a stair matrix to achieve a fast convergence rate, high performance, and low complexity. For the base station -to-user antenna ratio (BUAR) $= \frac{160}{30}, \frac{160}{40}, \frac{160}{50}, and \frac{160}{60}$ and the number of iterations (n) =2, 3, and 4, the performance of MMSE, NS, GS, JA, and proposed methods is compared using BER parameter. The suggested technique outperforms the NS, GS, and JA methods in terms of performance.

In (Yin et al., 2014), A soft-output data detection algorithm based on conjugate gradients is used to improve error-rate performance for massive MIMO systems with medium BS-to-user antenna ratios. The conjugate-gradient is used to reduce the signal detection’s high computational complexity. To reduce complexity, a modified version of the conjugate gradient least square (CGLS) algorithm is used. In contrast to current linear detection methods for massive MIMO systems, the suggested technique eliminates two of the most complicated tasks, namely Gram-matrix calculation and matrix inversion, while still being able to calculate soft-outputs. The performance of the CGLS, Neumann, and Cholesky inversion methods is compared using block error rate (BLER) for the antenna configuration of 8×128 *and* 32×256.

A Neumann series-based detection method for massive MIMO systems over correlated rician fading is proposed in (Ghacham et al., 2017). MMSE is a linear detection technique on the receiver side that is critical in terms of implementation complexity and contributes significantly to the improvement of transmission reliability. MMSE and ZF have comparable performance and outperform maximum ratio combination (MRC), particularly in high spectral efficiency. The two received techniques such as MMSE and ZF, on the other hand, involve matrix inversion computation, and the complexity grows with the number of users. In this paper, the initial polynomial expansion iterations are used instead of the inverse calculation. As a result, the computational complexity is significantly reduced.

The adaptive damped Jacobi (DJ) technique and the conjugate gradient algorithm developed in (Dan et al., 2020) are combined into a hybrid iterative algorithm for signal detection for uplink. The CG method is utilized to offer a good search direction for the adaptive DJ algorithm, and the Chebyshev approach is employed to speed up convergence. The method avoids complicated matrix inversion operations at the start of iteration by using the CG algorithm and the DJ algorithm. The suggested method's complexity is lowered from $\mathrm{O}(U^3)\, to\, \mathrm{O}(U^2)$. The proposed algorithm's performance is compared to that of MRC, DJ, CG, Neumann and MMSE for antenna scales of 16×64 and 16×128 using the BER parameter. It outperforms methods such as the MRC, DJ, Neumann, and CG. Under the conditions of low complexity, the proposed method achieves close but not superior MMSE linear detection performance.

A linear massive MIMO detector based on Gauss-Seidel algorithm and successive over-relaxation (SOR) algorithm is proposed in (Vasudevan, 2020). In this paper, a detector is presented that is based on the combined GS and SOR techniques, with the initial solution determined by the first iteration of the GS algorithm. Following that, the SOR iterative algorithm is used to detect the signal. The performance and complexity of a suggested approach for the massive MIMO UL detector are compared to the JA, GS, and SOR methods for BUAR = 2 or 64×128 antenna configuration. Performance is shown by the BER verses the signal-to-noise ratio (SNR), while the computational complexity is represented by the number of multiplications. Numerical results show that the suggested technique reduces complexity and improves performance when compared to methods such as JA, GS, and SOR.

In (H. Wu et al., 2020), a low complexity soft output signal detection algorithm based on improved kaczmarz method is proposed, which avoids the matrix inversion operation and thus reduces complexity by an order of magnitude. Furthermore, an appropriate relaxation parameter is introduced to further enhance the suggested algorithm's convergence speed. The MMSE-based linear signal detection technique yields good performance, but it is excessively complicated due to direct matrix inversion. The proposed algorithm is designed for uplink massive MIMO systems to avoid the high dimensional matrix inversion required by the MMSE criterion. The suggested method's performance is compared with CG, Neumann, and MMSE techniques in this work, and it outperforms the CG and Neumann algorithms in terms of BER.

A Massive MIMO uplink signal detection algorithm based on the alternating direction method of multipliers (ADMM) and Huber fitting techniques is proposed in (Chataut & Akl, 2018). The ADMM technique is primarily intended for addressing convex optimization problems by breaking larger problems into smaller ones which is used for complexity reduction. It makes variable updates much easier in each iteration, and variables are updated during each iteration by solving an unconstrained convex optimization problem. Huber fitting is a robust regression method that reduces the sensitivity of the function to outliers in the data. In this work, the complexity of the proposed detector is in the order of $O(U^2)$. Therefore, the complexity is reduced as compared to ZF and MMSE detectors. The simulation results have demonstrated that the proposed technique has equivalent BER performance to existing massive MIMO detection algorithms such as ZF and MMSE.

In (Ye & Min, 2020), a block matrix-based Gauss-Seidel method is presented to enhance the convergence rate and the performance of the traditional Gauss-Seidel method for signal detection in massive MIMO uplink systems. The Block Gauss-Seidel (BGS) algorithm, which is based on the block matrix, decomposes the filter matrix to generate the split matrix, and then iteratively solves the estimated value of the transmitted signal vector. The complexity of the BGS method is lowered by one order of magnitude when compared to the MMSE algorithm. In this paper, simulation results show that the suggested algorithm improves the conventional GS technique and approaches but does not exceed the MMSE algorithm's near-optimal BER performance.

Matrix inversion is required for minimum mean squared error and zero forcing detectors, which has significant computational complexity. (Shafivulla et al., 2020) proposed a detection algorithm for massive MIMO that computes an approximate inverse using the Cayley-Hamilton theorem and has quadratic complexity in terms of the number of users. To reduce the complexity caused by matrix inversion, the Cayley-Hamilton theorem is applied. The suggested technique in this paper does not involve the calculation of the Gram matrix. To reduce the complexity caused by matrix inversion, the Cayley-Hamilton theorem is applied. The proposed method's complexity is reduced from $\mathrm{O}(U^3)$ to $\mathrm{O}(U^2)$, and its performance is comparable to that of the ZF and MMSE methods based on the BER parameter.

In (Amiri & Naeiny, 2020), low-complexity iterative detection for uplink multiuser massive MIMO systems based on the Gram Schmidt algorithm, which is used for enhancing the convergence rate is suggested. Linear detection methods such as MMSE and ZF can achieve near maximum detector performance. However, the complexity of these detectors in massive MIMO systems is high due to the need to calculate the inverse of a large dimension matrix. The Gram Schmidt technique is applied in this paper by using the MMSE detector filtering matrix. The proposed method eliminates the direct calculation of matrix inversion in the MMSE and ZF detectors. The complexity order is reduced from $\mathrm{O}(U^3) to \mathrm{O}(U^2)$ .The simulation results show that the suggested method enhances convergence speed and achieves comparable BER performance to the MMSE detector while requiring significantly less computational complexity.

Table 2. 2: Summary of Some Related works

Authors/ year	Title	Theoretical model	Proposed method	Finding	Research gap
Dan et al., 2020	Low-Complexity Hybrid Iterative Signal Detection Algorithm for Massive MIMO	At initial conjugate gradient is applied to provide effective search for Jacobi.	Hybrid of damped Jacobi and conjugate gradient method.	Complexity is reduced.	Even though complexity is reduced, the performance is less perform than MMSE Not Applicable for small BUAR.
Shafivulla et al., 2020	Low Complexity Signal Detection for Massive-MIMO Systems	Cayley-Hamilton theorem used to reduce complexity due to direct matrix inversion.	MMSE and ZF based on Cayley-Hamilton theorem.	Computational Complexity is reduced.	Still it focuses on computational complexity but the performance is not better than MMSE. Not applicable for small BUAR.
Vasudevan, 2020	Hybrid Linear Massive MIMO Detector Using Gauss – Seidel And Successive Over - Relaxa tion	The initial solution is determined by Gauss-Seidel and after that successive over relaxation	Hybrid of Gauss-Seidel and Successive over relaxation.	Complexity is reduced.	Those two algorithms are almost similar when the relaxation parameter =1. The performance of the proposed method is not

		is employed to detect the signal.			better than MMSE especially for small number of iteration.
Chataut & Akl, 2018	Huber Fitting based ADMM Detection for Uplink 5G Massive MIMO Systems	ADMM break bigger problem into smaller and Huber fitting for robust regression.	ADMM algorithm based on Huber fitting method.	Computational is complexity reduced and convergence rate improved.	Even though the complexity is reduced the Performance is not better than conventional MMSE. Not applicable for small BUAR.
Albreem et al., 2020	A robust and joint low complexity detection algorithm based on the Jacobi (JA) and Gauss-Seidel methods	Proposed technique takes advantage of the JA and GS methods' minimal complexity.	Hybrid of JA and GS methods.	Computational is complexity reduced and convergence rate improved.	Not applicable for small BUAR.

CHAPTER THREE

3. MATERIALS AND METHODS

3.1 Introduction

In this thesis, related secondary sources of data about signal detection algorithms for uplink massive MIMO systems were reviewed, including former researchers' works, different Institute of Electrical and Electronics Engineers (IEEE) articles, and journals. Researchers applied their own proposed techniques to obtain high performance and low-complexity transmitted signal detecting methods in massive MIMO uplink systems. The methodology of this study is illustrated as follows, based on inputs obtained through a review of related literature, a problem statement, and bearing in mind the problem of existing signal detection algorithms.

3.2 Materials

In this thesis work, software such as MATLAB/R2021 and ConceptDraw DIAGRAM are used. MATLAB is a programming tool that was created specifically for engineers and scientists to study and design systems and products that will change the world. ConceptDraw DIAGRAM is drawing software that includes a professional set of drawing tools, ready-to-use templates, a large object library, and a range of custom printing and file export options.

3.3 Methods

3.3.1 System Design

- Analyzing the mathematical model of various signal detection algorithms in order to calculate the detected signal.
- Developing the hybrid signal detection algorithm for massive MIMO uplink systems.

3.3.2 Simulation Methods

- Perform a BER versus SNR simulation to compare the proposed signal detection method's performance to that of other algorithms.
- Perform a performance comparison of the proposed signal detection method with other algorithms based on SER versus SNR simulation.
- Perform a performance comparison of the proposed algorithm with other algorithms using MSE versus SNR simulation.

- Perform a computational complexity comparison of the proposed method with existing methods based on the real number of multiplications versus the number of users' simulations.

3.3.3 Mathematical Model of Signal Detection Algorithms for Massive MIMO Uplink

3.3.3.1 System Model

We consider a massive MIMO system with N total numbers of antennas at the base station to serve up to U single-antenna users concurrently, where the number of users is less than the number of base station antennas. The vector x = $[x_1, x_{2,} .....x_u]^T$ represents signal transmitted by all users and the symbol vector y = $[y_1, y_2 ...y_N]^T$ represents signal received at the base station. The received data is typically influenced by the channel effect and Gaussian noise (w). The channel matrix (H) entries are assumed to be independent and identically distributed (i.i.d) Gaussian random variables with mean, variance (δ^2) and $N \times U$ size. The detection model is determined by y, x, H and w, where w is additive white Gaussian noise. y is defined as;

$$y = Hx + w \tag{3.1}$$

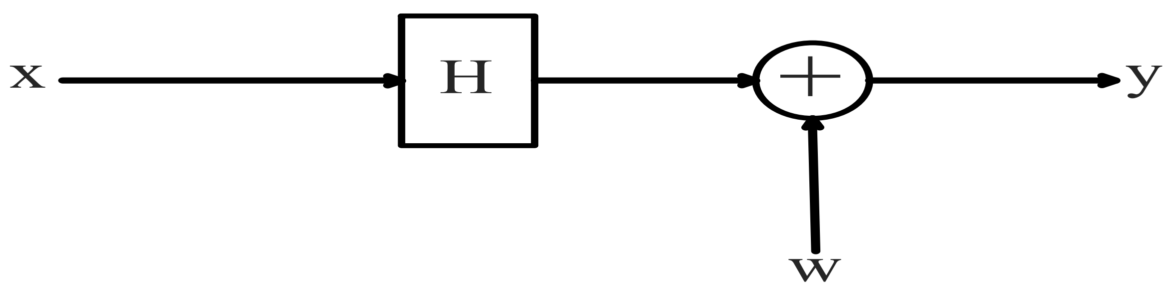

Figure 3. 1: System model

The figure 3.1 illustrates the system model of a massive MIMO uplink transmission system. While traveling via the communication channel, the transmitted message signal x is multiplied by the channel matrix H, and the noise is added to the transmitted message signal.

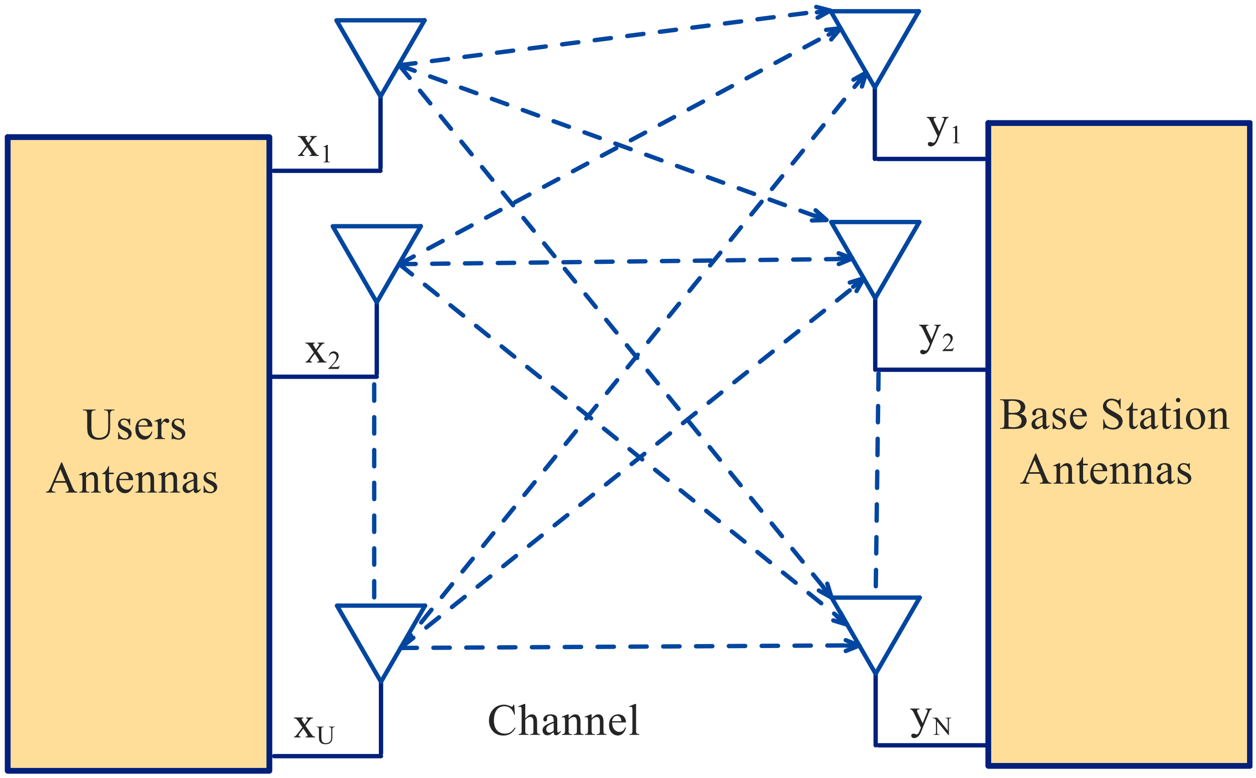

Figure 3. 2: Massive MIMO uplink transmission system

The figure 3.2 demonstrates the uplink transmission of massive MIMO system equipped with N antenna BS supporting U single-antenna users. In massive MIMO systems, detection at the base station is essential to distinguish the signal transmitted by each user from the received signal. The number of BS antennas is greater than the number of user antennas. Due to the enormous number of antennas in massive MIMO systems, uplink signal detection becomes computationally complex, lowering the possible throughput. There are various methods for detecting received signals, but in order to achieve higher performance, we need an efficient detector with manageable processing complexity. The main issues in signal detection algorithms for massive MIMO uplink systems are performance and complexity. Signal detection techniques in a massive MIMO system have a significant impact on overall system performance. In comparison to existing MIMO systems, base stations in the massive MIMO system are configured with a large number of antennas, resulting in a massive amount of data being created, putting increased demands on RF and baseband processing techniques. The massive MIMO detection algorithms are expected to have high performance and low computational complexity, but it faced challenges in finding such detection algorithms. The figure below shows signal detection for an uplink massive MIMO system with N base station antennas and U single antenna users. The following sections examine the most commonly used signal detection methods.

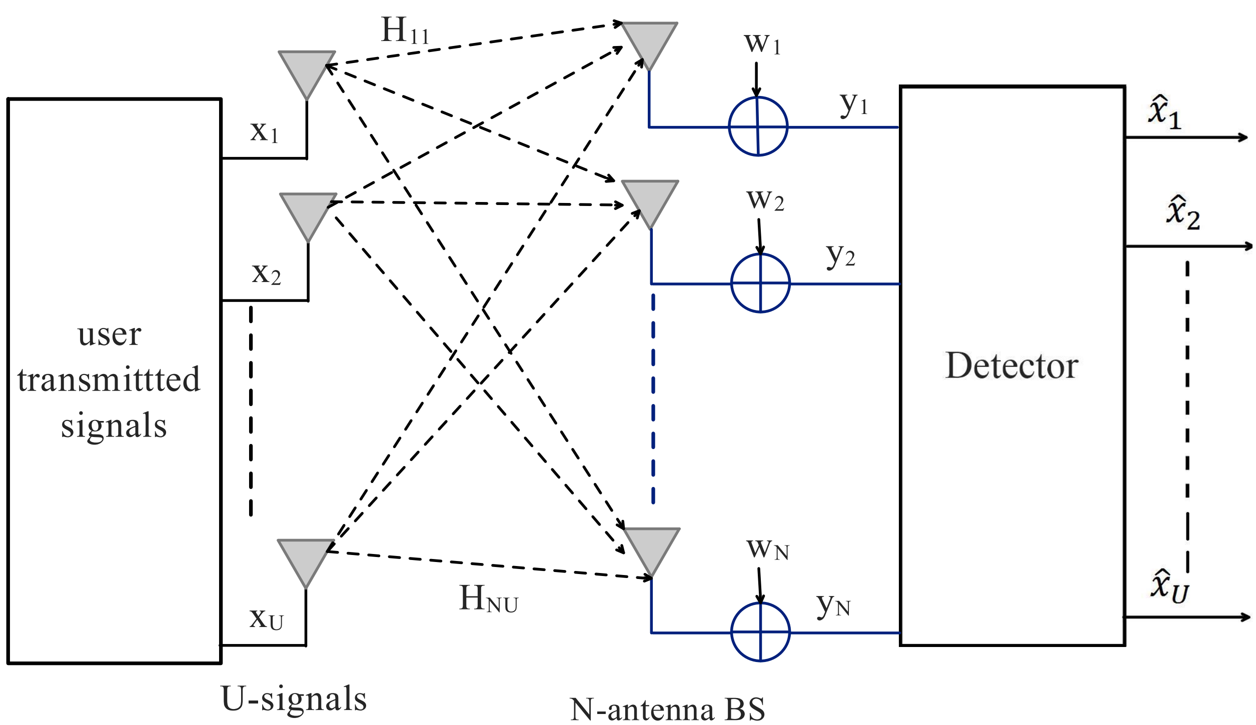

Figure 3. 3: Signal detection of massive MIMO uplink systems

3.3.3.2 Matched Filter Algorithm

By setting A=H, where A is the equalization matrix, the matched filter treats interference from other sub-streams as pure noise. Using MF, the estimated received signal is given by (Albreem et al., 2019):

$$x_{MF} = H^H y \tag{3.2}$$

When the number of user is significantly smaller than the number of antennas in the base station, it performs well, but as the number of user grows larger, it performs poorly compared to more complicated detectors.

3.3.3.3 Zero Forcing Algorithm

Zero forcing is a typical linear detection algorithm that deforms the channel matrix H to convert massive MIMO uplink signal detection into a linear matrix equation solution, which is

$y = Hx$. The zero forcing mechanism works by inverting the channel matrix H and so eliminating the channel effect. The received signal and the transmitted signal are related using equation (3.1) according to the massive MIMO system model. The ZF detection technique of massive MIMO is to concurrently left multiply both sides of Eq. (3.1) by the conjugate transpose H^H of the channel matrix, neglecting the additive noise w, to obtain Eq. (3.3).

$$H^H y = H^H Hx \tag{3.3}$$

Know multiply Eq. (3.3) by $(H^H H)^{-1}$ (Ghacham et al., 2017), then the equation becomes.

$$x = (H^H H)^{-1} H^H y = (H^H H)^{-1} y_{MF} \tag{3.4}$$

Where $y_{MF} = H^H y$

The detection of the transmitted signal x has been implemented. However, there is an error in Eq. (3.4) due to the presence of additive noise w. Based on the prior concept, the transmitted signal x can be calculated by a matrix A, causing Eq. (3.5) to hold.

$$\hat{x} = Ay \tag{3.5}$$

Where $A = (H^H H)^{-1} H^H$

Where $\hat{x}$ is the estimated transmitted signal, in this manner, massive MIMO linear detection is translated into matrix A estimation. The ZF is a widely used linear detection technique. Its fundamental idea is to neglect the additive noise w in the massive MIMO channel model in the analysis. However, because noise is frequently not negligible in real-world situations, the result achieved by employing this approach may not be the optimal solution. Since ZF algorithm involves direct matrix inversion the computational complexity is high.

3.3.3.4 Minimum Mean Square Error Algorithm

The minimum mean square error detector's main goal is to minimize the mean-square error (MSE) between the transmitted signal x and estimated signal. The MMSE detection technique is another linear detection algorithm. Its primary principle is to get the estimated signal $\hat{x} = Ay$ as close to the true value as possible. The objective function used in the MMSE detection technique is (Trimeche et al., 2012)

$$A_{MMSE} = \arg\min_{A} E\|x - Ay\|^2 \tag{3.6}$$

The following equation can be found by solving the matrix A using Eq. (3.6) (Trimeche et al., 2012):

$$A_{MMSE} = \arg\min_A E\|x - Ay\|^2$$

$$= \arg\min_A E\{(x - Ay)^H (x - Ay)\}$$

$$= \arg\min_A E\{tr[(x - Ay)(x - Ay)^H]\}$$

$$= \arg\min_A E\{tr[xx^H - xy^H A^H - Ayx^H + Ayy^H A^H]\} \tag{3.7}$$

Calculate the partial derivatives for Eq. (3.7) (Trimeche et al., 2012) and set them to zero to obtain

$$\frac{\partial tr[xx^H - xy^H A^H - Ayx^H + Ayy^H A^H]}{\partial w} = 0 \tag{3.8}$$

We can obtain by solving Eq. (3.8) (Trimeche et al., 2012)

$$A = (H^H H + \delta^2 I_U)^{-1} H^H \tag{3.9}$$

$$\hat{x}_{MMSE} = Ay = (H^H H + \delta^2 I_U)^{-1} H^H y \tag{3.10}$$

Where δ^2 is the noise variance, which is defined as $\frac{N_0}{E_s}$, N_0 is the noise spectral density, and E_s is the spectral density of the signal.

The matrix inverse is involved in both the ZF detection algorithm and the MMSE detection algorithm. In a massive MIMO system, the scale of the channel matrix H is usually very enormous. However, matrix inversion is more complex, which increases the computing complexity. Many techniques have been proposed to lower the algorithm complexity in order to avoid the enormous complexity of matrix inversion. To avoid direct matrix inversion, iterative algorithms such as CG, OCD, and GS have been developed.

3.3.3.5 Gauss-Seidel Algorithm

The Gauss-Seidel algorithm, also known as the successive displacement method, is used to solve the linear system depicted in equation (3.1). The GS method decomposes the equalization matrix **A** of MMSE algorithm into a diagonal matrix (**D**), an upper triangular matrix (**U**), and a lower triangular matrix (**L**).

$$A = D + L + U \tag{3.11}$$

The GS method converges quickly, if good initialization is considered. The estimated signal using GS algorithm written as (Vasudevan, 2020).

$$\hat{x}_{(n)} = (D - L)^{-1}(y_{MF} + U\hat{x}_{(n-1)})\text{, n = 1, 2……} \tag{3.12}$$

Where $y_{MF} = H^H y$ and n represents the number of iterations. The initial solution is determined based on the diagonal matrix.

$$\hat{x}_{(0)} = D^{-1} y_{MF} \tag{3.13}$$

Because there is no direct matrix inversion in the GS method, the complexity is lower than in the ZF and MMSE algorithms.

3.3.3.6 Conjugate Gradient Algorithm

Another method for solving linear equations using n iterations is the conjugate gradients method. The signal calculated using the CG technique is written as (Yin et al., 2015):

$$\hat{x}_{(n+1)} = \hat{x}_{(n)} + \alpha_{(n)} p_{(n)} \tag{3.14}$$

Where n is the number of iterations, $\alpha_{(n)}$ is a scale parameter, $p_{(n)}$ is the conjugate direction with respect to A. $p_{(n)}$ can be related with equalization matrix A as follow:

$$(p_{(n)})^H A p_{(j)} = 0 \tag{3.15}$$

$\alpha_{(n)}$ can be calculated in Eq. (3.16)

$$\alpha_{(n)} = \frac{(r_{(n)}, r_{(n)})}{(Ap_{(n)}, r_{(n)})} \tag{3.16}$$

Here, r is the residual vector, which is given by Eq. (3.17) (Yin et al., 2015)

$$r_{(n+1)} = r_{(n)} + \alpha_{(n)} A p_{(n)} \tag{3.17}$$

Equation 3.15 is applicable for $n \neq j$. The linear matrix equation can solve using the CG technique. As a result, this approach may be used to detect massive MIMO signals. However, the traditional CG algorithm still has significant flaws. To start with, while each element in the vector can be multiplied and accumulated in parallel with each row element of the matrix when matrix times vector, there is a good data dependence between the steps in the original algorithm, so the computation must be done step by step according to the algorithm's order and the degree of parallelism is low (Yin et al., 2015). Second, the conventional CG technique does not provide information about the beginning value of iteration, yet the zero vectors is commonly employed in an iteration. Obviously, a zero vector can only satisfy the constraints that are achievable, but it is not optimal. As a result, finding a better initial iterative value can cause the algorithm to converge faster and reduce the number of iterations, lowering the algorithm's computational complexity indirectly.

3.3.3.7 Optimized coordinate descent Algorithm

Optimized coordinate descent is a low complexity iterative approach for inverting a high dimensional linear system. Using a sequence of simple, coordinate wise updates, it achieves an approximate solution to a wide number of convex optimizations. The estimated solution is as follows (M. Wu et al., 2016):

$$\hat{x}_n = (\|h_{(n)}\|_2^2 + N_o)^{-1} h_{(n)}{}^H (y - \sum_{j \neq n} h_j x_j) \tag{3.18}$$

The Eq. (3.18), is computed sequentially for each user, u = 1...U with the new result applied immediately to the u_{th} user in subsequent stages. These methods will be performed for a total of n iterations.

3.3.4 Proposed Method

The main issues for transmitted signal detection algorithms in massive MIMO systems are performance and complexity. The performance-complexity profiles as well as the convergence rate are influenced by the initialization of detection algorithms. The proposed method takes MMSE equalization matrix and applies cholesky decomposition to it, then uses the ADMM technique on this decomposed matrix to solve the system for the first iteration to obtain good initialization, and then the GS algorithm is applied. The GS algorithm has a low complexity and a high rate of convergence if appropriate initial solution is selected. Based on the diagonal matrix, the starting solution is computed. The ADMM technique is an iterative strategy for solving an issue by breaking it down into smaller problems. ADMM makes variable updates easier in each iteration, and variables are updated throughout each iteration by solving convex optimization problem. It is a well-known numerical method for solving convex optimization problems with convex objective functions and constraints. ADMM combines the decomposability of the dual ascent technique with the improved convergence qualities of the multiplier method. A constrained convex optimization problem in general:

Minimize $f(x)$ subject to $x \in C$ (Boyd et al., 2011)

With a variable, $x \in \Re$ can be rewritten in ADMM form as

Minimize $f(x) + g(z)$, subject to $x = z$

where g is a convex set of C indicator functions. This problem's scaled ADMM form is (Boyd et al., 2011)

$$x_{n+1} = \arg\min_x \left\{ f(x) + \frac{\rho}{2} \|x - z_n + u_n\|_2^2 \right\}$$

$$z_{n+1} = \arg\min_z \left\{ g(z) + \frac{\rho}{2} \|x_{n+1} - z + u_n\|_2^2 \right\}$$

$$u_{n+1} = u_n + x_{n+1} - z_{n+1}$$

where u is the dual variable that has been scaled. In this case, the x-update includes minimizing f, whereas the z-update entails minimizing g. The z update can be stated as g is an indicator function of a closed nonempty convex set C (Boyd et al., 2011)

$$z_{n+1} = \arg\min_z \left\{ g(z) + \frac{\rho}{2} \|z - v\|_2^2 \right\} = \prod\nolimits_C (v) \tag{3.19}$$

Where $v = x_{n+1} + u_n$ a constant vector for z-update is purposes and $\prod_C (v)$ is the Euclidean projection onto C. As a result, the scaled ADMM problem may be expressed as (Shahabuddin et al., 2021)

$$x_{n+1} = \arg\min_x \left\{ f(x) + \frac{\rho}{2} \|x - z_n + u_n\|_2^2 \right\}$$

$$z_{n+1} = \prod\nolimits_C (x_{n+1} + u_n)$$

$$u_{n+1} = u_n + x_{n+1} - z_{n+1}$$

Box convex optimization problem is given by:

$$\hat{x}_{BOX} = \arg\min_{x \in C_{\mathrm{O}}^U} \|y - Hx\|_2^2 \tag{3.20}$$

We rewrite (3.20) into the following equivalent form (Shahabuddin et al., 2021)

$$\min_{x,z \in C^U} imize \frac{1}{2} \|y - Hx\|_2^2 + g(z) \text{ subject to } z = x \tag{3.21}$$

Where g(z) is the indicator function for the convex set C_{O} defined by

$$g(z) = \begin{cases} 0, if z \in C_{\mathrm{O}}^U \\ \infty, otherwise \end{cases}$$

The augmented Lagrangian for the problem in (3.21) is (Shahabuddin et al., 2021)

$$L_\beta(x, z, \lambda) = \frac{1}{2} \|y - Hx\|_2^2 + g(z) + \frac{\beta}{2} \|z - x - \lambda\|_2^2 \tag{3.22}$$

where λ is the scaled dual variable associated with the constraint z = x and $\beta > 0$ is a suitable regularization parameter. We can now utilize ADMM to solve the augmented Lagrangian over x and z. In concrete terms, the procedure is as follows:

$$\hat{x}_{n+1} = \arg\min_{x} L_{\beta}(x, z_n, \lambda_n)$$

$$\hat{z}_{n+1} = \arg\min_{z} L_{\beta}(\hat{x}_{n+1}, z, \lambda_n)$$

$$\lambda_{n+1} = \lambda_n + \hat{z}_{n+1} - \hat{x}_{n+1}$$

In the first stage of the ADMM iteration, we minimize x while keeping z constant. To compute the first step of ADMM, we take the derivative of (3.22) with respect to x and set it to zero.

$$H^H(y - Hx) - \beta(z - x - \lambda) = 0$$

$$\hat{x} = (H^H H + \beta I)^{-1}(H^H y + \beta(z - \lambda)) \tag{3.23}$$

Here, $A = H^H H + \beta I$ is the equalization matrix in MMSE algorithm with β is the scaled form of $\delta^2 I$ and $H^H y = y_{MF}$ .In this case, we used the Cholesky decomposition to get the matrix's inverse in order to avoid direct matrix inversion, which is a decomposition of the form:

$$A = LL^H$$

$$A^{-1} = (L^{-1})^H * L^{-1}$$

Equation (3.23) indicates the MMSE with ADMM technique, it is important to note that setting z and λ to zero at (3.23), gives us the linear MMSE equalization, but in this thesis z in initialized based on diagonal matrix. This technique used to obtain good initial point for GS method at the first iteration. The z update step is denoted as (Shahabuddin et al., 2021)

$$\hat{z} = \arg\min_{z \in C_O^U} \left(\frac{\beta}{2}\right) \left\| z - (\hat{x} + \lambda) \right\|_2^2 \tag{3.24}$$

Equation (3.24) is an orthogonal projection of $\hat{x} + \lambda$ onto the convex C_O^U .

By substituting the Cholesky decomposed matrix in Eq. (3.23), we obtain

$$\hat{x} = (L^{-1})^H L^{-1}(H^H y + \beta(z - \lambda)) \tag{3.25}$$

Equation (3.25) is used to reduce the complexity because it avoids the direct matrix inversion computation in the MMSE algorithm and to obtain a good initial point at the first iteration, which is used as an input to the GS algorithm for the remaining iterations.

The proposed detector's block diagram is depicted in Figure.

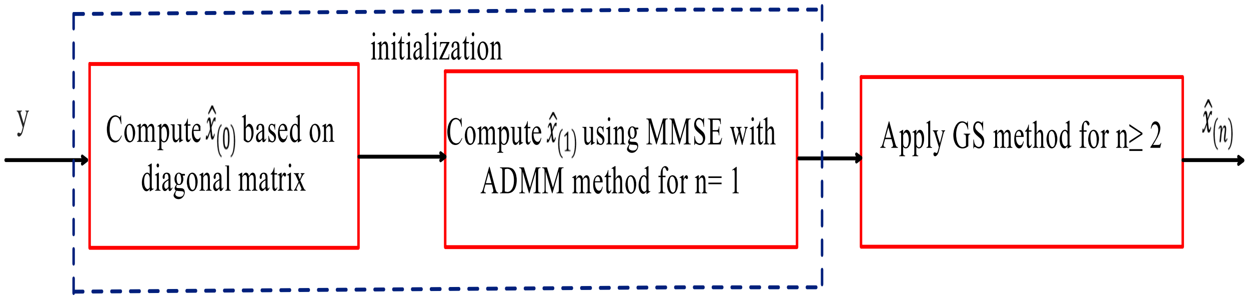

Figure 3. 4: Block diagram of proposed detector based on MMSE with ADMM technique and GS method

The proposed detector has two stages: initialization and detection, as shown on the above figure. The general steps of the proposed detector are as follows:

Step 1: the initial solution $\hat{x}_{(0)}$ is calculated based on diagonal matrix as follows indicated in equation (3.13):

$$\hat{x}_{(0)} = D^{-1} y_{MF}$$

Where $y_{MF} = H^H y$

Step 2: use the MMSE with ADMM method with n=1, where n denotes the number of iteration required to obtain the lowest BER, MSE and SER. Compute the first iteration solution $\hat{x}_{(1)}$ using equation (3.25) as follows:

$$\hat{x} = (L^{-1})^H L^{-1}(H^H y + \beta(z - \lambda)), \text{ where n=1}$$

Where β is a scaled version of $\delta^2 I$, $z = \hat{x}_{(0)}$ and λ is initialized with zero vector.

Step 3: Apply the GS algorithm where $n \geq 2$ as shown in (3.12) to estimate the transmitted signal.

$$\hat{x}_{(n)} = (D - L)^{-1}(y_{MF} + U\hat{x}_{(n-1)}), \text{ where n=2,3 ….}$$

The flowchart of the proposed detector's two steps, initialization and final detection, is shown in figure below.

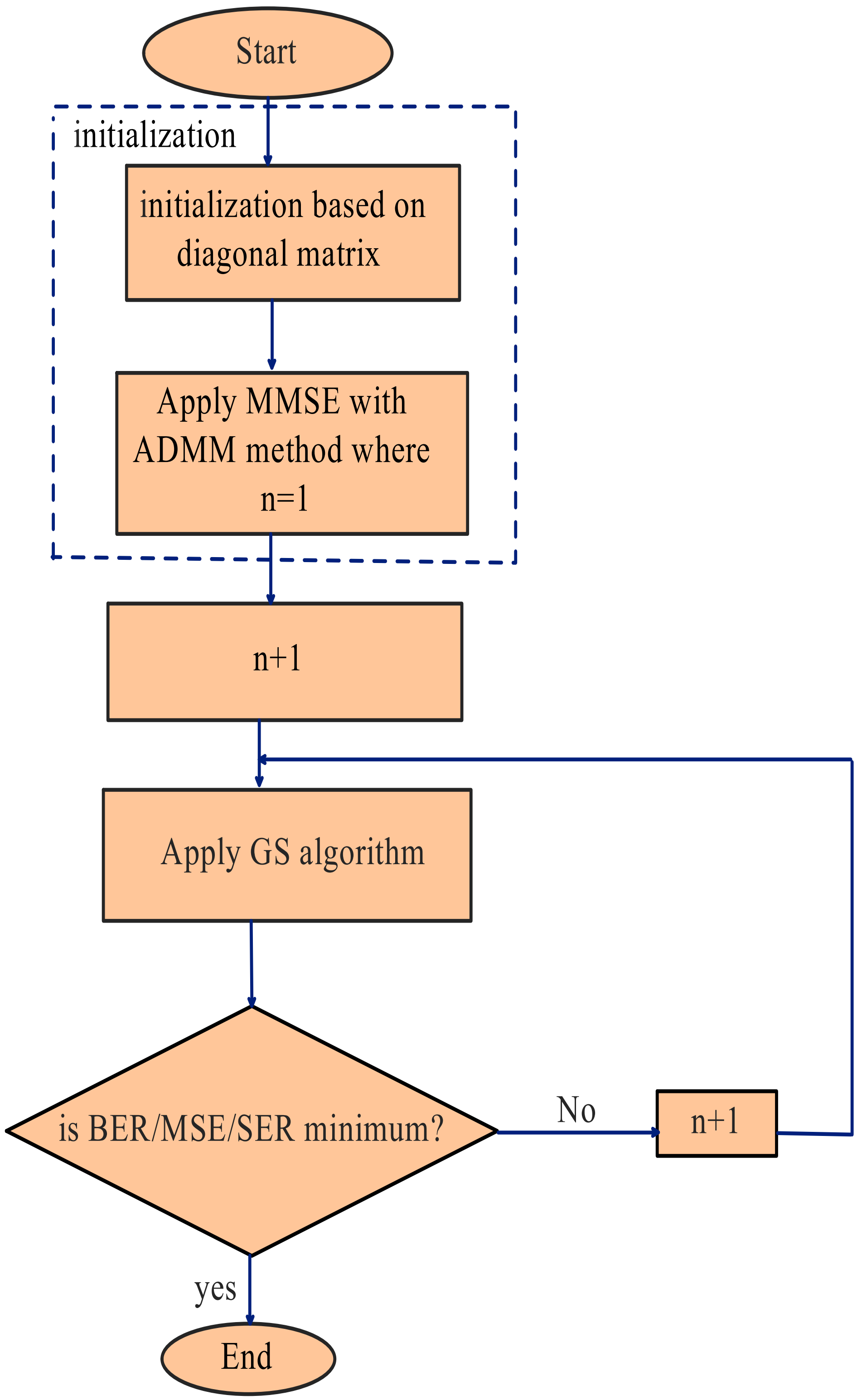

Figure 3. 5: Flowchart of proposed detector based on MMSE with ADMM technique and GS method

Algorithm 1: proposed detection method based on hybrid MMSE with ADMM and GS methods

Inputs: y, H, N_O, n, and E_s

Output: detected signal $\hat{x}$

Initialization:

λ =0

$\beta = N_O / E_s$

$A = H^H H + \beta I_U$

$A = LL^H$

D = daig(A), U = -triu(A), L = -tril(A)

$y_{MF} = H^H y$

Initial detection:

$z_{(0)} = \hat{x}_{(0)} = D^{-1} y_{MF}$

$\hat{x}_{(1)} = (L^{-1})^H L^{-1}(y_{MF} + \beta(z_{(0)} - \lambda))$

Iteration:

for i =2 : 1 : n

$\hat{x}_{(n)} = (D - L)^{-1}(y_{MF} + U\hat{x}_{(n-1)})$

end

Return $\hat{x}$

3.3.4.1 Computational complexity of proposed method

Computation complexity of the algorithm is largely depends on the total number of multiplication and division requires in the algorithm. To drive the multiplication complexity of the proposed algorithm considers the formulas that used in Algorithm 1:

$\hat{x}_{(1)} = (L^{-1})^H L^{-1}(y_{MF} + \beta(z_{(0)} - \lambda))$, in this formula U number of division is required to find $(L^{-1})^H$ and again U number of division is required to find (L^{-1}), and for the multiplication between $(L^{-1})^H$ and L^{-1} , U^2 computation is required, then for $(L^{-1})^H L^{-1}$, $U+U+U^2=U^2+2U$, computation is required, where U is the number of users. Since $\beta(z_{(0)}-\lambda)$ is scalar computation its computational complexity is negligible. Again to multiply, $(L^{-1})^H L^{-1}$ and $y_{MF}+\beta(z_{(0)}-\lambda)$, U^2 additional computation is required. Then for computing, $\hat{x}_{(1)}=(L^{-1})^H L^{-1}(y_{MF}+\beta(z_{(0)}-\lambda))$, $U^2+U^2+2U=2U^2+2U$ computation is required. U real number of divisions are required to compute the inverse diagonal matrix (D^{-1}) for finding $\hat{x}_{(0)}$. For the first iteration, $2U^2+2U+U=2U^2+3U$ number of multiplications is required. Then the remaining n-1 iterations solution is calculated based on GS method, which is defined by $\hat{x}_{(n)}=(D-L)^{-1}(y_{MF}+U\hat{x}_{(n-1)})$. To find $(D-L)^{-1}$, U^2 multiplications is required. To compute $y_{MF}+U\hat{x}_{(n-1)}$, $2U^2$ multiplications computation is required. Again, to multiply $(D-L)^{-1}$ and $y_{MF}+U\hat{x}_{(n-1)}$, U^2 multiplications computation is required. Then for each iteration $2U^2+U^2+U^2=4U^2$ multiplications is required. Since there are $n-1$ iterations, then total computational complexity for GS method is given by $(n-1)4U^2=4nU^2-4U^2$. Then the total computational complexity of the proposed algorithm becomes:

$$\begin{aligned}&4nU^2-4U^2+2U^2+3U\\&=4nU^2-2U^2+3U\end{aligned} \tag{3.26}$$

Where U indicates the number of Users and n represents the number of iteration

3.4 Performance Metrics of Signal Detection Algorithm

The performance of signal detection algorithms in massive MIMO uplink systems can be measured using metrics such as MSE, BER, and SER.

3.4.1 Mean Squared Error (MSE)

Mean squared error (MSE) is employed as a performance parameter to demonstrate the detector's efficiency. The MSE of a detector is the average of the squares of the errors that is, the average squared difference between the detected and actual values. Let x be the original transmitted signal and $\hat{x}$ represents the detected signal, MSE is given as:

$$MSE=\frac{1}{U}\sum_{k=1}^{U}(x-\hat{x})^2 \tag{3.27}$$

Where U is the number of users in a base station,

3.4.2 Bit Error Rate (BER)

The bit error rate (BER) in telecommunication transmission is the percentage of received bits that have errors relative to the total number of transmitted bits in a communication. BER is a critical parameter for assessing the performance of signal detection algorithms. BER is the ratio of the number of detected bits with errors to the total number of transmitted bits.

$$\text{BER}=\frac{\text{No.of bits in error}}{\text{Total No. of transmitted bits}} \tag{3.28}$$

3.4.3 Symbol Error Rate (SER)

In a communication system, the symbol error rate represents the probability of receiving a symbol with an error. A symbolic error rate is expressed as the product of BER and the number of bits in a symbol.

$$\text{SER}=\frac{\text{No. of symbols in error}}{\text{Total No. of transmitted symbols}} \tag{3.29}$$

3.4.4 Signal-to-Noise Ratio (SNR)

The signal-to-noise ratio (SNR) in a digital communication system is defined as the ratio of signal power in a symbol p_S to noise power p_W. A SNR is a measure of the strength of the desired signal in comparison to background noise (undesired signal).

$$SNR = \frac{p_S}{p_W} \tag{3.30}$$

Alternatively, signal-to-noise ratio also can be calculated in terms of symbol energy and power spectral density of noise (N_O) which used in this thesis work is given by:

$$\text{SNR}=\frac{E_S}{No} \tag{3.31}$$

In addition, energy of symbol is given by:

$$E_S = \frac{1}{Ns}(sum(abs(x)^2) \tag{3.32}$$

Where N_S indicates the total number of symbol and x the transmitted signal.

CHAPTER FOUR

4. RESULTS AND DISCUSSIONS

The simulation results to achieve the study's specific objective are presented in this chapter. The simulation results and discussions on the performance of the proposed detector and other detectors for massive MIMO uplink signal detection based on BER, SER, MSE, and SNR parameters under AWGN channel are provided. In addition, the complexity of the proposed detector and other detectors based on real number of multiplications is presented. The simulation parameters used in this thesis work to evaluate the performance and complexity of proposed signal detection algorithm with other algorithms for massive MIMO uplink signal detection are listed in the table below.

Table 4. 1: Simulation parameters

No.	Simulation parameters	Type and Value	comment
1	Modulation schemes	8-QAM, 16-QAM,32-QAM and 64-QAM	
2	Channel	AWGN	
3	Noise	AWGN	
4	SNR Range	0dB to 30dB	
5	BER range	1 to 10^{-4}	
6	SER range	1 to 10^{-4}	
7	MSE range	1 to 10^{-4}	
8	Number of users	64,80, 120, and 128	Based on $1<\text{BUAR}\leq 2$
9	Number of Base Station antenna	120, 128, 180, and 256	Based on $1<\text{BUAR}\leq 2$
10	Number of iteration	n = 2,3,4 and 5	

4.1 Performance comparison of the proposed detector and other detectors

In order to evaluate the performance comparison between the proposed detector and other existing detectors, parameters such as Bit Error Rate, Symbol Error Rate, and Mean Squared Error are considered.

4.1.1 Performance comparisons of the proposed detector with other detectors based on Bit Error Rate

The transmission channel is set to additive white Gaussian noise(AWGN) channel, the noise is independent and identically distributed additive Gaussian white noise, and the baseband signal modulation techniques are 8-QAM, 16-QAM, 32-QAM and 64-QAM, respectively, in order to simulate the performance. The antenna scale is set to 80x120 (BUAR=1.5), 120x180 (BUAR=1.5), 64x128 (BUAR=2) and 128x256 (BUAR = 2), where the first number indicates the number of MS user's antennas, and the second number represents the number of base station antennas, with n representing the number of iterations. The simulation results compare the performance of the proposed algorithm with that of recently introduced Massive MIMO (M-MIMO) uplink detectors. The performance is shown in terms of bit error rate versus signal to noise ratio. MATLAB software is used to generate simulation results.

Figure 4.1 compares the proposed algorithm's BER to that of other currently available methods for an 80x120 (BUAR = 1.5) antenna arrangement utilizing 8QAM modulation and n=2 iterations. At n=2, the proposed algorithm outperformed MMSE and GS, whereas other methods require more iterations. The proposed algorithm achieved a BER = 3.33×10^{-5} at signal to noise ratio (SNR) = 21dB, whereas the GS algorithm achieved a BER = 5.55×10^{-2} at the same SNR = 21dB and the MMSE algorithm achieved a BER = 7.50×10^{-5} at the same SNR. The detectors based on MF, and conjugate-gradient methods perform the worst. The detectors based on OCD and GS methods perform moderately well. The detectors based on MMSE and ZF algorithms have good performance but the computational complexity is very high. The proposed algorithm outperformed from those methods with only two iterations. The detectors such as CG and OCD require a large number of iterations to obtain moderate performance, but it causes an increase in computational complexity.

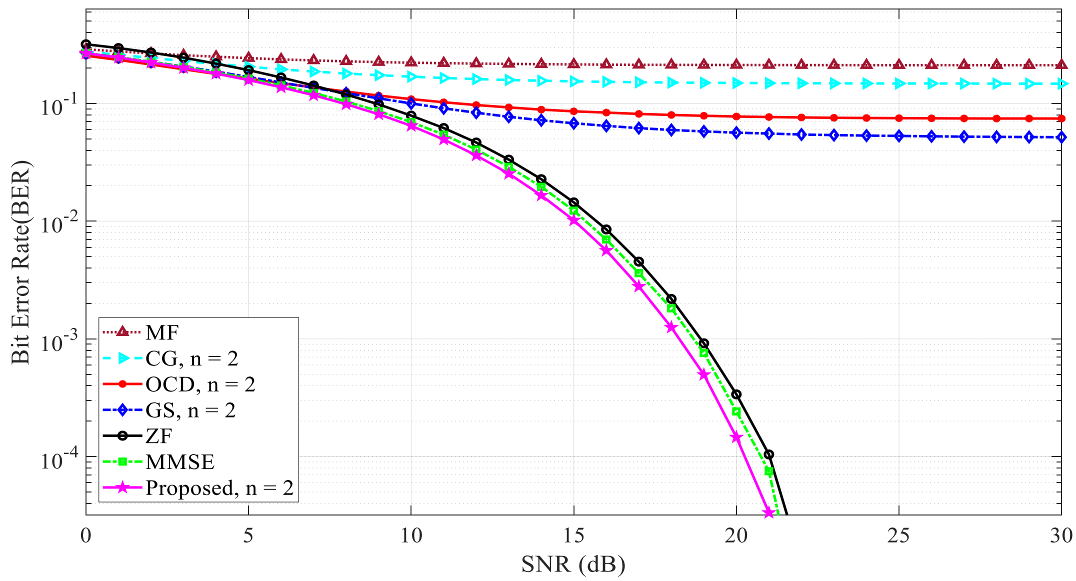

Figure 4. 1: BER performance of proposed algorithm and other methods at 80x120 M-MIMO system, 8QAM, and n=2

Table 4.2 shows that the performance comparison of proposed detector and other methods for the number of users = 80, number of base station antennas = 120, and number of iterations = 2 over 8QAM at SNR = 17dB to 21dB. As we observed from the table the performance of proposed detector is better than from the other methods. The table below indicates the tabular form of figure 4.1 by considering some value of SNR.

Table 4. 2: BER performance comparison of proposed and other methods at 80x120 M-MIMO, 8QAM and n=2

SNR (dB)	BER						
	Proposed	MMSE	ZF	GS	OCD	CG	MF
17	2.79×10^{-3}	3.62×10^{-3}	4.53×10^{-3}	6.18×10^{-2}	8.16×10^{-2}	1.52×10^{-1}	2.131×10^{-1}
18	1.25×10^{-3}	1.82×10^{-3}	2.81×10^{-3}	5.95×10^{-2}	7.99×10^{-2}	1.51×10^{-1}	2.129×10^{-1}
19	4.96×10^{-4}	7.58×10^{-4}	9.17×10^{-4}	5.79×10^{-2}	7.86×10^{-2}	1.50×10^{-1}	2.125×10^{-1}
20	1.46×10^{-4}	2.47×10^{-4}	3.38×10^{-4}	5.65×10^{-2}	7.75×10^{-2}	1.49×10^{-1}	2.123×10^{-1}
21	3.33×10^{-5}	7.50×10^{-5}	1.04×10^{-4}	5.55×10^{-2}	7.67×10^{-2}	1.49×10^{-1}	2.121×10^{-1}

Figure 4.2 demonstrates the BER performance of the proposed method and other algorithms for an 80x120 antenna configuration, n = 3 iterations, and the same modulation technique as in the previous figure. At SNR = 19dB, the proposed algorithm obtained a BER $=4.583\times10^{-4}$, while the GS method acquired a BER $=3.368\times10^{-2}$, and the MMSE method achieved a BER

$=7.167\times10^{-4}$. At SNR = 20dB, the proposed detector obtained a BER $=1.292\times10^{-4}$, whereas the GS detector reached a BER $=3.189\times10^{-2}$ and the MMSE detector achieved a BER = 2.458×10^{-4}. The proposed algorithm requires only two iterations to achieve the desired performance, whereas other algorithms require more iteration, increasing computational complexity.

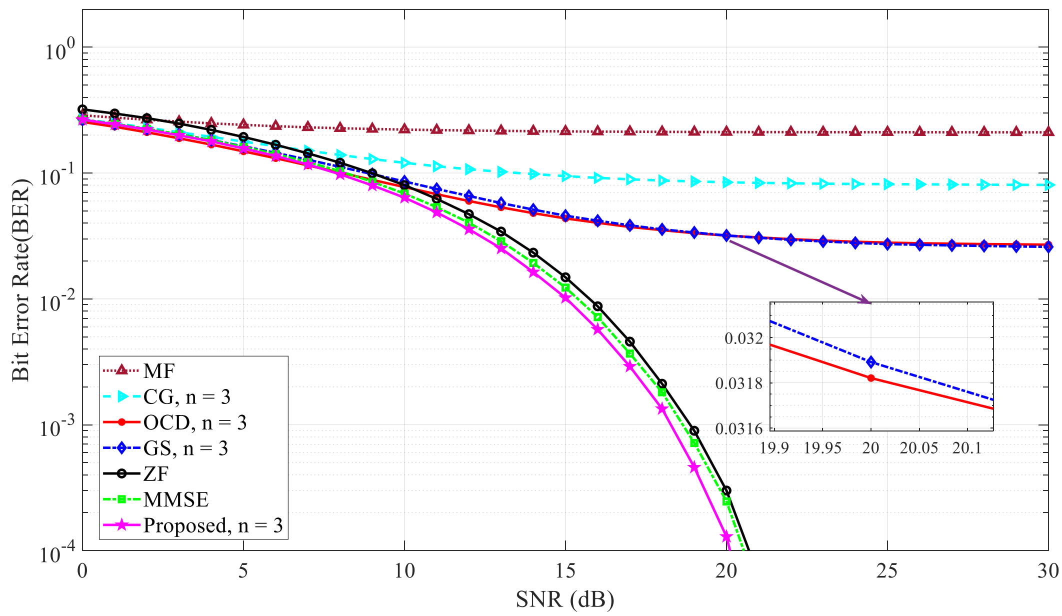

Figure 4. 2: BER performance of proposed algorithm and other methods at 80x120 M-MIMO system, 8QAM, and n=3

Figure 4.3 depicts the BER performance of the proposed method and other algorithms for a 120x180 antenna configuration, n = 4 iterations, and the same modulation technique as in the previous figure. The proposed algorithm attained a BER $=4.306\times10^{-4}$ at SNR = 19dB, while the GS method achieved a BER $=1.918\times10^{-2}$, and the MMSE method achieved a BER $=6.944\times10^{-4}$ at the same SNR value. At SNR = 20dB, the proposed detector acquired a BER $=1.222\times10^{-4}$, whereas the GS detector showed a BER $=1.725\times10^{-2}$ and the MMSE detector obtained a BER $=2.222\times10^{-4}$. All of the figures above show that the proposed detector outperforms other detectors. The matched filter detector and the conjugate gradient detector perform poorly.

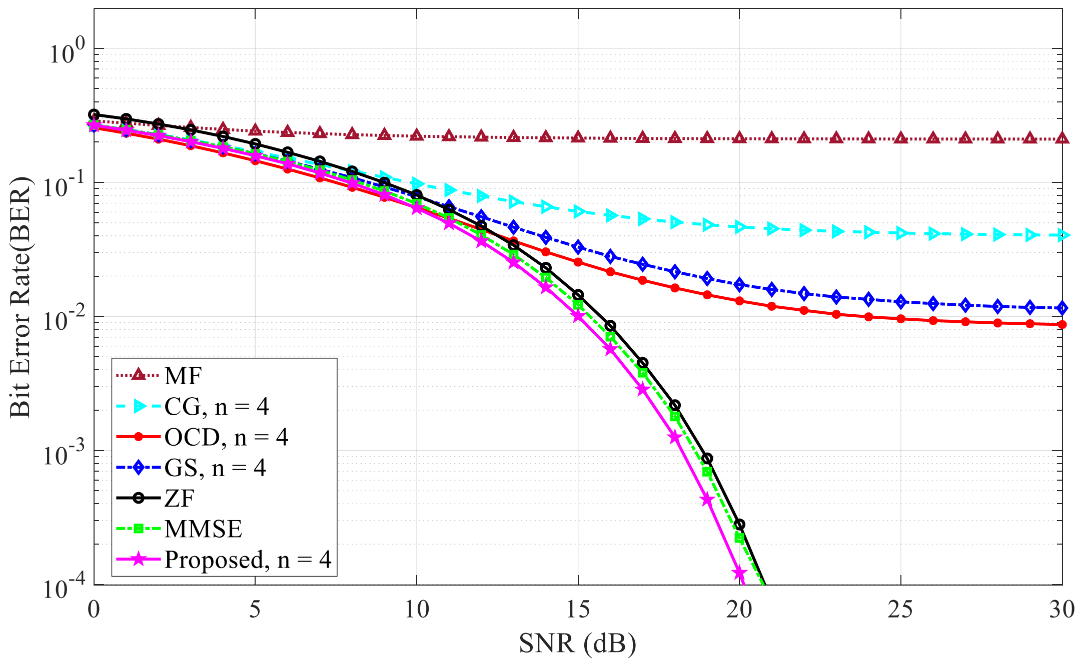

Figure 4. 3: BER performance of proposed algorithm and other methods at 120x180 M-MIMO system, 8QAM, and n=4

The simulation results presented below are obtained by changing the modulation scheme from 8-QAM to 16-QAM. Figure 4.4 compares the performance of the proposed algorithm to other algorithms for an 80x120 massive MIMO system with n = 2 and 16QAM modulation. The proposed detector obtained a BER= 7.19×10^{-5} at SNR = 21dB, whereas the GS algorithm reached a BER= 8.44×10^{-2} and MMSE algorithm obtained a BER= 1.59×10^{-4} at the same SNR = 21dB. The MF and the CG detectors showed very poor bit error rate performance as compared to the other detectors. The ZF and the MMSE detectors showed good bit error rate performance, but these detectors have high computational complexity. The OCD and the GS detectors showed better performance as compared to MF and CG detectors, but less performance as compared to proposed detector, MMSE, and ZF detectors. As shown in the figure, the proposed detector outperformed the MMSE, ZF, and other detectors.

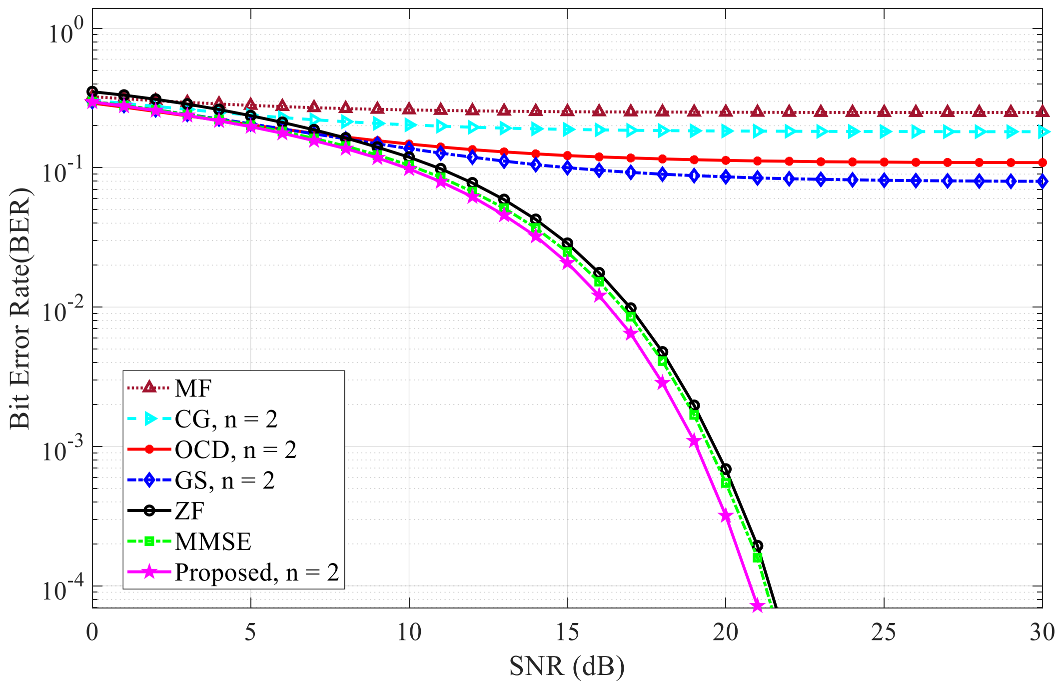

Figure 4. 4: BER performance of proposed algorithm and other methods at 80x120 M-MIMO system, 16QAM, and n=2

Table 4.3 indicates the performance comparison of proposed detector and other detectors for SNR = 17dB to 21dB, at the number of users = 80, number of base station antennas = 120 and n = 2 over 16QAM. As we observed from the table, the proposed detector achieved the best performance. CG and MF methods are the poor performance method as indicated in table. The table below indicates the tabular form of the figure 4.4 by considering some value of SNR.

Table 4. 3: BER performance comparison of proposed and other methods at 80x120 M-MIMO, 16QAM and n=2

SNR	BER						
(dB)	Proposed	MMSE	ZF	GS	OCD	CG	MF
17	6.45×10^{-3}	8.54×10^{-3}	9.82×10^{-3}	9.25×10^{-2}	1.17×10^{-1}	1.85×10^{-1}	2.509×10^{-1}
18	2.86×10^{-3}	4.10×10^{-3}	4.76×10^{-3}	8.98×10^{-2}	1.16×10^{-1}	1.84×10^{-1}	2.506×10^{-1}
19	1.10×10^{-3}	1.68×10^{-3}	1.97×10^{-3}	8.77×10^{-2}	1.14×10^{-1}	1.84×10^{-1}	2.503×10^{-1}
20	3.19×10^{-4}	5.47×10^{-4}	6.88×10^{-4}	8.60×10^{-2}	1.13×10^{-1}	1.83×10^{-1}	2.499×10^{-1}
21	7.19×10^{-5}	1.59×10^{-4}	1.94×10^{-4}	8.44×10^{-2}	1.12×10^{-1}	1.83×10^{-1}	2.495×10^{-1}

Figure 4.5 compares the proposed algorithm's performance to that of other recently used detectors in a massive MIMO system with an 80x120 antenna configuration and n = 3 over

16QAM modulation. The proposed algorithm achieved a $\mathrm{BER} = 1.084 \times 10^{-3}$ at SNR = 19dB while the GS method acquired a BER $= 5.624 \times 10^{-2}$ and the MMSE method obtained a BER $= 1.644 \times 10^{-3}$ at the same SNR. At SNR = 20dB, the proposed detector showed a BER $= 3.343 \times 10^{-4}$, while the GS detector achieved a BER $= 5.379 \times 10^{-2}$ and the MMSE detector obtained a $\mathrm{BER} = 5.750 \times 10^{-4}$. At SNR = 21dB, the proposed detector showed a BER $= 6.875 \times 10^{-5}$, while the GS detector achieved a BER $= 5.197 \times 10^{-2}$ and the MMSE detector obtained a $\mathrm{BER} = 1.531 \times 10^{-4}$.

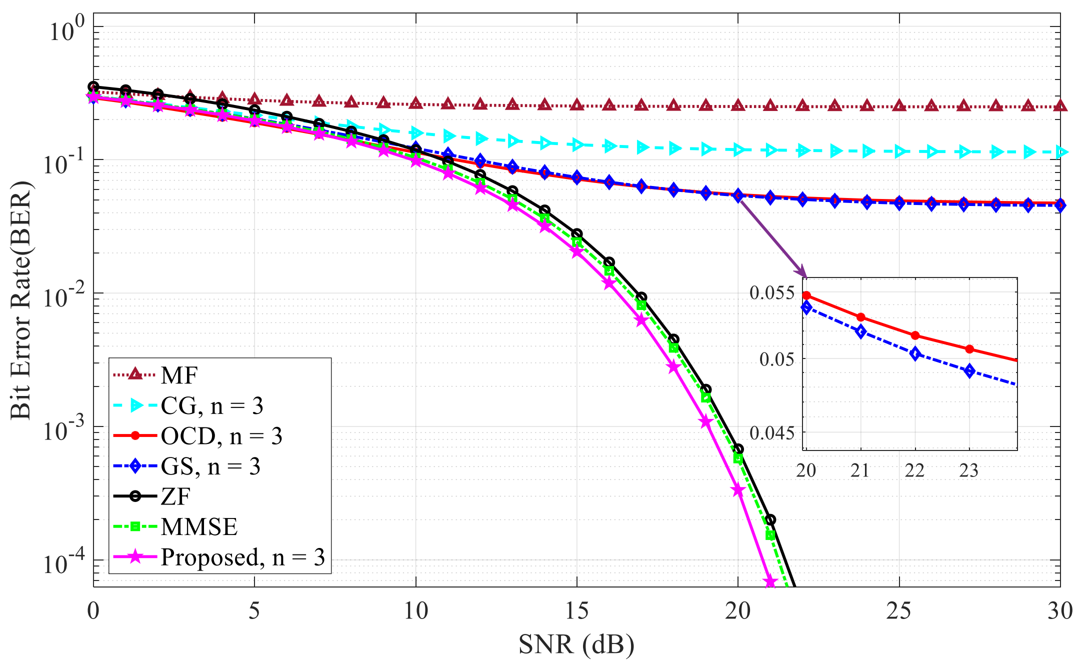

Figure 4. 5: BER performance of proposed detector and other detectors at 80x120 M-MIMO system, 16QAM and n=3

Figure 4.6 compares the proposed algorithm's performance to that of other recently used detectors in a massive MIMO system with an 120x180 antenna configuration and n = 4 over 16QAM modulation. The proposed algorithm achieved a $\mathrm{BER} = 1.139 \times 10^{-3}$ at SNR = 19dB while the GS method acquired a BER $= 3.662 \times 10^{-2}$ and the MMSE method obtained a BER $= 1.727 \times 10^{-3}$ at the same SNR. At SNR = 20dB, the proposed detector showed a BER $= 2.979 \times 10^{-4}$, while the GS detector achieved a BER $= 3.378 \times 10^{-2}$ and the MMSE detector obtained a $\mathrm{BER} = 5.500 \times 10^{-4}$. At SNR = 21dB, the proposed detector showed a BER

$= 6.667\times10^{-5}$, while the GS detector achieved a BER $= 2.266\times10^{-2}$ and the MMSE detector obtained a BER $= 1.604\times10^{-4}$.

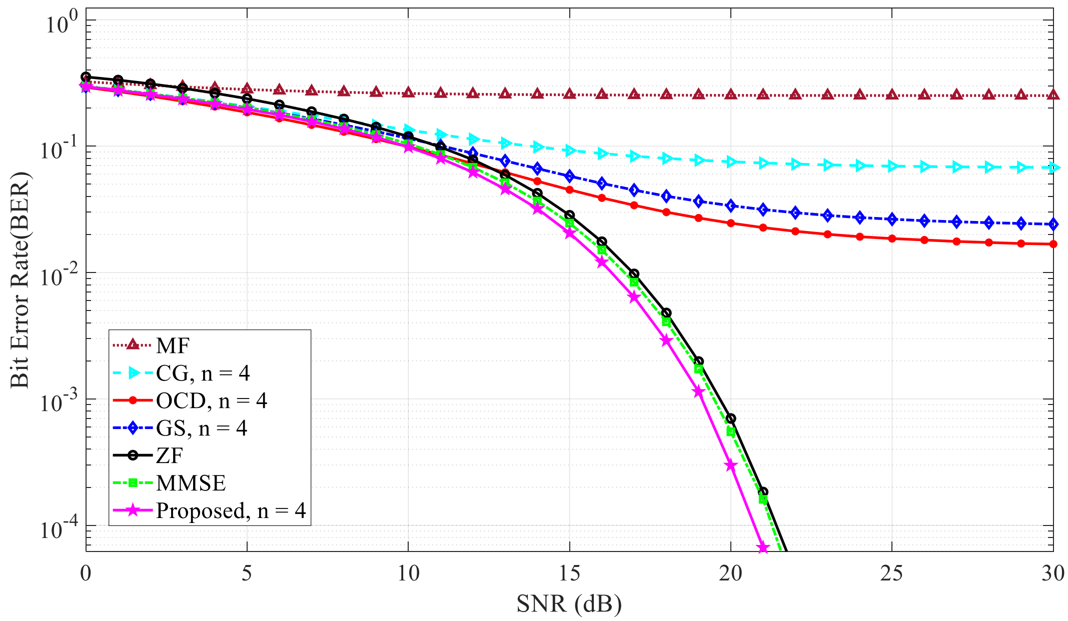

Figure 4. 6: BER performance of proposed detector and other detectors at 120x180 M-MIMO system, 16QAM and n=4

The simulation results presented below are obtained by changing the modulation scheme from 16-QAM to 32-QAM. Figure 4.7 shows a performance comparison of the proposed detector with other currently available massive MIMO detectors for an 80x120 antenna configuration, n = 2, and 32QAM. The proposed algorithm achieved a BER = 5.80×10^{-5} at SNR = 25dB, but the GS method achieved a BER = 2.36×10^{-1} and MMSE obtained a BER $= 8.80\times10^{-5}$ at the same SNR = 25dB, indicating that the GS method required additional iterations to achieve the target performance. Table 4.4 depicts the BER performance comparison of the proposed detector and other detectors at SNR = 20dB to 25dB, the number of users = 80, the number of base station antennas = 120, n = 2 over 32QAM. As indicated in the table, the proposed algorithm outperformed from the other methods. The table below indicates the tabular representation of figure 4.7 by considering some value of SNR. The MF, OCD and CG show poor performance.

Table 4. 4: BER performance comparison of proposed and other methods at 80x120 M-MIMO, 32QAM and n=2

SNR (dB)	BER						
	Proposed	MMSE	ZF	GS	OCD	CG	MF
20	1.41×10^{-2}	1.62×10^{-2}	1.75×10^{-2}	2.43×10^{-1}	2.86×10^{-1}	3.54×10^{-1}	3.663×10^{-1}
21	6.73×10^{-3}	8.07×10^{-3}	8.58×10^{-3}	2.41×10^{-1}	2.85×10^{-1}	3.54×10^{-1}	3.661×10^{-1}
22	2.75×10^{-3}	3.57×10^{-3}	3.57×10^{-3}	2.39×10^{-1}	2.84×10^{-1}	3.53×10^{-1}	3.659×10^{-1}
23	9.50×10^{-4}	1.16×10^{-3}	1.30×10^{-3}	2.38×10^{-1}	2.83×10^{-1}	3.53×10^{-1}	3.658×10^{-1}
24	2.00×10^{-4}	3.13×10^{-4}	3.30×10^{-4}	2.37×10^{-1}	2.83×10^{-1}	3.53×10^{-1}	3.658×10^{-1}
25	5.80×10^{-5}	8.80×10^{-5}	9.50×10^{-5}	2.36×10^{-1}	2.81×10^{-1}	3.52×10^{-1}	3.658×10^{-1}

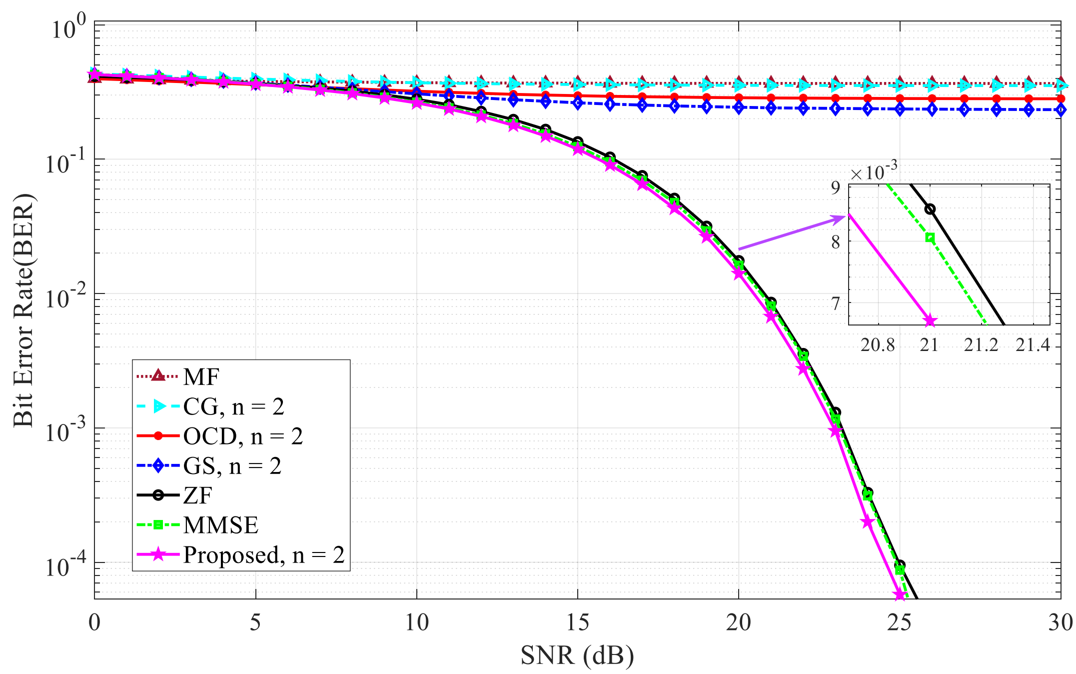

Figure 4. 7: BER performance of proposed detector and other detectors at 80x120 M-MIMO system, 32QAM and n=2

Figure 4.8 demonstrates a BER performance comparison of a proposed detector with other detectors for a massive MIMO system with a 120x180 antenna configuration, n = 4 and 32QAM. At SNR = 20dB, the proposed detector showed a $\text{BER} = 1.475\times10^{-2}$, while the GS detector achieved a BER $= 1.489\times10^{-1}$ and the MMSE detector obtained a $\text{BER} = 1.684\times10^{-2}$.

At SNR = 23dB, the proposed detector showed a $BER = 9.367 \times 10^{-4}$, while the GS detector achieved a BER $= 1.342 \times 10^{-1}$ and the MMSE detector obtained a $BER = 1.197 \times 10^{-3}$. The proposed algorithm achieved a $BER = 2.100 \times 10^{-4}$ at SNR = 24dB while the GS method acquired a BER $= 1.313 \times 10^{-1}$ and the MMSE method obtained a $BER = 3.050 \times 10^{-4}$ at the same SNR. At SNR = 25dB, the proposed detector showed a $BER = 2.333 \times 10^{-5}$, while the GS detector achieved a BER $= 1.289 \times 10^{-1}$ and the MMSE detector obtained a BER $= 5.000 \times 10^{-5}$.

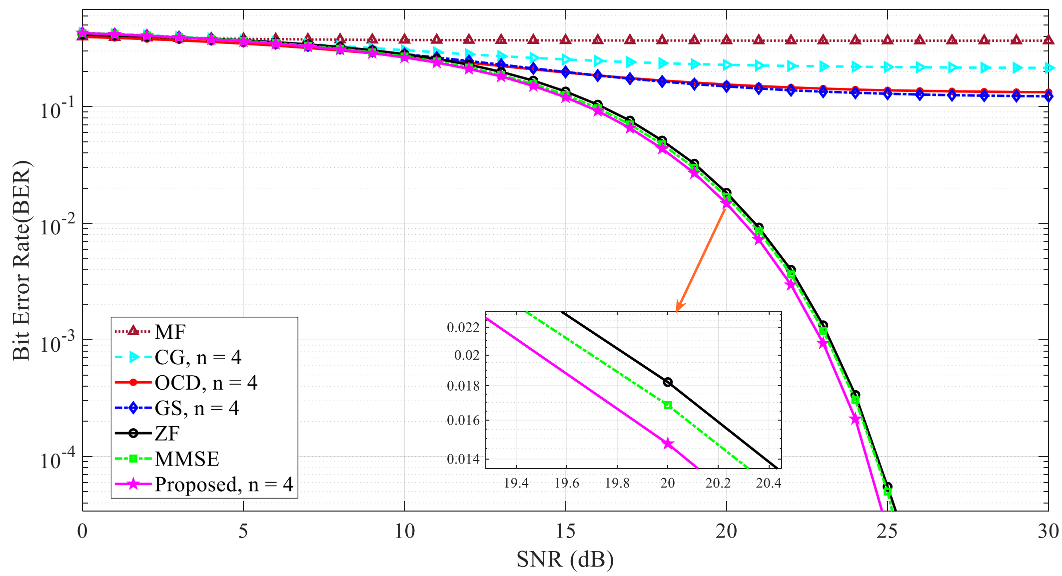

Figure 4. 8: BER performance of proposed detector and other detectors at 120x180 M-MIMO system, 32QAM and n=4

Figure 4.9 depicts a BER performance comparison of a proposed detector with other detectors for a massive MIMO system with an antenna configuration of 64x128 (BUAR = 2), n = 4, and 32QAM. At SNR=19dB, the proposed detector achieved a $BER = 3.353 \times 10^{-3}$, whereas the GS detector achieved a $BER = 2.043 \times 10^{-2}$ and the MMSE detector acquired a $BER = 3.850 \times 10^{-3}$. The proposed detector achieved a BER = 1.100×10^{-3} at SNR = 20dB, while the GS detector achieved a BER = 2.201×10^{-2} and the MMSE detector obtained a $BER = 1.275 \times 10^{-3}$ at the same SNR = 20dB. At SNR = 21dB, the proposed detector achieved a $BER = 2.875 \times 10^{-4}$, whereas the GS detector achieved a $BER = 1.774 \times 10^{-2}$ and the MMSE detector acquired a

$\mathrm{BER} = 3.689 \times 10^{-4}$. The proposed detector achieved a BER = 5.938×10^{-5} at SNR = 22dB, while the GS detector achieved a BER = 1.463×10^{-2} and the MMSE detector obtained a BER $= 8.750 \times 10^{-5}$ at the same SNR = 22dB.

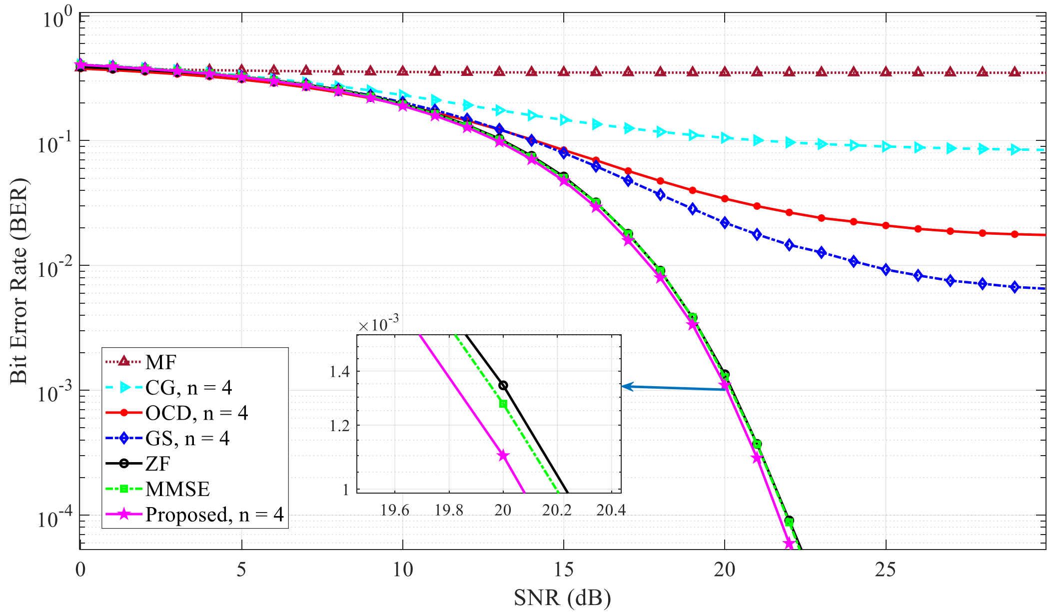

Figure 4. 9: BER performance of proposed detector and other detectors at 64x128 M-MIMO system, 32QAM and n=4

Figure 4.10 depicts a BER performance comparison of a proposed detector with other detectors for a massive MIMO system with an antenna configuration of 128x256 (BUAR = 2), n = 5, and 32QAM. At SNR=20dB, the proposed detector achieved a $\mathrm{BER} = 9.766 \times 10^{-4}$, whereas the GS detector achieved a $\mathrm{BER} = 1.031 \times 10^{-2}$ and the MMSE detector acquired a $\mathrm{BER} = 1.142 \times 10^{-3}$. The proposed detector achieved a BER = 2.391×10^{-4} at SNR = 21dB, while the GS detector achieved a BER = 6.857×10^{-3} and the MMSE detector obtained a BER $= 3.375 \times 10^{-4}$ at the same SNR = 21dB. At SNR = 22dB, the proposed detector achieved a $\mathrm{BER} = 2.656 \times 10^{-5}$, whereas the GS detector achieved a $\mathrm{BER} = 4.633 \times 10^{-3}$ and the MMSE detector acquired a $\mathrm{BER} = 6.250 \times 10^{-5}$. As number of iteration increased the performance of detectors such as GS and OCD become improved, but as the number of iteration increased, the computational complexity also increased. In signal detection, system small iteration methods are required, so the proposed detector required only two iterations to obtained better performance.

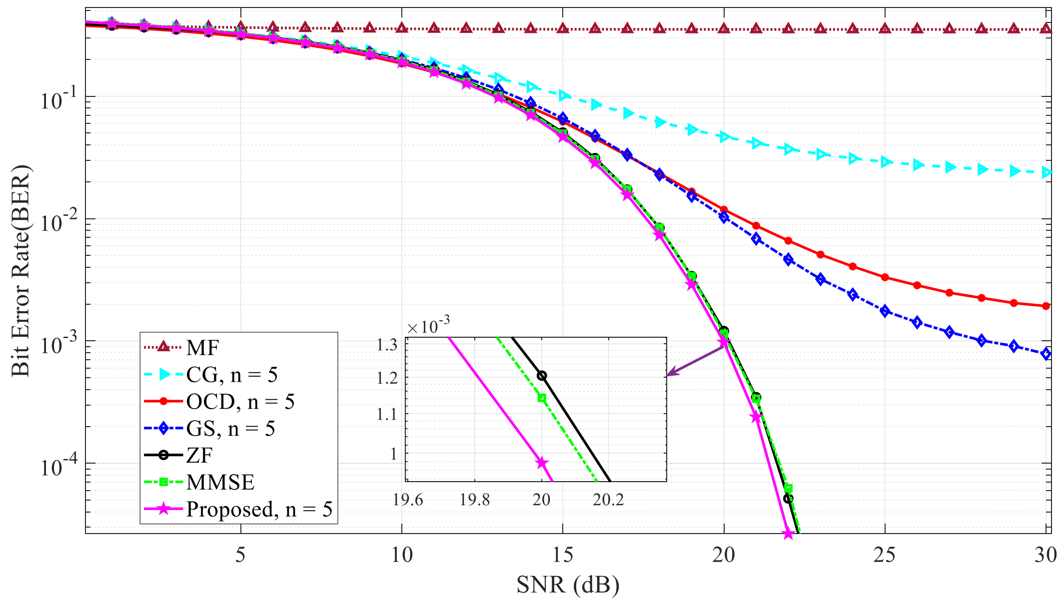

Figure 4. 10: BER performance of proposed algorithm and other methods at 128x256 M-MIMO system, 32QAM and n=5

The simulation results presented below are obtained by changing the modulation scheme from 32-QAM to 64-QAM. Figure 4.11 depicts a BER performance comparison of a proposed detector with other detectors for massive MIMO system with an 80x120 antenna configuration, n = 3, and 64QAM. At SNR=25dB, the proposed detector achieved a BER $=1.638\times10^{-3}$, whereas the GS detector achieved a BER$=1.394\times10^{-1}$and the MMSE detector acquired a BER$=1.971\times10^{-3}$. The proposed detector achieved a BER = 5.812×10^{-4} at SNR = 26dB, while the GS detector achieved a BER = 1.386×10^{-1} and the MMSE detector obtained a BER$=7.562\times10^{-4}$ at the same SNR = 26dB. At SNR = 27dB, the proposed detector achieved a BER$=1.542\times10^{-4}$, whereas the GS detector achieved a BER$=1.379\times10^{-1}$and the MMSE detector acquired a BER$=2.292\times10^{-4}$. At SNR = 28dB, the proposed detector achieved a BER$=3.542\times10^{-5}$, whereas the GS detector achieved a BER$=1.374\times10^{-1}$and the MMSE detector acquired a BER$=4.792\times10^{-5}$.

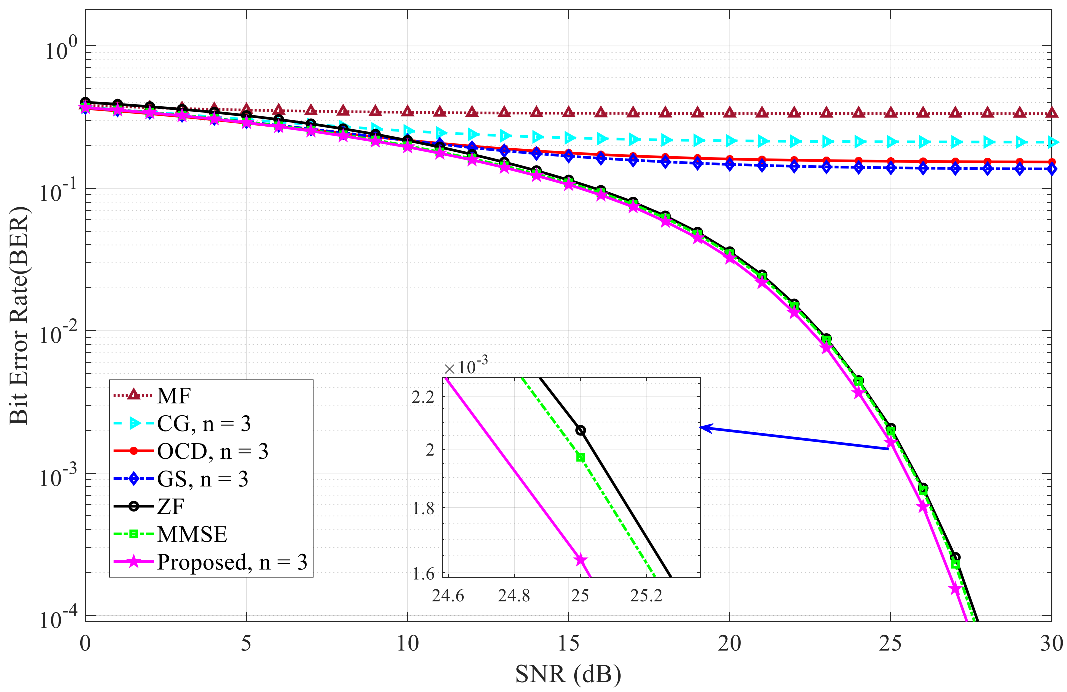

Figure 4. 11: BER performance of proposed algorithm and other methods at 80x120 M-MIMO system, 64QAM and n=3

Figure 4.12 compares the BER performance of a proposed detector to that of other detectors for a massive MIMO system with a 120x180 antenna configuration, n = 4, and 64QAM. The proposed detector achieved a $BER = 1.453\times10^{-3}$ at SNR = 25dB, while the GS detector achieved a BER 1.126×10^{-1} and the MMSE detector obtained a $BER = 1.844\times10^{-3}$ at the same SNR = 25dB. At SNR=26dB, the proposed detector achieved a $BER = 5.153\times10^{-4}$, whereas the GS detector achieved a $BER = 1.115\times10^{-1}$ and the MMSE detector acquired a BER $= 6.556\times10^{-4}$. At SNR = 27dB, the proposed detector achieved a $BER = 1.361\times10^{-4}$, whereas the GS detector achieved a $BER = 1.105\times10^{-1}$ and the MMSE detector acquired a BER $= 2.028\times10^{-4}$. At SNR = 28dB, the proposed detector achieved a $BER = 2.500\times10^{-5}$, whereas the GS detector achieved a $BER = 1.099\times10^{-1}$ and the MMSE detector acquired a BER $= 4.028\times10^{-5}$.

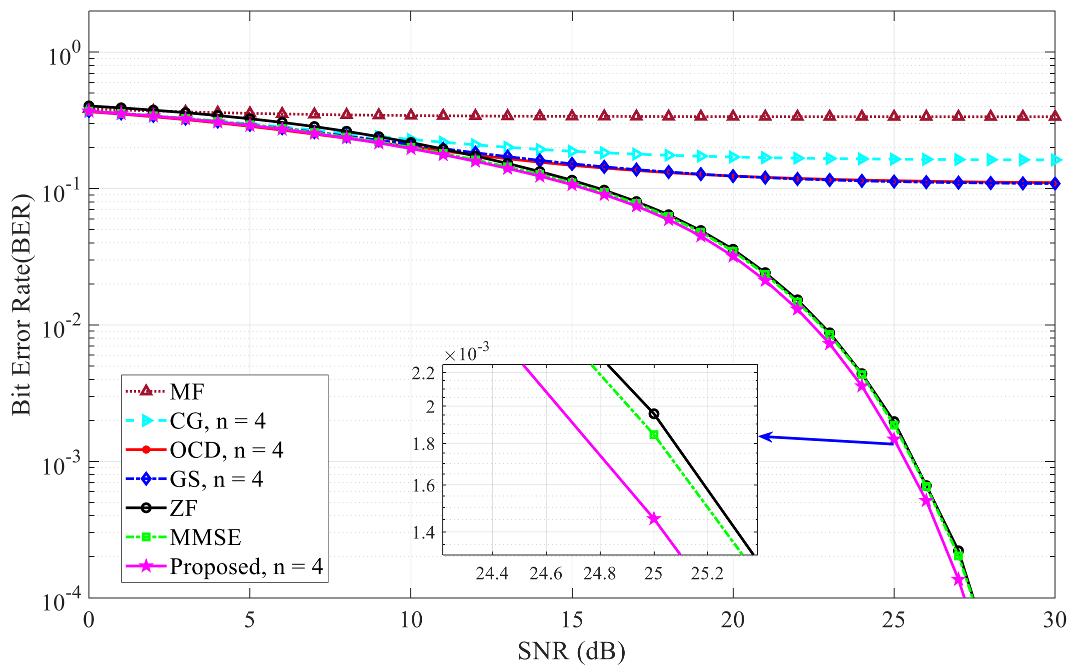

Figure 4. 12: BER performance of proposed algorithm and other methods at 120x180 M-MIMO system, 64QAM and n=4

Figure 4.13 compares the BER performance of a proposed detector to that of other detectors for a massive MIMO system with a 128x256 (BUAR = 2) antenna configuration, n = 5, and 64QAM. The proposed detector achieved a BER = 2.73×10^{-5} at SNR = 25dB, whereas the GS detector obtained a BER = 9.31×10^{-3} and the MMSE detector achieved a BER $= 3.91\times10^{-5}$ at the same SNR = 25dB.

Table 4.5 shows the performance comparison of the proposed detector with the other detectors at SNR = 20dB to 25dB, the number of users = 128, the number of base station antennas = 256, n = 5, and 64QAM based on BER. The table below indicates tabular representation of figure 4.13 by considering some value of SNR. Generally, from all numerical result figures and tables the proposed detector achieved the best bit error rate performance with small number of iterations and outperformed from the other detectors.

Table 4. 5: BER performance comparison of proposed and other methods at 128x256 M-MIMO, 64QAM and n=5

SNR (dB)	BER						
	Proposed	MMSE	ZF	GS	OCD	CG	MF
20	7.91×10^{-3}	8.75×10^{-3}	8.81×10^{-3}	2.61×10^{-2}	2.67×10^{-2}	6.05×10^{-2}	3.218×10^{-1}
21	3.89×10^{-3}	4.35×10^{-3}	4.42×10^{-3}	2.07×10^{-2}	2.19×10^{-2}	5.63×10^{-2}	3.216×10^{-1}
22	1.63×10^{-3}	1.88×10^{-3}	1.89×10^{-3}	1.60×10^{-2}	1.83×10^{-2}	5.28×10^{-2}	3.215×10^{-1}
23	5.36×10^{-4}	6.41×10^{-4}	6.60×10^{-4}	1.34×10^{-2}	1.54×10^{-2}	5.01×10^{-2}	3.214×10^{-1}
24	1.51×10^{-4}	2.01×10^{-4}	1.90×10^{-4}	1.10×10^{-2}	1.33×10^{-2}	4.77×10^{-2}	3.214×10^{-1}
25	2.73×10^{-5}	3.91×10^{-5}	4.30×10^{-5}	9.31×10^{-3}	1.17×10^{-2}	4.61×10^{-2}	3.214×10^{-1}

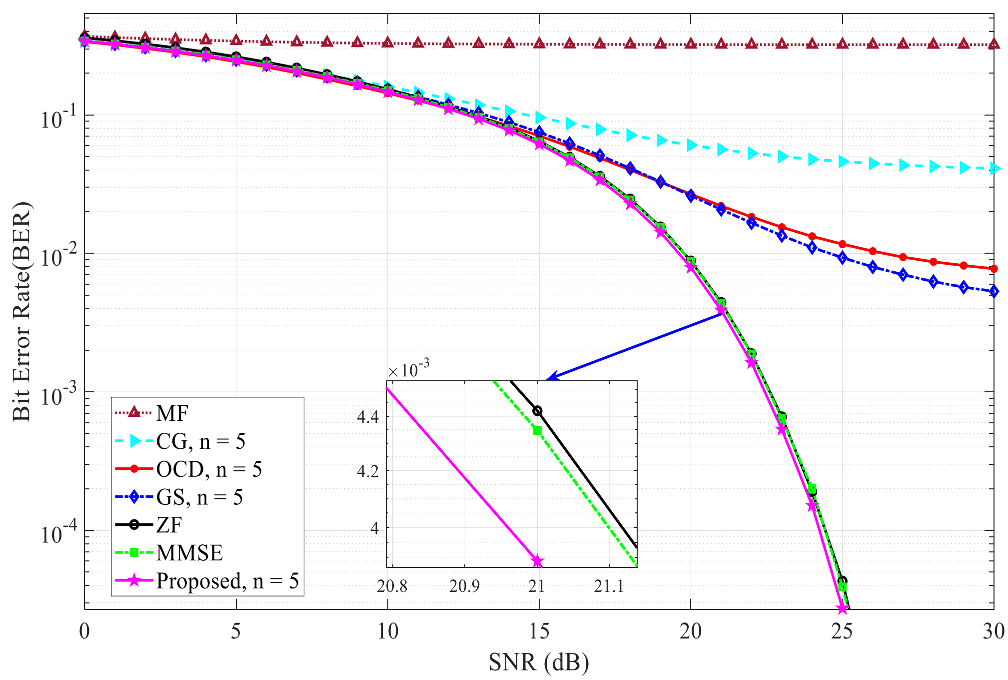

Figure 4. 13: BER performance of proposed detector and other methods at 128x256 M-MIMO system, 64QAM and n=5

4.1.2 Performance comparisons of the proposed detector with other detectors based on Mean Squared Error

The mean squared error is calculated based on the original signal and detected signal. The following simulation results are presented in order to evaluate the MSE performance of the proposed and other currently available detectors. The simulation results compare the performance of the proposed algorithm with that of recently introduced massive MIMO uplink detectors based on the MSE. The performance is shown in terms of mean squared error versus signal to noise ratio by varying the number of users, number of base station antennas, modulation schemes and number of iterations.

For a massive MIMO system with an 80x120 (BUAR = 1.5) antenna configuration, n = 2, and 8QAM, Figure 4.14 compares the MSE performance of a proposed detector to that of other detectors. At SNR = 20dB, the proposed detector achieved an $MSE = 4.38\times10^{-4}$, whereas the GS detector achieved an $MSE=1.63\times10^{-1}$ and the MMSE detector achieved an MSE $= 7.25\times10^{-4}$. At SNR = 21dB, the proposed detector achieved an $MSE = 1.00\times10^{-4}$, whereas the GS detector achieved an $MSE = 1.60\times10^{-1}$ and the MMSE detector achieved an MSE $= 2.25\times10^{-4}$.

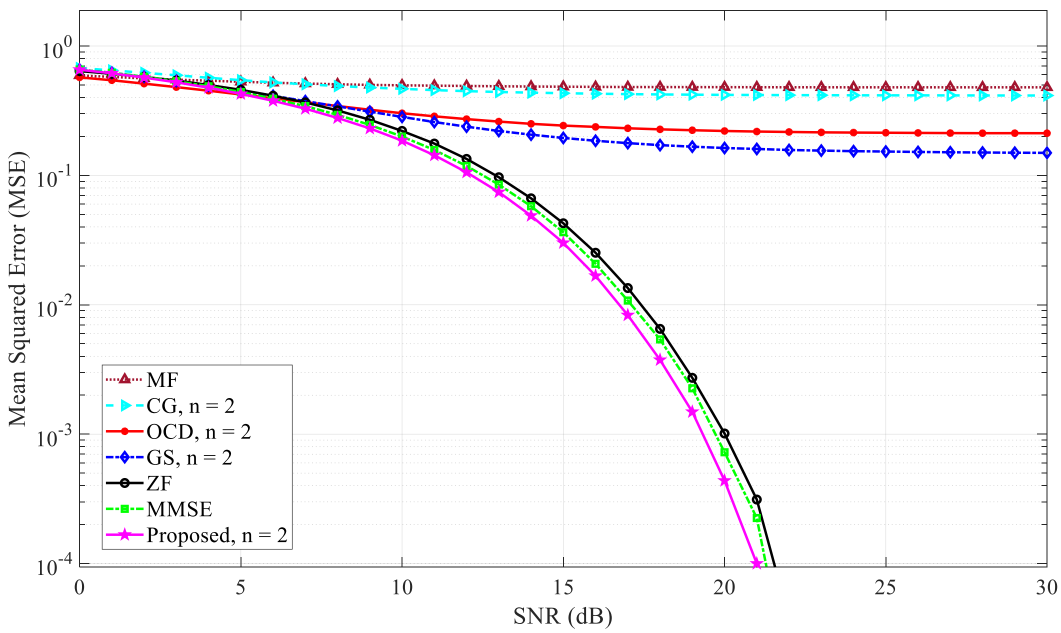

Figure 4. 14: MSE performance of proposed detector and other methods at 80x120 M-MIMO system, 8QAM and n=2

Table 4.6 compares the proposed detector's performance to that of the other detectors at SNR = 15dB to 21dB, 80 users, 120 base station antennas, n = 2, and 8QAM based on MSE. The table below indicates tabular representation of figure 4.14 by considering some value of SNR.

As shown, from the table and the figure the proposed detector achieved the better mean squared performance than other detectors with in two numbers of iterations.

Table 4. 6: MSE performance comparison of proposed and other methods at 80x120 M-MIMO, 8QAM and n=2

SNR (dB)	MSE						
	Proposed	MMSE	ZF	GS	OCD	CG	MF
15	3.01×10^{-2}	3.64×10^{-2}	4.27×10^{-2}	1.95×10^{-1}	2.43×10^{-1}	4.32×10^{-1}	4.845×10^{-1}
16	1.67×10^{-2}	2.07×10^{-2}	2.54×10^{-2}	1.85×10^{-1}	2.37×10^{-1}	4.28×10^{-1}	4.829×10^{-1}
17	8.31×10^{-3}	1.08×10^{-2}	1.35×10^{-2}	1.78×10^{-1}	2.31×10^{-1}	4.25×10^{-1}	4.816×10^{-1}
18	3.75×10^{-3}	5.40×10^{-3}	6.51×10^{-3}	1.71×10^{-1}	2.27×10^{-1}	4.22×10^{-1}	4.814×10^{-1}
19	1.49×10^{-3}	2.26×10^{-3}	2.73×10^{-3}	1.67×10^{-1}	2.23×10^{-1}	4.20×10^{-1}	4.810×10^{-1}
20	4.38×10^{-4}	7.25×10^{-4}	1.01×10^{-3}	1.63×10^{-1}	2.20×10^{-1}	4.19×10^{-1}	4.807×10^{-1}
21	1.00×10^{-4}	2.25×10^{-4}	3.13×10^{-4}	1.60×10^{-1}	2.18×10^{-1}	4.18×10^{-1}	4.802×10^{-1}

Figure 4.15 demonstrates an MSE performance comparison of a proposed detector with other detectors for a massive MIMO system with a 120x180 antenna configuration, n = 3 and 16QAM.

The proposed algorithm achieved an $\mathrm{MSE}=4.915\times10^{-2}$ at SNR = 16dB, while the GS method acquired an $\mathrm{MSE}=2.599\times10^{-1}$ and the MMSE method obtained an $\mathrm{MSE}=5.989\times10^{-2}$ at the same SNR. At SNR = 17dB, the proposed detector showed an $\mathrm{MSE}=2.633\times10^{-2}$, while the GS detector achieved an $\mathrm{MSE}=2.446\times10^{-1}$and the MMSE detector obtained an MSE $=3.435\times10^{-2}$. At SNR = 18dB, the proposed detector showed an $\mathrm{MSE}=1.200\times10^{-2}$, while the GS detector achieved an $\mathrm{MSE}=2.314\times10^{-1}$and the MMSE detector obtained an MSE $=1.691\times10^{-2}$. The proposed algorithm achieved an $\mathrm{MSE}=4.683\times10^{-3}$ at SNR = 19dB, while the GS method acquired an $\mathrm{MSE}=2.209\times10^{-1}$ and the MMSE method obtained an MSE $=7.225\times10^{-3}$ at the same SNR. At SNR = 20dB, the proposed detector showed an MSE $=1.433\times10^{-3}$, while the GS detector achieved an $\mathrm{MSE}=2.126\times10^{-1}$ and the MMSE detector obtained an $\mathrm{MSE}=2.525\times10^{-3}$. The proposed algorithm achieved an $\mathrm{MSE}=3.750\times10^{-4}$ at SNR = 21dB, while the GS method acquired an $\mathrm{MSE}=2.057\times10^{-1}$ and the MMSE method obtained an $\mathrm{MSE}=8.000\times10^{-4}$ at the same SNR.

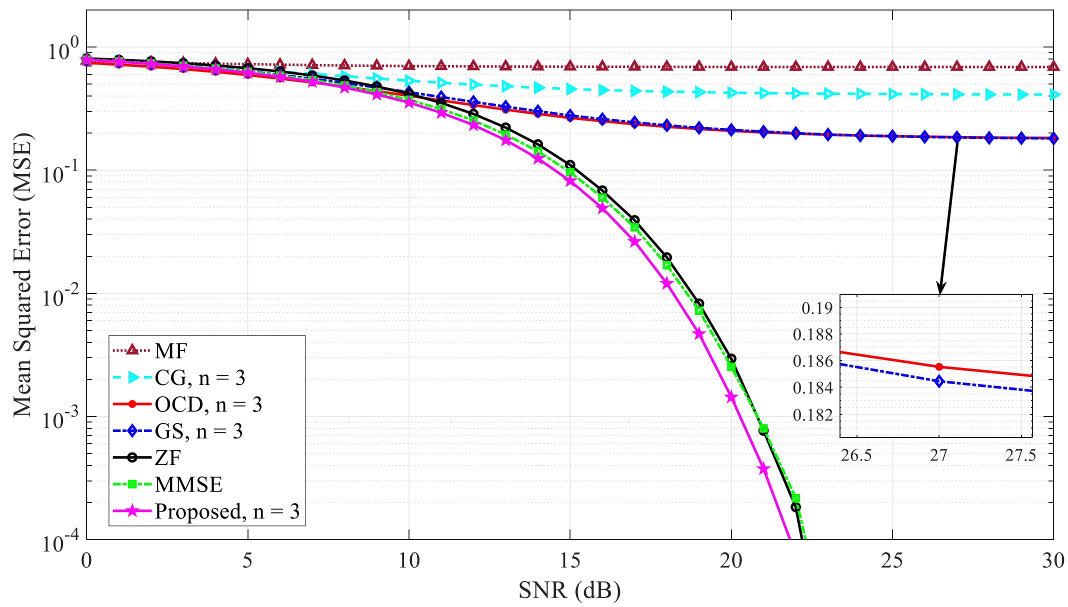

Figure 4. 15: MSE performance of proposed detector and other methods at 120x180 M-MIMO system, 16QAM and n=3

Figure 4.16 shows an MSE performance comparison of a proposed detector with other detectors for a massive MIMO system with a 120x180 antenna configuration, n = 4, and 32QAM. The proposed algorithm achieved an $MSE = 1.704 \times 10^{-2}$ at SNR = 21dB, while the GS method achieved an $MSE = 3.283 \times 10^{-1}$ and the MMSE method obtained an MSE $= 1.974 \times 10^{-2}$ at the same SNR. At SNR = 22dB, the proposed detector obtained an MSE $= 6.517 \times 10^{-3}$, while the GS detector achieved an $MSE = 3.186 \times 10^{-1}$ and the MMSE detector obtained an $MSE = 8.025 \times 10^{-3}$. The proposed algorithm achieved an $MSE = 2.117 \times 10^{-3}$ at SNR = 23dB, while the GS method achieved an $MSE = 3.097 \times 10^{-1}$ and the MMSE method obtained an $MSE = 2.792 \times 10^{-3}$ at the same SNR. At SNR = 24dB, the proposed detector showed an $MSE = 5.167 \times 10^{-4}$, while the GS detector achieved an $MSE = 3.027 \times 10^{-1}$ and the MMSE detector obtained an $MSE = 7.500 \times 10^{-4}$. The proposed algorithm achieved an MSE $= 5.833 \times 10^{-5}$ at SNR = 25dB, while the GS method achieved an $MSE = 2.971 \times 10^{-1}$ and the MMSE method obtained an $MSE = 1.333 \times 10^{-4}$ at the same SNR.

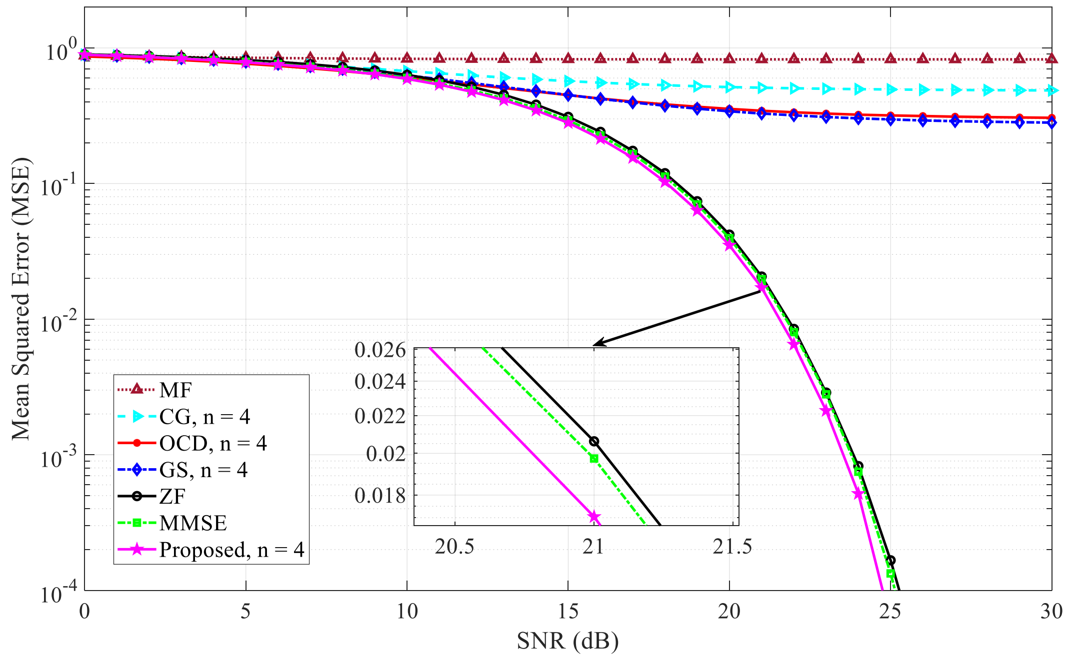

Figure 4. 16: MSE performance of proposed detector and other methods at 120x180 M-MIMO system, 32QAM and n=4

Figure 4.17 compares the MSE performance of a proposed detector to that of other detectors in a massive MIMO system with a 128x256 antenna configuration, n = 5, and 64QAM. At SNR = 22dB, the proposed detector obtained an $MSE = 9.234\times10^{-3}$, while the GS detector achieved an $MSE = 9.727\times10^{-2}$ and the MMSE detector obtained an $MSE = 1.069\times10^{-2}$. The proposed algorithm achieved an $MSE = 3.086\times10^{-3}$ at SNR = 23dB, while the GS method achieved an $MSE = 7.855\times10^{-2}$ and the MMSE method obtained an $MSE = 3.633\times10^{-3}$ at the same SNR. At SNR = 24dB, the proposed detector showed an $MSE = 7.500\times10^{-4}$, while the GS detector achieved an $MSE = 6.560\times10^{-2}$ and the MMSE detector obtained an MSE $= 1.047\times10^{-3}$. The proposed algorithm achieved an $MSE = 1.172\times10^{-4}$ at SNR = 25dB, while the GS method achieved an $MSE = 5.531\times10^{-2}$ and the MMSE method obtained an MSE $= 1.797\times10^{-4}$ at the same SNR. As indicated in all MSE simulation results the MF detector and CG detector showed the poor performance.

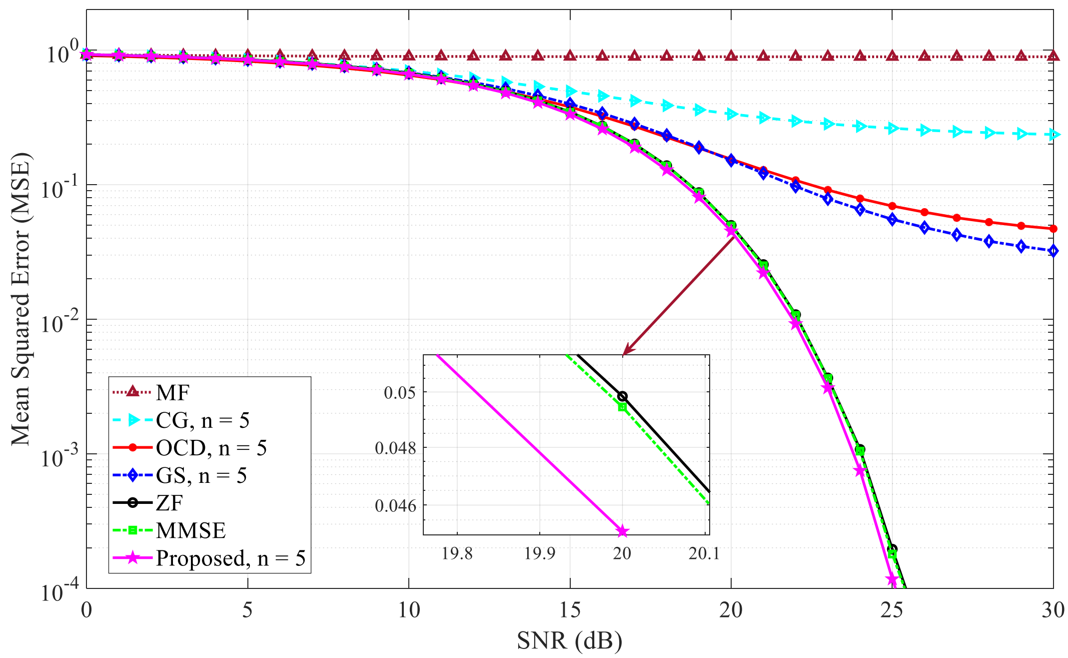

Figure 4. 17: MSE performance of proposed detector and other methods at 128x256 M-MIMO system, 64QAM and n=5

4.1.3 Performance comparisons of the proposed detector with other detectors based on Symbol Error Rate

In order to evaluate the performance of massive MIMO uplink detectors, the simulation results presented below are based on the symbol error rate versus signal to noise ratio. The number of symbols with errors in a detected signal and the total number of transmitted symbols are used to calculate the SER. The performance is shown in terms of symbol error rate versus signal to noise ratio by varying the number of users, number of base station antennas, modulation schemes and number of iterations.

In Figure 4.18, the SER performance of a proposed detector is compared to that of other detectors in a massive MIMO system with an 80x120 antenna configuration, n = 2, and 8QAM. The proposed algorithm obtained a $SER = 4.50\times10^{-4}$, at SNR = 20dB, whereas the GS method obtained a $SER = 1.65\times10^{-1}$, and the MMSE method obtained a $SER = 6.88\times10^{-4}$ at the same SNR.

Table 4.7 compares the performance of the proposed detector to the other detectors at SNR = 15dB to 20dB, 80 users, 120 base station antennas, n = 2, and 8QAM based on SER. The table below shows a tabular representation of figure 4.18 when some value of SNR is taken into account.

Table 4. 7: SER performance comparison of proposed and other methods at 80x120 M-MIMO, 8QAM and n=2

SNR (dB)	SER						
	Proposed	MMSE	ZF	GS	OCD	CG	MF
15	3.07×10^{-2}	3.70×10^{-2}	4.42×10^{-2}	1.98×10^{-1}	2.41×10^{-1}	4.29×10^{-1}	4.861×10^{-1}
16	1.74×10^{-2}	2.18×10^{-2}	2.64×10^{-2}	1.89×10^{-1}	2.34×10^{-1}	4.26×10^{-1}	4.847×10^{-1}
17	9.01×10^{-3}	1.17×10^{-2}	1.39×10^{-2}	1.81×10^{-1}	2.29×10^{-1}	4.24×10^{-1}	4.835×10^{-1}
18	4.09×10^{-3}	5.68×10^{-3}	6.69×10^{-3}	1.74×10^{-1}	2.24×10^{-1}	4.22×10^{-1}	4.824×10^{-1}
19	1.53×10^{-3}	2.34×10^{-3}	2.76×10^{-3}	1.69×10^{-1}	2.21×10^{-1}	4.19×10^{-1}	4.822×10^{-1}
20	4.50×10^{-4}	6.88×10^{-4}	9.88×10^{-4}	1.65×10^{-1}	2.18×10^{-1}	4.17×10^{-1}	4.818×10^{-1}

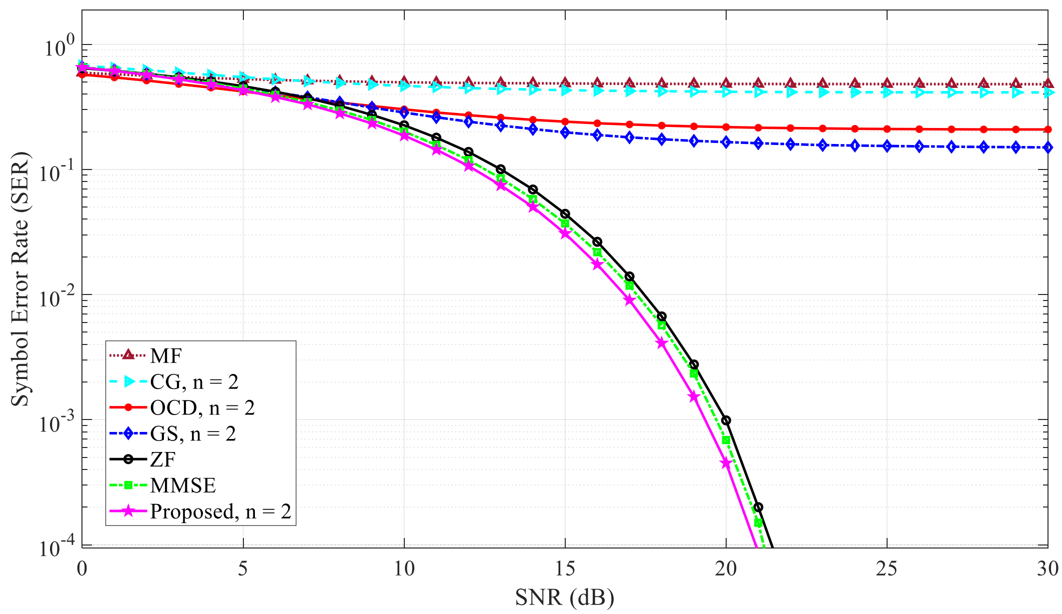

Figure 4. 18: SER performance of proposed detector and other methods at 80x120 M-MIMO system, 8QAM and n=2

The SER performance of a proposed detector is compared to that of other detectors in figure 4.19 in a massive MIMO system with a 120x180 antenna configuration, n = 3, and 16QAM. The proposed algorithm obtained a $SER = 4.525\times10^{-3}$, at SNR = 19dB, whereas the GS method obtained a $SER = 2.160 \times 10^{-1}$, and the MMSE method obtained a $SER = 6.825 \times 10^{-3}$ at the same SNR. At SNR = 20dB, the proposed detector showed a $SER = 1.442 \times 10^{-3}$, while the GS detector achieved a $SER = 2.068 \times 10^{-1}$ and the MMSE detector obtained a $SER = 2.392 \times 10^{-3}$. The proposed algorithm obtained a $SER = 3.583 \times 10^{-4}$, at SNR = 21dB, whereas the GS method obtained a $SER = 1.996 \times 10^{-1}$, and the MMSE method obtained a $SER = 7.333 \times 10^{-4}$ at the same SNR.

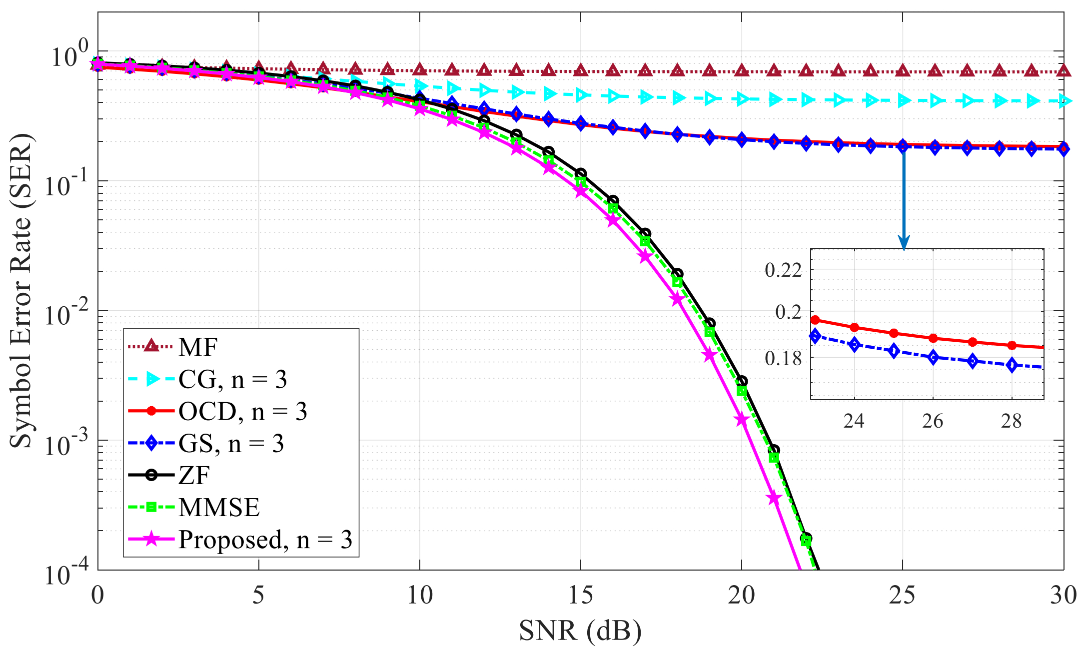

Figure 4. 19: SER performance of proposed detector and other methods at 120x180 M-MIMO system, 16QAM and n=3

In figure 4.20, the SER performance of a proposed detector is compared to that of other detectors in a massive MIMO system with a 120x180 antenna configuration, n = 4, and 32QAM. The proposed algorithm achieved a $SER = 6.750 \times 10^{-3}$, at SNR = 22dB, whereas the GS method obtained a $SER = 3.205 \times 10^{-1}$, and the MMSE method obtained a $SER = 8.200 \times 10^{-3}$ at the same SNR. At SNR = 23dB, the proposed detector showed a $SER = 2.150 \times 10^{-3}$, while the GS detector achieved a $SER = 3.118 \times 10^{-1}$ and the MMSE detector obtained a $SER = 3.125 \times 10^{-3}$. The proposed algorithm obtained a $SER = 4.917 \times 10^{-4}$, at SNR = 24dB, whereas the GS method obtained a $SER = 3.048 \times 10^{-1}$, and the MMSE method obtained a $\text{SER} = 7.333\times10^{-4}$ at the same SNR. At SNR = 25dB, the proposed detector showed a $\text{SER} = 1.083\times10^{-4}$, while the GS detector achieved a $\text{SER} = 2.996\times10^{-1}$ and the MMSE detector obtained a $\text{SER} = 1.333\times10^{-4}$.

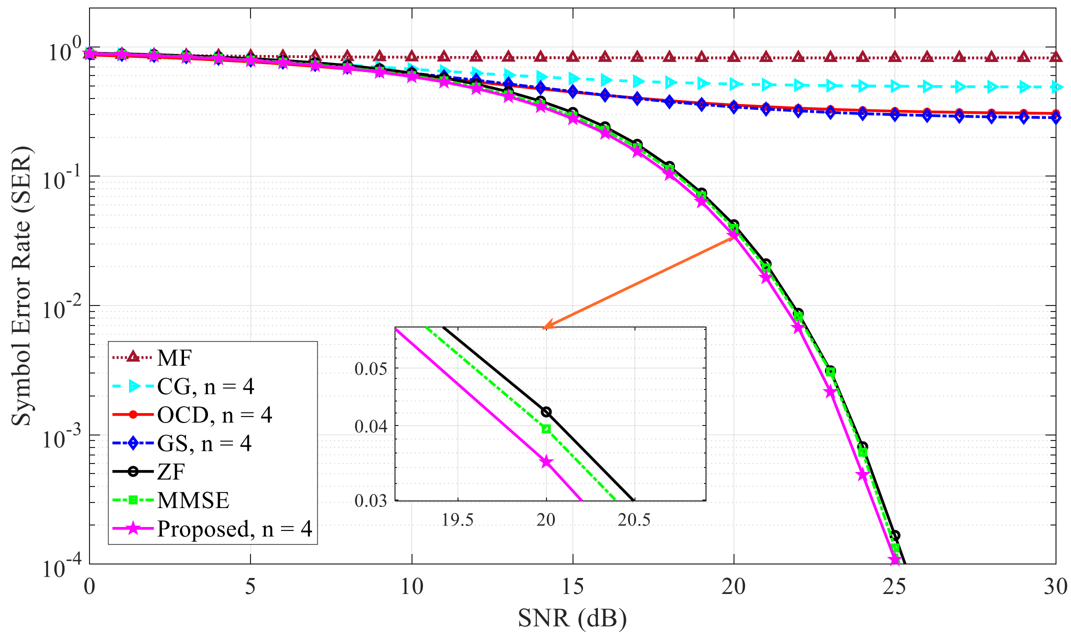

Figure 4. 20: SER performance of proposed detector and other methods at 120x180 M-MIMO system, 32QAM and n=4

In figure 4.21, the SER performance of a proposed detector is compared to that of other detectors in a massive MIMO system with a 64x128 antenna configuration, n = 4, and 32QAM. The proposed algorithm achieved a $\text{SER} = 7.094\times10^{-3}$, at SNR = 19dB, whereas the GS method obtained a $\text{SER} = 6.936\times10^{-2}$, and the MMSE method obtained a $\text{SER} = 8.547\times10^{-3}$ at the same SNR. At SNR = 20dB, the proposed detector showed a $\text{SER} = 2.484\times10^{-3}$, while the GS detector achieved a $\text{SER} = 5.513\times10^{-2}$ and the MMSE detector obtained a $\text{SER} = 2.969\times10^{-3}$. The proposed algorithm obtained a $\text{SER} = 5.938\times10^{-4}$, at SNR = 21dB, whereas the GS method obtained a $\text{SER} = 4.441\times10^{-2}$, and the MMSE method obtained a $\text{SER} = 6.719\times10^{-4}$ at the same SNR. At SNR = 22dB, the proposed detector showed a $\text{SER} = 1.094\times10^{-4}$, while the GS detector achieved a $\text{SER} = 3.667\times10^{-2}$ and the MMSE detector obtained a $SER = 1.563 \times 10^{-4}$. The proposed detector outperformed from the other detectors.

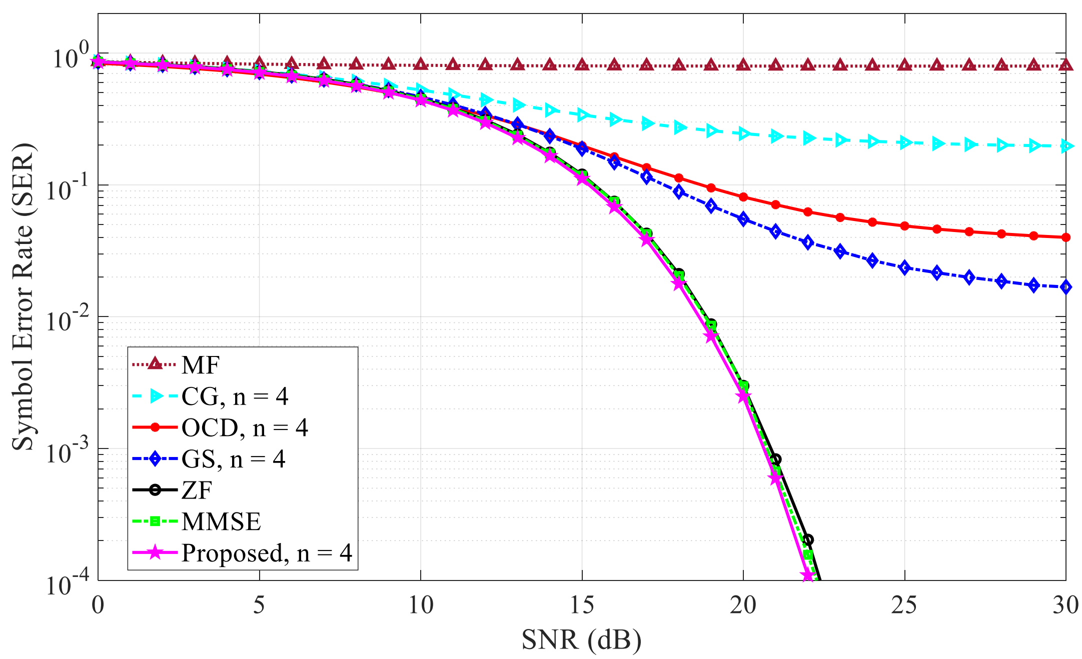

Figure 4. 21: SER performance of proposed detector and other methods at 64x128 M-MIMO system, 32QAM and n=4

In figure 4.22, the SER performance of a proposed detector is compared to that of other detectors in a massive MIMO system with a 128x256 antenna configuration, n = 5, and 64QAM. The proposed algorithm achieved a $SER = 9.484 \times 10^{-3}$, at SNR = 22dB, whereas the GS method obtained a $SER = 9.832 \times 10^{-2}$, and the MMSE method obtained a $SER = 1.107 \times 10^{-2}$ at the same SNR. At SNR = 23dB, the proposed detector showed a $SER = 3.125 \times 10^{-3}$, while the GS detector achieved a $SER = 8.043 \times 10^{-2}$ and the MMSE detector obtained a $SER = 3.961 \times 10^{-3}$. The proposed algorithm obtained a $SER = 8.594 \times 10^{-4}$, at SNR = 24dB, whereas the GS method obtained a $SER = 6.647 \times 10^{-2}$, and the MMSE method obtained a $SER = 1.086 \times 10^{-3}$ at the same SNR. At SNR = 25dB, the proposed detector showed a $SER = 1.484 \times 10^{-4}$, while the GS detector achieved a $SER = 5.618 \times 10^{-2}$ and the MMSE detector obtained a $SER = 2.344 \times 10^{-4}$. As indicated in all SER simulation results the MF, CG and OCD show poor performance.

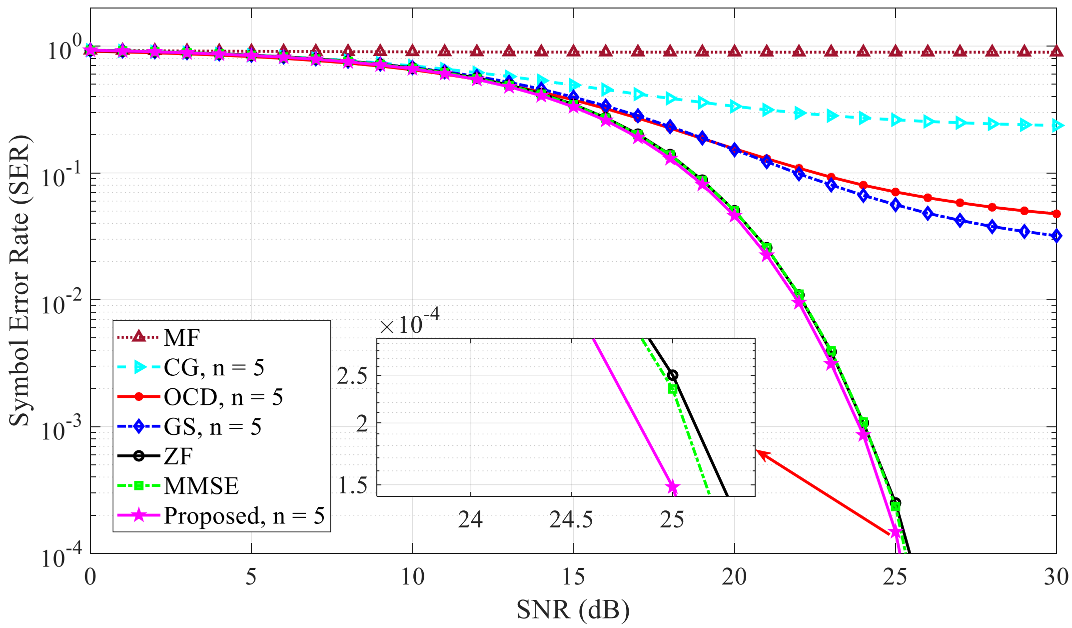

Figure 4. 22: SER performance of proposed detector and other methods at 128x256 M-MIMO system, 64QAM and n=5

4.1.4 Summary of Performance Comparison

As shown in the above all-performance simulation results, the proposed detector has achieved the best BER, MSE, and SER performance as compared to, GS, OCD, and CG and achieved comparable performance with MMSE and Zero forcing detectors.

The proposed detector achieved the optimal $BER = 3.33\times10^{-5}$ at the SNR=21dB, whereas GS detector achieved $BER = 5.55\times10^{-2}$ for 8-QAM, 80x120 antenna configuration and n=2. At this condition the percentage performance improvement of the proposed detector from the GS detector is given by $\frac{(5.55\times10^{-2} - 3.33\times10^{-5})}{5.55\times10^{-2}}\times100 = 99.94\%$. The proposed detector achieved the optimal $BER = 2.73\times10^{-5}$ at the SNR=25dB, whereas GS detector achieved $BER = 9.31\times10^{-3}$ for 64-QAM, 128x256 antenna configuration and n=5. At this condition the percentage performance improvement of the proposed detector from the GS detector is 99.71%. The proposed algorithm achieved an $MSE = 1.172\times10^{-4}$ at SNR = 25dB, while the GS method achieved an $MSE = 5.531\times10^{-2}$ for a massive MIMO system with a 128x256 antenna configuration, n = 5, and 64QAM. At this condition the percentage performance improvement of the proposed detector from the GS detector is 99.78%. At SNR = 22dB, the proposed detector showed a $\text{SER} = 1.094 \times 10^{-4}$, while the GS detector achieved a $\text{SER} = 3.667 \times 10^{-2}$ for a massive MIMO system with a 64x128 antenna configuration, n = 4, and 32QAM. At this condition the percentage performance improvement of the proposed detector from the GS detector is 99.70%. These improvements are occurred due to taking of best initial condition by using ADMM technique.

4.2 Complexity Analysis Based on Number of Multiplications

As discussed in chapter three, the number of mathematical operations performed, such as multiplications and divisions, is well known to have a significant impact on complexity. Furthermore, a large number of iterations lead to an increase in computational complexity. U real number of divisions are required to compute the inverse diagonal matrix (D^{-1}) for finding $\hat{x}_{(0)}$. To find the solution for the first iteration $\hat{x}_{(1)}$ by taking MMSE equalization matrix using ADMM solution finding technique, the computational complexity is $2U^2 + 2U$ .The GS method necessitates a computational complexity of $4nU^2 - 4U^2$. As a result, the computational complexity of the proposed algorithm is $4nU^2 - 2U^2 + 3U$. the proposed detector achieves the desired complexity reduction. The proposed algorithm's complexity is reduced to $\text{O}(U^2)$. where U indicates the number users. Table 4.8 compares the proposed method to other methods in terms of complexity.

Table 4. 8: Complexity of proposed algorithm, CG, GS, OCD, ZF, and MMSE.

Algorithm	computational complexity
CG (Yin et al., 2014)	$nU^2 + 6nU$
GS (Vasudevan, 2020)	$4nU^2$
OCD (M. Wu et al., 2016)	$2nNU + nU$
ZF (Shafivulla et al., 2020)	$\frac{1}{2}(U^3 + NU^2 + 5U^2 + 3NU)$
MMSE (Shahabuddin et al., 2021)	$4U^3 + 4N^2U + 4NU$
Proposed	$4nU^2 - 2U^2 + 3U$

Figure 4.23 shows a comparison of the proposed detector's complexity to that of other detection algorithms based on the number $\text{users} = 80$, base station $\text{antennas} = 120$ and $\text{n} = 2$.

The complexity of the proposed algorithm is far lower than that of the MMSE algorithm, as shown in the figure 4.23. When compared to other methods, the ZF and MMSE algorithms have high computational complexity. The proposed method met the requirements for low computational complexity. The number of users, base station antenna, and iterations used in the simulation determine the computational complexity.

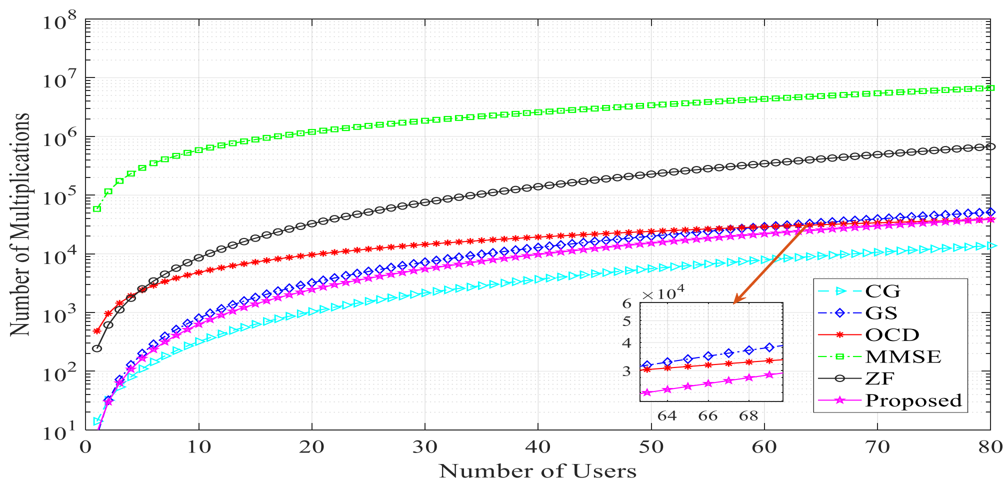

Figure 4. 23: Complexity comparison of proposed detector with other methods at 80x120 M-MIMO and n=2

By considering some numbers of users, we can express figure 4.23 in tabular form. As the number of user increase, the computational complexity also increased as shown in table 4.9. Table 4.9 shows complexity comparison of proposed method and other methods for some value of users from 76 to 80 and the number of iterations $n = 2$.

Table 4. 9: Complexity comparison of proposed detector and other methods at 80x120 M-MIMO and n=2

Number of users	Number of multiplications in algorithms					
	Proposed	MMSE	ZF	GS	OCD	CG
76	34,884	6,169,984	594,168	46,208	36,632	12,464
77	35,805	6,298,292	612,689	47,432	37,114	12,782
78	36,738	6,428,448	631,566	48,672	37,596	13,104
79	37,683	6,560,476	650,802	49,928	38,078	13,430
80	38,640	6,694,400	670,400	51,200	38,560	13,760

Figure 4.24 shows a comparison of the proposed detector's complexity to that of other detection algorithms based on the number of users $=120$, base station antennas $=180$ and $n=3$.

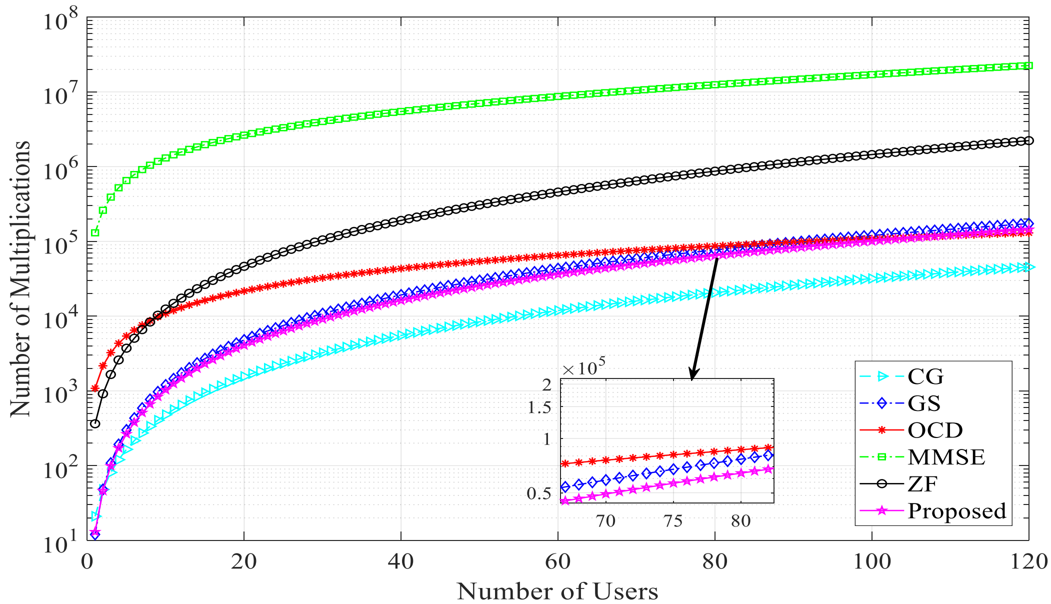

Figure 4. 24: Complexity comparison of proposed detector with other methods at 120x180 M-MIMO and n=3

By considering some users value from the figure 4.24, we can obtain the following table. Table 4.10 shows complexity comparison of proposed method and other methods for some value of users from 115 to 120 and the number of iterations $n=3$.

Table 4. 10: Complexity comparison of proposed detector and other methods at 120x180 M-MIMO and n=3

Number of users	Number of multiplications in algorithms					
	Proposed	MMSE	ZF	GS	OCD	CG
115	132,595	21,070,300	2,014,800	158,700	124,545	41,745
116	134,908	21,360,704	2,056,448	161,472	125,628	42,456
117	137,241	21,653,892	2,098,629	164,268	126,711	43,173
118	139,594	21,949,888	2,141,346	167,088	127,794	43,896
119	141,967	22,248,716	2,184,602	169,932	128,877	44,625
120	144,360	22,550,400	2,228,400	172,800	129,960	45,360

Figure 4.25 shows a comparison of the proposed detector's complexity to that of other detection algorithms based on the number of users $= 64$, base station antennas $= 128$ and $n = 4$.

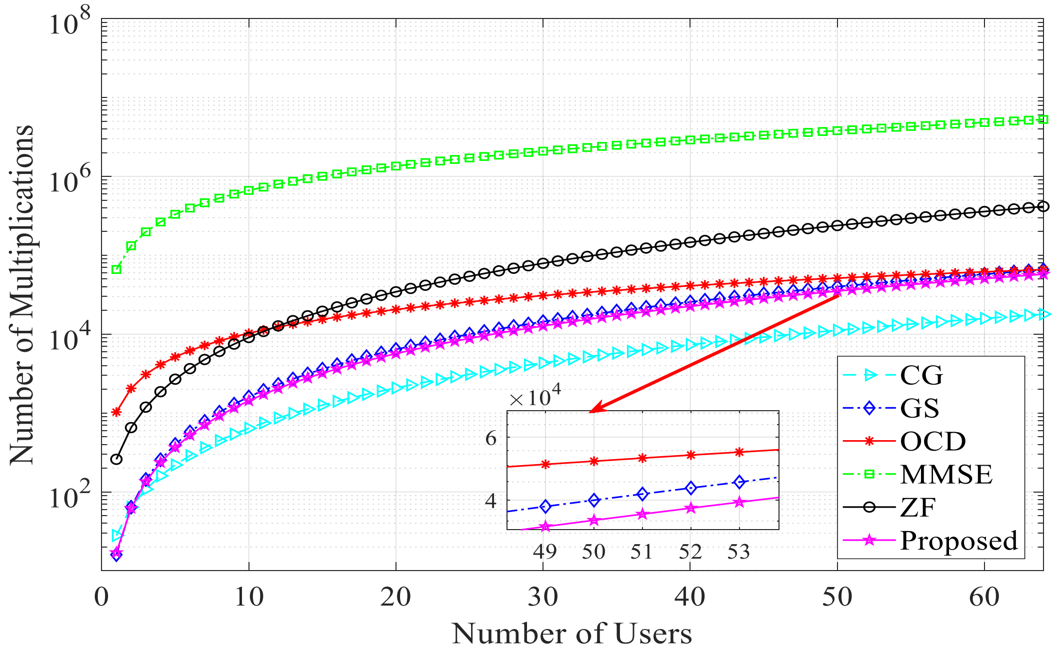

Figure 4. 25: Complexity comparison of proposed detector with other methods at 64x128 M-MIMO and n=4

By considering some users value from the figure 4.25, we can obtain the following table. Table 4.11 shows complexity comparison of proposed method and other methods for some value of users from 60 to 64 and the number of iterations $n = 4$.

Table 4. 11: Complexity comparison of proposed detector and other methods at 64x128 M-MIMO and n=4

Number of users	Number of multiplications in algorithms					
	Proposed	MMSE	ZF	GS	OCD	CG
60	50,580	4,826,880	358,920	57,600	61,680	15,840
61	52,277	4,936,852	372,649	59,536	62,708	16,348
62	54,002	5,048,288	386,694	61,504	63,736	16,864
63	55,755	5,161,212	401,058	63,504	64,764	17,388
64	57,536	5,275,648	415,744	65,536	65,792	17,920

Figure 4.26 shows a comparison of the proposed detector's complexity to that of other detection algorithms based on the number of users $= 128$, base station antennas $= 256$ and n $= 5$.

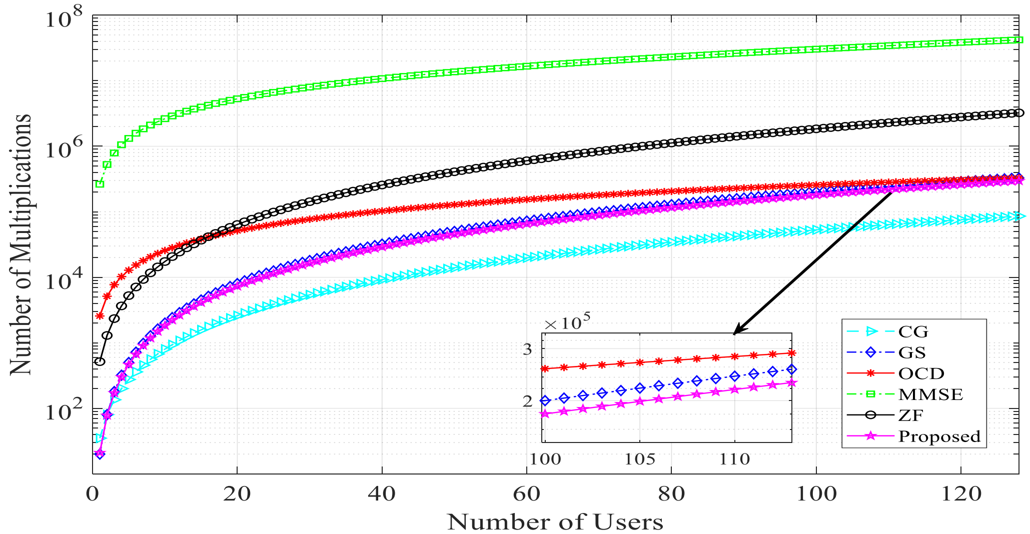

Figure 4. 26: Complexity comparison of proposed detector with other methods at 128x256 M-MIMO and n=5

By considering some users value from the figure 4.26, we can obtain the following table. Table 4.12 shows complexity comparison of proposed method and other methods for some value of users from 124 to 128 and the number of iterations n $= 5$.

Table 4. 12 : Complexity comparison of proposed detector and other methods at 128x256 M-MIMO and n=5

Number of users	Number of multiplications in algorithms					
	Proposed	MMSE	ZF	GS	OCD	CG
124	277,140	40,259,328	3,007,496	307,520	318,060	80,600
125	281,625	40,708,500	3,063,625	312,500	320,625	81,875
126	286,146	41,160,672	3,120,390	317,520	323,190	83,160
127	290,703	41,615,868	3,177,794	322,580	325,755	84,455
128	295,296	42,074,112	3,235,840	327,680	328,320	85,760

As indicated in the above all complexity simulation results, the proposed detector has low computational complexity as compared to MMSE, ZF, GS, and OCD.

5. CONCLUSIONS AND RECOMMENDATIONS

5.1 Conclusions

Massive MIMO is a key enabling technology for 5G and B5G communication networks due to its high spectral efficiency, high energy efficiency, high link reliability, and high data rate. However, the deployment of massive MIMO systems faces a number of challenges. One of the major challenges in the deployment of massive MIMO systems is the detection of uplink signals. To mitigate this challenge, several signal detection algorithms have been used. Performance and complexity are the major issues in signal detection. A detector with low complexity and high performance is required. The performance-complexity profile of signal detection algorithms is greatly influenced by good initialization. A low-complexity, efficient hybrid MMSE with ADMM technique and GS-based signal detection algorithm for massive MIMO uplink systems is proposed in this thesis. Initialization using the MMSE with ADMM technique and detection using the GS algorithm are the two stages of the proposed hybrid detector. In addition, a diagonal matrix is also used to initialize the proposed detector.

As shown in the simulation results, the performance of the proposed detector is evaluated using parameters such as BER, MSE, SER and SNR for antenna configurations of 80x120, 120x180, 64x128 and 128x256 over 8QAM, 16QAM, 32QAM, and 64QAM modulation schemes at various iterations. The proposed algorithm achieved the best BER, MSE and SER performance with only two iterations, as demonstrated by the simulation results. The proposed detector has improved performance with a small number of iterations and low computational complexity. The proposed detector complexity is reduced from $\mathrm{O}(U^3)$ to $\mathrm{O}(U^2)$. The proposed detector achieves the required performance with only two iterations, whereas other detectors such as OCD and GS require more iterations to perform better, but this causes the complexity to increase. The MMSE and ZF detectors perform well, but their complexity is high. Detectors such as CG and MF show very low performance.

5.2 Recommendations

In this thesis, the proposed detector performance is only evaluated at the simulation level. In the future scope of this thesis, the practical performance of the proposed detector can also be investigated by designing very large scale integration (VLSI) architecture and implementing it on a Xilinx Virtex-7 field-programmable gate array (FPGA). In the future work of this thesis, machine learning and deep learning based massive MIMO uplink signal detection algorithms will be developed.

Research Fund Acknowledgement

This research project is funded by Adama Science and Technology University under the grant number ASTU/SM-R/403/22, Adama, Ethiopia.

6. REFERENCES

Borges, D., Montezuma, P., Dinis, R., & Beko, M. (2021). Massive mimo techniques for 5g and beyond—opportunities and challenges. Electronics (Switzerland), 10(14), 1–29. https://doi.org/10.3390/electronics10141667

Huang, C.-W., Chou, Y.-C., Chen, H.-Y., & Chou, C.-F. (2021). Joint QoS-Aware Scheduling and Precoding for Massive MIMO Systems via Deep Reinforcement Learning. arXiv preprint arXiv:2104.04492 Ml, 1–12. http://arxiv.org/abs/2104.04492

Rahmawati, P., Nashiruddin, M. I., & Nugraha, M. A. (2021). Capacity and coverage analysis of 5g nr mobile network deployment for indonesia's urban market. 2021 IEEE International Conference on Industry 4.0, Artificial Intelligence, and Communications Technology (IAICT), 90–96.

Shahabuddin, S., Hautala, I., Juntti, M., & Studer, C. (2021). ADMM-Based Infinity-Norm Detection for Massive MIMO: Algorithm and VLSI Architecture. IEEE Transactions on Very Large Scale Integration (VLSI) Systems, 29(4), 747–759. https://doi.org/10.1109/TVLSI.2021.3056946

Albreem, M. A., Alsharif, M. H., & Kim, S. (2020). Massive MIMO Uplink Systems. Journal of SS symmetry Ml, 1–12. https://doi.org/10.3390/sym12020306

Amiri, M., & Naeiny, M. F. (2020). Low-Complexity Iterative Detection for Uplink Multiuser Large-Scale MIMO. Journal of Information Systems and Telecommunication (JIST), 1(29), 25.

Chataut, R., & Akl, R. (2020). Massive MIMO systems for 5G and beyond networks—overview, recent trends, challenges, and future research direction. Sensors (Switzerland), 20(10), 1–35. https://doi.org/10.3390/s20102753

Dan, Z., Dong, S., Xiaofang, C., Xia, H., & Xin, W. (2020). A Low-Complexity Hybrid Iterative Signal Detection Algorithm for Massive MIMO. 2020 IEEE 8th International Conference on Information, Communication and Networks, ICICN 2020, 85–89. https://doi.org/10.1109/ICICN51133.2020.9205094

Elsherbiny, H., Abbas, H. M., Abou-zeid, H., Hassanein, H. S., & Noureldin, A. (2020). 4g lte network throughput modelling and prediction. GLOBECOM 2020-2020 IEEE Global Communications Conference, 1–6.

Shafivulla, S., Patel, A., & Khan, M. Z. A. (2020). Low Complexity Signal Detection for Massive-MIMO Systems. IEEE Wireless Communications Letters, 9(9), 1467–1470.

https://doi.org/10.1109/LWC.2020.2994058

Vasudevan, M. A. M. A. K. (2020). Efficient Hybrid Linear Massive MIMO Detector Using Gauss – Seidel And Successive Over - Relaxation. International Journal of Wireless Information Networks, 0123456789. https://doi.org/10.1007/s10776-020-00493-5

Wu, H., Shen, B., Zhao, S., & Gong, P. (2020). Low-complexity soft-output signal detection based on improved kaczmarz iteration algorithm for uplink massive MIMO system. Sensors (Switzerland), 20(6). https://doi.org/10.3390/s20061564

Yang, X., Cao, F., Matthaiou, M., & Jin, S. (2020). On the uplink transmission of extra-large scale massive MIMO systems. IEEE Transactions on Vehicular Technology, 69(12), 15229–15243.

Ye, Q., & Min, X. (2020). Block Gauss-Seidel Method for Signal Detection in Uplink Massive MIMO Systems. Proceedings of the 2020 The 2nd World Symposium on Software Engineering 122–127.

Albreem, M. A., Juntti, M., & Shahabuddin, S. (2019). Massive MIMO Detection Techniques: A Survey. IEEE Communications Surveys and Tutorials, 21(4), 3109–3132. https://doi.org/10.1109/COMST.2019.2935810

Mohammadghasemi, H., Sabahi, M. F., & Forouzan, A. R. (2019). Pilot-decontamination in massive MIMO systems using interference alignment. IEEE Communications Letters, 24(3), 672–675.

Yarrabothu, R. S., & Telagathoti, P. (2019). Massive Mimo and Beamforming Techniques of 5G Networks. CERC 1, 139–142. https://doi.org/10.35940/ijeat.A1034.1291S52019

Chataut, R., & Akl, R. (2018). Huber Fitting based ADMM Detection for Uplink 5G Massive MIMO Systems. 2018 9th IEEE Annual Ubiquitous Computing, Electronics and Mobile Communication Conference, UEMCON 2018, 33–37. https://doi.org/10.1109/UEMCON.2018.8796735

Meng, X., Chang, Y., Wang, Y., & Wu, J. (2018). Multi-user grouping based scheduling algorithm in massive MIMO uplink networks. 2018 IEEE 4th International Conference on Computer and Communications (ICCC), 409–413.

Nguyen, M. T. (2018). Massive MIMO: A Survey of Benefits and Challenges. ICSES Trans. Comput. Hardw. Electr. Eng4(4), 1–4.

Yang, H. (2018). User scheduling in massive MIMO. 2018 IEEE 19th International Workshop on Signal Processing Advances in Wireless Communications (SPAWC), 1–5.

Adhikary, A., Ashikhmin, A., & Marzetta, T. L. (2017). Uplink interference reduction in large-scale antenna systems. IEEE Transactions on Communications, 65(5), 2194–2206.

Chen, X., Lu, J., Fan, P., & Letaief, K. Ben. (2017). Massive MIMO beamforming with transmit diversity for high mobility wireless communications. IEEE Access, 5, 23032–23045.

Ghacham, S., Benjillali, M., & Guennoun, Z. (2017). Low-Complexity Detection For Massive MIMO Systems Over Correlated Rician Fading. IEEE, 1677–1682.

Gustafsson, O., Bertilsson, E., Klasson, J., & Ingemarsson, C. (2017). Approximate neumann series or exact matrix inversion for massive MIMO? Proceedings - 24th IEEE Symposium on Computer Arithmetic, ARITH 2017, 62–63. https://doi.org/10.1109/ARITH.2017.11

MOQBEL, M. A. M., Wangdong, W., & Ali, A. Z. (2017). MIMO Channel Estimation Using the LS and MMSE Algorithm. IOSR Journal of Electronics and Communication Engineering, 12(01), 13–22. https://doi.org/10.9790/2834-1201021322

Mukubwa, E., Sokoya, O. A., & Ilcev, D. S. (2017). Comparison and analysis of massive MIMO linear precoding schemes in the downlink. 2017 IEEE AFRICON, 187–191.

Varasteh, M., Rassouli, B., & Clerckx, B. (2017). Wireless information and power transfer over an AWGN channel: Nonlinearity and asymmetric Gaussian signaling. 2017 IEEE Information Theory Workshop (ITW), 181–185.

Xia, X., Xu, K., Zhang, D., Xu, Y., & Wang, Y. (2017). Beam-domain full-duplex massive MIMO: Realizing co-time co-frequency uplink and downlink transmission in the cellular system. IEEE Transactions on Vehicular Technology, 66(10), 8845–8862.

Lyu, T. K. (2016). Capacity of multi-user MIMO systems with MMSE and ZF precoding. 2016 IEEE Conference on Computer Communications Workshops (INFOCOM WKSHPS), 1083–1084.

Wu, M., Dick, C., Cavallaro, J. R., & Studer, C. (2016). High-Throughput Data Detection for Massive MU-MIMO-OFDM Using Coordinate Descent. IEEE Transactions on Circuits and Systems I: Regular Papers, 63(12), 2357–2367. https://doi.org/10.1109/TCSI.2016.2611645

Wu, Z., Zhang, C., Xue, Y., Xu, S., & You, X. (2016). Efficient architecture for soft-output massive MIMO detection with Gauss-Seidel method. Proceedings - IEEE International Symposium on Circuits and Systems, 2016-July, 1886–1889. https://doi.org/10.1109/ISCAS.2016.7538940

Besnoff, J., & Ricketts, D. (2015). Quadrature amplitude modulated (QAM) communication link for near and mid-range RFID systems. 2015 IEEE International Conference on RFID (RFID), 151–157.

Yin, B., Wu, M., Cavallaro, J. R., & Studer, C. (2015). VLSI design of large-scale soft-output MIMO detection using conjugate gradients. Proceedings - IEEE International Symposium on Circuits and Systems, 2015-July, 1498–1501. https://doi.org/10.1109/ISCAS.2015.7168929

Iwakuni, T., Maruta, K., Ohta, A., Shirato, Y., Kurosaki, S., Arai, T., & Iizuka, M. (2015). Massive MIMO effect for multiuser spatial multiplexing in time varying channel. IEICE Communications Express, 4(8), 270–275.

Bjornson, E., Hoydis, J., Kountouris, M., & Debbah, M. (2014). Massive MIMO systems with non-ideal hardware: Energy efficiency, estimation, and capacity limits. IEEE Transactions on Information Theory, 60(11), 7112–7139. https://doi.org/10.1109/TIT.2014.2354403

Björnson, E., Hoydis, J., Kountouris, M., & Debbah, M. (2014). Massive MIMO systems with non-ideal hardware: Energy efficiency, estimation, and capacity limits. IEEE Transactions on Information Theory, 60(11), 7112–7139.

Ding, W., Yang, F., Pan, C., Dai, L., & Song, J. (2014). Compressive sensing based channel estimation for OFDM systems under long delay channels. IEEE Transactions on Broadcasting, 60(2), 313–321.

Gao, Xinyu, Dai, L., Hu, Y., Wang, Z., & Wang, Z. (2014). Matrix inversion-less signal detection using SOR method for uplink large-scale MIMO systems. 2014 IEEE Global Communications Conference, 3291–3295.

Gustavsson, U., Sanchéz-Perez, C., Eriksson, T., Athley, F., Durisi, G., Landin, P., Hausmair, K., Fager, C., & Svensson, L. (2014). On the impact of hardware impairments on massive MIMO. 2014 IEEE Globecom Workshops (GC Wkshps), 294–300.

Jiang, J.-D., Lin, T.-C., & Phoong, S.-M. (2014). New subspace-based blind channel estimation for orthogonally coded MIMO-OFDM systems. 2014 IEEE International Conference on Acoustics, Speech and Signal Processing (ICASSP), 6489–6493.

Larsson, E. G., Edfors, O., Tufvesson, F., & Marzetta, T. L. (2014). Massive MIMO for next generation wireless systems. IEEE Communications Magazine, 52(2), 186–195.

Lu, L., Li, G. Y., Swindlehurst, A. L., Ashikhmin, A., & Zhang, R. (2014). An overview of massive MIMO: Benefits and challenges. IEEE Journal on Selected Topics in Signal Processing, 8(5), 742–758. https://doi.org/10.1109/JSTSP.2014.2317671

Müller, R. R., Cottatellucci, L., & Vehkaperä, M. (2014). Blind pilot decontamination. IEEE Journal of Selected Topics in Signal Processing, 8(5), 773–786.

Park, C.-S., Byun, Y.-S., Bokiye, A. M., & Lee, Y.-H. (2014). Complexity reduced zero-forcing beamforming in massive MIMO systems. 2014 Information Theory and Applications Workshop (ITA), 1–5.

Yin, B., Wu, M., Cavallaro, J. R., & Studer, C. (2014). Conjugate gradient-based soft-output detection and precoding in massive MIMO systems. 2014 IEEE Global Communications Conference, GLOBECOM 2014, 1, 3696–3701. https://doi.org/10.1109/GLOCOM.2014.7037382

Li, Y., Nam, Y.-H., Ng, B. L., & Zhang, J. (2012). A non-asymptotic throughput for massive MIMO cellular uplink with pilot reuse. 2012 IEEE Global Communications Conference (GLOBECOM), 4500–4504.

Trimeche, A., Boukid, N., Sakly, A., & Mtibaa, A. (2012). Performance analysis of ZF and MMSE equalizers for MIMO systems. 7th International Conference on Design & Technology of Integrated Systems in Nanoscale Era, 1–6.

Gao, Xiang, Edfors, O., Rusek, F., & Tufvesson, F. (2011). Linear pre-coding performance in measured very-large MIMO channels. 2011 IEEE Vehicular Technology Conference (VTC Fall), 1–5.

Boyd, S., Parikh, N., Chu, E., Peleato, B., & Eckstein, J. (2011). Distributed optimization and statistical learning via the alternating direction method of multipliers. Foundations and Trends® in Machine Learning, 3(1), 1–122.

Appaiah, K., Ashikhmin, A., & Marzetta, T. L. (2010). Pilot contamination reduction in multi-user TDD systems. 2010 IEEE International Conference on Communications, 1–5.

Studer, C., Wenk, M., & Burg, A. (2010). MIMO transmission with residual transmit-RF impairments. 2010 International ITG Workshop on Smart Antennas (WSA), 189–196.

Van der Veen, A.-J., Talwar, S., & Paulraj, A. (1997). A subspace approach to blind space-time signal processing for wireless communication systems. IEEE Transactions on Signal Processing, 45(1), 173–190.

7. APPENDIX

The followings are algorithms that we used for comparisons with proposed algorithm:

Algorithm 2: Signal detection based on MMSE algorithm.

Inputs: y, H, N_O, and E_s

Output: detected signal $\hat{x}$

Initialization:

$\beta = N_O / E_s$

$A = H^H H + \beta I_U$

$y_{MF} = H^H y$

Detection:

$\hat{x} = A^{-1} y_{MF}$

Return $\hat{x}$

Algorithm 3: Signal detection based on ZF algorithm.

Inputs: y, and H

Output: detected signal $\hat{x}$

Initialization:

$A = H^H H$

$y_{MF} = H^H y$

Detection:

$\hat{x} = A^{-1} y_{MF}$

Return $\hat{x}$

Algorithm 4: Signal detection based on GS algorithm.

Inputs: y, H, N_O, n and E_s

Output: detected signal $\hat{x}$

Initialization:

$\beta = N_O / E_s$

$A = H^H H + \beta I_U$

$y_{MF} = H^H y$

D = daig(A), U = -triu(A), L = -tril(A)

Detection:

for i=1:1: n

$\hat{x}_{(n)} = (D - L)^{-1}(y_{MF} + U\hat{x}_{(n-1)})$

end

Return $\hat{x}$

Algorithm 5: Signal detection based on OCD algorithm.

Inputs: y, H, n and N_O

Output: detected signal $\hat{x}$

Initialization:

$r = y$

$\alpha = 0$

$d_u^{-1} = (\|h_u\|_2^2 + \alpha)^{-1}$

$p_u = d_u^{-1} \|h_u\|_2^2$

Detection:

for i= 1:1:n

for u = 1:1:U

$x_u^{(n)} = proj(d_u^{-1} h_u^H r + p_u x_u^{(n-1)})$

$\Delta x_u^{(k)} = x_u^{(n)} - x_u^{(n-1)}$

$r = r - h_u \Delta x_u^{(n)}$

end

end

Return $\hat{x} = \left[x_1^{(n)}, ... x_U^{(n)} \right]^T$

Algorithm 6: Signal detection based on CG algorithm.

Inputs: y, H, N_O, n and E_s

Output: $\hat{x}$

Initialization:

$\beta = N_O / E_s$

$A = H^H H + \beta I_U$

$y_{MF} = H^H y$

$r = y_{MF}$

p = r

v = 0

Detection:

for i = 1:1: n

$e = Ap$

$\alpha = \frac{\|r\|^2}{p^* e}$

$v = v + \alpha p$

$r_{new} = r - \alpha e$

$\gamma = \frac{\|r_{new}\|^2}{\|r\|^2}$

$p = r_{new} + \gamma p$

$r = r_{new}$

end

Return $\hat{x} = v$

Algorithm 7: Signal detection based on MF algorithm.

Inputs: y and H

Output: $\hat{x}$

Detection:

$\hat{x} = H^{H} y$

Return $\hat{x}$